The Biochemical Dynamics of Monoclonal Antibody Production in High Density Perfused Fermentors

by

Michael Alexander Tyo

B.S., Biology, Massachusetts Institute of Technology (1976)
M.S., Biochemical Engineering, Massachusetts Institute of Technology (1978)

SUBMITTED TO THE DEPARTMENT OF APPLIED BIOLOGICAL SCIENCES
IN PARTIAL FULFILLMENT OF THE REQUIREMENTS FOR THE DEGREE
OF

DOCTOR OF PHILOSOPHY

in
BIOCHEMICAL ENGINEERING

at the
MASSACHUSETTS INSTITUTE OF TECHNOLOGY

February, 1992

Signature of Author _____ *Signature redacted*
Department of Applied Biological Sciences
October 8, 1991

Certified by _____ *Signature redacted*
W. G. Thilly
Professor of Applied Biological Sciences
Thesis Supervisor

Accepted by _____ *Signature redacted*
Steven R. Tannenbaum
Chairman, Departmental Committee on Graduate Students

1

"This doctoral thesis has been examined by a Committee of the Department of

Applied Biological Sciences as follows:"

Professor Helmut Zarbl   Signature redacted
                                               Chairman
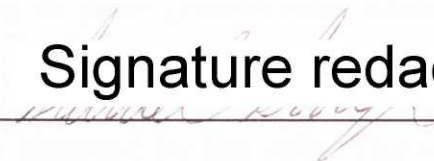
Professor William Thilly   Signature redacted
                                        Thesis Supervisor

Professor Henri Brunengraber   Signature redacted

Professor Randall Swartz   Signature redacted

Professor Sam Singer   Signature redacted

The Biochemical Dynamics of Monoclonal Antibody Production in High Density Perfused Fermentors

by Michael A. Tyo
Submitted to the Department of Applied Biological Sciences on October 8, 1991 in partial fulfillment of the requirements for the degree of Doctor of Philosophy in Biochemical Engineering

Abstract

Monoclonal antibody producing cells based on the Sp2/0 murine hybridoma cell line were used in a series of experiments to investigate their patterns of metabolic responses to environmental stresses while growing at high density. As part of the research project, a novel perfusion bioreactor system was developed which permitted the cells to grow to a density of 2×10^7 cells/ml with a viability in excess of 80%.

It was observed that as the cells increased in density from 10^6 to 10^7 cells/ml, the specific productivity of IgG declined by 99%. At low cell density ($<3 \times 10^6$ cells/ml), the IgG productivity was typically around 0.20 pg/cell-h. However, as the cell density approached 10^7 cells/ml, IgG productivity fell to less than 0.01 pg/cell-h. Coincident with this decline in IgG secretion was a dramatic drop in the uptake rates of amino acids. For example, at a perfusion rate of three volumes/day, the uptake rate of leucine dropped from 30 to 2.3 fmol/cell-h when the cell density increased from 10^6 to 10^7 cells/ml. This density dependence of amino acid uptake rates is only one manifestation of a larger pattern of coordinated down-regulation of metabolic rates in response to the condition of high cell density which includes protein synthesis, oxygen uptake, and inorganic ion uptake.

When the response of the cells to steady-state conditions of waste metabolite limitation and nutrient limitation was examined, it was found that waste and nutrient limitations caused declines in net amino acid uptake rates of 73% and 12%, respectively. Waste-limited and nutrient-limited conditions both produced decreases in steady state cell density and viability. Waste-limited cells exhibited a decrease in their growth rate, while nutrient-limited cells showed an increase in the death rate.

Another novel finding of this research project was that the product of spontaneous glutamine breakdown, pyrollidone carboxylic acid (PCA, also known as oxoproline), is quantitatively ingested by the cells. The uptake rate of PCA is exceeded only by glucose and glutamine. In order to close the net amino acid balance, PCA must be included. At 5 volumes/day perfusion rate, for example, a net of 26 fmol/cell-h amino acids are required for growth. The observed net amino acid uptake rate (excluding PCA) was only 20 fmol/c-h. After accounting for the PCA, I measured a net amino acid flux of 34 fmol/c-h, more than enough to meet the amino acid requirement.

Thesis Supervisor: Dr. William G. Thilly
          Title: Professor of Applied Biological Sciences

Acknowledgments

I wish to acknowledge the contributions of the many friends and colleagues whose efforts made this work possible. This research project could not have been conducted in isolation and therefore represents a truly collective enterprise. For all of your help I am sincerely grateful. In particular, my friends and lab partners Claudia Buser and Joyce Morrill, who joined me in working late nights and weekends running the experimental cultures, and who did all the IgG assays, were wonderful collaborators. Yakov Makarovsky, Art Lafleur, and all the staff of the Analytical Chemistry Laboratory of the Center for Environmental Health Sciences kindly taught me everything I needed to know about HPLC analysis. Lori Tsuruda isolated and tested hundreds of clones to find the one that would produce enough material to work with. Peter Becker and Quintaniay Holifield, my undergraduate assistants, helped me immensely in the analytical lab and cell lab, running assays and counting cells.

For their guidance, advice, and kind words, I wish to thank Professor Thilly, my advisor, and all the members of my thesis committee. Professor Thilly especially deserves a word of appreciation for having allowed me the freedom to answer the questions regarding cell metabolism which I had been asking for years.

For their financial support, I wish to thank all our friends at Centocor, Inc., especially Michael Wall and Hubert Schoemaker. In addition, Centocor graciously provided the cells used for these experiments and invaluable recommendations on their cultivation.

Finally, I wish to thank all the members of my family, who, with long-suffering patience, endured years of missed dinners, lost weekends, and postponed attention. This thesis is dedicated to them.

Table of Contents

List of Figures

9

List of Tables

List of Symbols and Abbreviations

aib   = α-aminoisobutyric acid

Ala   = alanine

Arg   = arginine

Asp   = aspartate

Asn   = asparagine

ATP   = adenosine triphosphate

cm   = centimeter

Cys   = cysteine

d_p = particle diameter (cm)

D   = bioreactor dilution rate (hr^{-1})

DABS= 4-N,N-dimethylaminobenzene-4'sulfate

DMEM=Dulbecco's modified Eagle's medium

E_h = observed redox potential of redox couple (mV)

E'_0 = standard potential of redox couple (mV)

F   = medium flow rate (cm^3/h)

F   = Faraday constant (96,406 joule/volt)

fmol   = femtomole (10^{-15} mole)

g   = gravitational acceleration (981 cm/s^2)

Gln   = glutamine

Glu   = glutamate

Gly   = glycine

h   = time (hour)

His   = histidine

IgG   = immunoglobulin G; gamma-type antibody molecules

Ile   = isoleucine

K_S = substrate concentration giving half-maximal growth (mole/l)

L   = tube length needed to capture all particles (cm)

l   = volume (liter)

Leu   = leucine

M   = molar concentration (mole/l)

m   = maintenance requirement for substrate (mole/cell-hr)

Met   = methionine

mM = millimolar (10^{-3} mole/l)

mV = millivolt (10^{-3} volt)

PCA = pyrollidone carboxylic acid

Phe = phenylalanine

pmol = picomole (10^{-12} mole)

Pro = proline

Q = volumetric flow rate (cm^3/s)

Q_P = volumetric product formation rate (mole/l-h or g/l-h)

q_P = specific product formation rate (mole/cell-h or g/cell-h)

Q_S = volumetric substrate uptake rate (mole/l-h)

q_S = specific substrate uptake rate (mole/cell-h)

r = radial coordinate (cm)

r_c = critical radius for particle capture (cm)

R = radial distance (cm), or

R = gas constant (8.31 joule/°K-mole)

S = substrate concentration in system (mole/l)

s = time (seconds)

S_0 = substrate concentration at t=0 (mole/l)

S_i = inlet substrate concentration (mole/l)

Ser = serine

S_{yx} = standard error of estimate

t = time (hours or seconds)

TCA = tricarboxylic acid

THF = tetrahydrofolate

Thr = threonine

Trp = tryptophan

Tyr = tyrosine

V = bioreactor volume (cm^3)

Val = valine

V_{max} = maximum velocity (cm/s or mol/s)

V(r) = fluid velocity as a function of radius (cm/s)

V_T = particle terminal velocity (cm/s)

V_Z = fluid velocity in Z axis (cm/s)

X = cell concentration (cell/cm^3)

X_0 = cell density at t = 0 (cell/cm^3)

X_D = dead cell concentration (cell/cm^3)

X_{D0} = dead cell concentration at time = 0 (cell/cm^3)

$\overline{X_{LM}}$ = log-mean cell density

X_V = viable cell density (cell/cm^3)

$X_{V\ LM}$ = log-mean viable cell density (cell/cm^3)

Y_G = yield of cells on substrate (growth-related)
(cells/mole substrate)

Y_{obs} = observed yield of cells on substrate (cells/mole substrate)

Z = distance along z coordinate (cm)

α = specific death rate (h^{-1})

$\Delta\rho$ = density difference (particle-fluid) (g/cm^3)

δ = diameter (cm)

ε = fraction of cells removed by a separator (dimensionless)

ε_D = separation ratio for dead cells (dimensionless)

ε_V = separation ratio for viable cells (dimensionless)

μ = fluid viscosity (g/cm-s), or

μ = specific growth rate (h^{-1})

μ_{MAX} = the maximum possible cell growth rate (h^{-1})

μM = micromolar (10^{-6} moles/l)

τ = time for a particle to cross a fluid gap (seconds)

I. Introduction

A. Historical Perspectives

Although the current scale of commercial production of mammalian cell-derived products is a recent development, the technological history upon which current processes are based began in the early part of this century. Prior to 1900, it was widely believed that living tissues were inherently incapable of life outside of the whole organism, which provided some "vital force" necessary to sustain the cells. Alexis Carrel (1912) conclusively laid this notion to rest by introducing the concept of feeding the cells. By periodic replenishment of a nutrient solution bathing a section of chicken muscle tissue, Carrel kept the cells alive for many years. Widespread interest in cell culture was sparked when the explant outlived the life expectancy of the donor chicken. It became evident that long-term growth of animal cells in culture was possible.

Carrel had demonstrated the long-term growth of tissues outside the organism. It was not until several decades had passed that Sanford *et al* (1948) showed how to clone individual cells. Sanford's solution to the problem of cloning was, like Carrel's solution, nutritional. It seemed that in order for cells to proliferate, they needed to alter the medium into which they were seeded. Although thousands of cells could easily modify the medium in a petri dish, a single cell was unable to. Sanford and co-workers simply pulled a cell into the tip of a micropipette and allowed it to grow there. In the limited

volume within the pipette tip, even a single cell could adjust the medium sufficiently so as to permit growth. This medium was composed mostly of animal bodily fluids, totally undefined in composition, with a little saline buffer added in.

The difficulties of working with serum and chick embryo extract as a culture medium led Harry Eagle to undertake a rational study to develop a defined culture medium. After animal nutritionists such as Rose *et al* (1955) developed the concept of eight "essential" amino acids on the basis of feeding studies with young animals, Eagle (1955) showed that cells grown in culture required five additional amino acids. By adding all these amino acids to a mixture of glucose, vitamins, trace minerals, and buffers, he was able to obtain the growth of cells with the addition of just 1% horse serum as a nutritional supplement. The requirement for additional amino acids in cell culture implies that some specialized amino acid metabolic transformations occurs *in vivo* to supply these amino acids to distant tissues, and that cells grown in culture lack these biochemical pathways. Cells grown in culture, therefore, have specific, exacting nutritional requirements which must be met if the cells are to grow over many generations.

B. Metabolic Studies in Cell Cultures

The creation of (mostly) chemically defined media opened the door for a burgeoning of nutritional studies in cell culture, leading to the development of a variety of media. Amino acid metabolism in cell cultures, as opposed to studies of whole organisms, was studied by Eagle (1959), who investigated the sources of amino acids synthesized by the cells through feeding the cells with ^{14}C- and ^{15}N-labelled amino acids, glucose, and ammonium. He also reported nutritional and metabolic differences between various cell strains in culture. As research progressed, it became apparent that there were many factors which affected the nutritional requirements of cells. Eagle and Piez (1962) reported that a variety of cell types, including HeLa, KB, liver, conjunctiva, and intestine, required serine for growth at low cell densities. At higher densities, serine was not absolutely needed for cell growth, although it did increase final cell densities. The authors postulated that at low cell densities, the serine which the cells synthesized leaked across the cell membranes before the cells could incorporate it into proteins. At high cell densities, the cells were able to cross-feed each other. Thus, the notion was created of a dependence of nutritional requirements on cell density.

From these early beginnings, many investigators developed their own cell culture media. Some media were minimal, containing only those ingredients which the cells absolutely required, such as those of Waymouth (1959) and Nagle *et al.* (1963). Other media, such as NCTC 109 of Evans *et al.*

16

(1956), are especially complex, designed especially for growing fastidious cells (or for the cloning of cells). These have a wide variety of additional ingredients, including purines and pyrimidines, non-essential amino acids, lipids, and other vitamins.

The supplementation of medium with small amounts of animal serum is a practice which is still widespread. The use of serum introduces many difficulties. There is a substantial variation in growth-promoting qualities between different lots of serum, making necessary tedious screening procedures to select appropriate batches of sera. These growth-promoting activities vary between different cell types, so that a batch of serum good for one cell line may be unacceptable for another, and vice versa. Economic considerations apply, as well. As agrimarket conditions change with the weather, so does the price of serum. Manyfold price fluctuations in the span of a few months have occurred in recent years, creating difficulties in an industry that is dependent on a steady supply of serum. Physical complications arise from the addition of serum to medium. Since serum contains five to ten percent protein by weight, even a low concentration serum supplement contributes a significant amount of protein to the medium. This protein, when exposed to an air-liquid interface, can denature and creates a persistent foam. Consequently, cell cultures which are oxygenated through aeration must deal with a foaming problem. Finally, the presence of extraneous proteins in the culture medium complicates the recovery of economically valuable proteins which the cells may be secreting.

These difficulties introduced through the use of serum led naturally to studies in serum-free media which could support the growth of cells. Birch

17

and Pirt (1969) developed a medium containing polyvinylpyrrolidone and methocel which supported the growth of mouse LS fibroblast cells without proteins. Birch and Pirt (1970) improved the performance of this medium through the addition of trace minerals. Despite the intensity of efforts to produce media which will support the growth of cells without the addition of animal sera, only recently have media been described which work well without sera. An understanding of the essential components in serum has been critical to the success of these researchers. Murakami *et al.* (1982) showed that ethanolamine (or phosphoethanolamine) is an essential growth-stimulating component of serum. Sasai *et al.* (1985) developed a protein-free medium based on insulin, transferrin, ethanolamine, and selenium supplementations to a blend of commercial basal media.

C. Glutamine Metabolism

As investigations into the nutritional needs of mammalian cells progressed, it was gradually realized that the amino acid glutamine plays a central role. Its carbon skeleton is converted into five different amino acids (glutamate, alanine, aspartate, asparagine, and proline). The amino nitrogen atoms appear in many other amino acids, and the amide nitrogens appear in amino acids, purines, and pyrimidines. In addition, the rapid conversion of (U-^{14}C) labelled glutamine atoms into $^{14}CO_2$ implies that glutamine is rapidly oxidized.

Glucose was considered by many investigators to be a primary energy source. However, as early as 1958, Darnell and Eagle observed that either glutamine or glutamic acid could substitute for glucose in the growth of HeLa cells. They also reported that fructose could replace glucose in the medium provided that sufficient quantities of glutamine were present. This finding was applied to media design by Leibovitz (1963), who developed a glucose-free medium based on galactose. Kovacevic and Morris (1972) examined the role of glutamine in the oxidative metabolism of tumor cells. They reported that glutamine was an excellent substrate for oxidation in isolated mitochondria, and that as the tumor cells grew faster, their mitochondria showed a greater affinity for glutamine. Zielke *et al.* (1976) were able to grow normal human fibroblasts without glucose. Reitzer *et al.* in 1979 demonstrated that glutamine was indeed the major source of energy for HeLa cells.

With excess glucose, some cells uncontrollably undergo glycolysis, but still use glutamine oxidation to supply the majority of energy needs. McKeehan (1982) observed that the oxidation of glutamine is usually incomplete, yielding a mixture of amino acids and organic acids. He termed this partial oxidation of glutamine "glutaminolysis." When a cell is deprived of glucose, some carbohydrate still is needed for growth. The sugar is needed to supply the ribose moiety of nucleic acids as well as for the glycosylation of proteins and lipids. Not only does the requirement for hexose go down when glutamine is present in sufficient amounts, but the lactic acid which is produced by glycolysis no longer contributes to a major load on the pH buffer. Imamura *et al.* in 1982 demonstrated the advantages of glucose-free media when culturing MDCK cells on microcarriers. These medium formulations permit a culture to maintain stable pH and redox parameters without the requirement of external control systems.

Eagle (1959) considered the fate of glutamine in cell culture systems. He showed that alanine, serine, aspartate, glutamate, and proline carbons were derived, at least in part, from glutamine. A more detailed study of the endproducts of glutamine metabolism was conducted by Zielke *et al.* (1980). Working with human fibroblasts, they showed that glutamine was converted into the organic acids lactate, citrate, and malate and the organic acids glutamate and aspartate. Lanks and Li (1988) measured the rates of production of 11 compounds (organic acids and amino acids) from 13 different cell lines. With the exception of a glycolysis-defective mutant, all the cell lines produced pyruvate, lactate, alanine, proline, aspartate and citrate. Their data were consistent with a model characterized by incomplete glutamine oxidation

leading to endproduct accumulation. It was shown that most of the glucose or glutamine carbon which entered the TCA cycle was not oxidized to CO_2, but instead was released into the culture medium as a waste product. However, their experiments were performed with non-growing confluent monolayers exposed to test media for 24 hours. Consequently, they did not determine the spectrum of endproducts formed during cell growth, which might be very different from the products formed by quiescent cells. Significantly, though, their work revealed fundamental differences between various cell lines with regard to their patterns of endproduct formation. For instance, the ratio of glutamate:alanine formation was 7.2 in MRC-5 cells and 0.3 in HeLa cells. An examination of the differences between growing and resting cells in glutamine metabolism was made by Brand *et al.* (1989). They showed that the distribution of ^{14}C-labelled glutamine into glutamate, aspartate, alanine, pyruvate, lactate, and CO_2 by primary rat thymocytes was altered substantially when the cells were stimulated into growth by Con A. Overall rates of glutaminolysis increased almost tenfold by growth stimulation. In addition, they examined tumorigenic lymphoblastoid cell lines and found more than double the overall rate of glutaminolysis that they had observed with the thymocytes. Working with isolated tumor cell mitochondria, Moreadith and Lehninger (1984) demonstrated that the amino group of glutamic acid is transferred by alanine aminotransferase (E.C. 2.6.1.2) to pyruvate, yielding alanine and oxoglutarate. Under conditions of pyruvate (or malate) deprivation, the amino group from glutamic acid was transferred to oxaloacetate by aspartate aminotransferase (E.C. 2.6.1.1), yielding aspartate and oxoglutarate. Thus, in this model system, they demonstrated that the

21

endproducts of glutamine oxidation were dependent on what amino group acceptor was available.

Ever since Reitzer *et al.* (1979) showed that glutamine is a major energy source in cell culture, others have been extending their observations. Sumbilla *et al.* (1981) compared the rates of oxidation of glutamine, glucose, ketone bodies, and fatty acids by human diploid fibroblasts. Examining cells during log-phase growth, they found that the rates of glutamine oxidation were two orders of magnitude higher than the rates of oxidation of the other substrates. A comparison of the relative efficiencies of glucose and glutamine as energy sources was made by Barbehenn *et al.* (1984). Working with pigmented epithelial cells, they were surprised to find that glucose was required to incorporate leucine, in light of Reitzer's and Zielke's reports of the efficiency of glutamine utilization. They also reported that glucose inhibits the oxidation of glutamine. This finding agreed with Zielke *et al.* (1978), who reported that human fibroblasts could use either glucose or glutamine alone for energy, but glucose inhibited glutaminolysis whenever both substrates were present. Finally, Reed *et al.* (1981) showed that glutamine could serve as a precursor to saponifiable (fatty acids) and non-saponifiable (sterols) lipids in human diploid fibroblasts. Thus, studies from many laboratories over the course of two decades have shown that glutamine is a direct precursor for a wide variety of metabolites, including amino acids, organic acids, nucleic acids, lipids, and CO_2. Because of its central role in cellular metabolism, glutamine has come to be recognized as a key parameter in the development of cell culture media and process design.

D. The Search for Unifying Paradigms

The realization that glutamine is used as a primary energy source led to efforts to develop paradigms which could take advantage of these findings. These paradigms would be useful to design new processes from a rational perspective. Some of the metabolites of glutamine, like lactate and ammonia, are toxic to the cells at some concentrations. Other metabolites, such as alanine and aspartate, are relatively benign. Some combination of medium design and perfusion rate is sought which can minimize the formation of harmful metabolites while at the same time maximize the formation of cell-derived product. This requires a detailed consideration of the metabolic sources of cellular energy metabolism. A way to study this is to determine the specific uptake rates of compounds which enter energy yielding metabolic pathways. Thilly *et al.* (1982) measured the rates of amino acid uptake or formation glucose/lactate rates, and ammonia formation rates using MDCK cells in batch microcarrier culture. Through an analysis of all these rates, they offered an attempt to integrate amino acid and carbohydrate metabolism in culture. Glacken *et al.* in 1986 inferred the specific ATP production rates of MDCK and FS-4 cells in batch culture by measuring lactate production and oxygen uptake. In order to determine how much energy was being yielded by each pathway, they assumed a value for ATP yield from the oxidation of glutamine as well as the ATP yield for glycolysis. However, their measurements were for a batch culture, with the subsequent rapidly varying concentrations of nutrients and wastes. Moreover, they inferred the glutamine energy flux by the lactate, ammonia, and glutamine concentration data. It is quite possible that glutamine metabolism in their experimental

23

system produced endproducts from glutamine metabolism other than lactate. A more thorough knowledge of overall uptake and excretion rates for a wider variety of metabolized compounds will enable a more precise calculation of cellular energy demands, and thus provide the information needed to impedance match the bioreactor design to the cells genetic potential. Furthermore, it is critical to examine cell culture systems under transient conditions as well as at steady-state to elucidate the full range of behaviors which mammalian cells exhibit.

E. Perfusion Culture and Cell Separation Technology

1. Cell Culture Kinetics

In a batch culture, the cells will continue dividing until the critical component in the medium is exhausted, or the concentration of a metabolic endproduct reaches toxic levels, or both. During the growth phase the cells rapidly change the chemical composition of the medium. However, it can take the cells hours or days to respond to a change in their environment. Consequently, measurements made of the behavior of the cells growing in batch culture to any particular environment actually reflect the response of the cells to some previously existing environment. Microbiologists long ago solved this problem with the invention of the chemostat. By continuously diluting a constant volume system with a nutrient solution, a steady-state is attained wherein the growth rate of the cells equals the dilution rate. Since the system is at steady-state, the behavior of the cells properly reflects the environment. The process of constantly diluting the contents of a cell culture bioreactor is called perfusion.

An understanding of the mathematics of continuous culture is necessary to properly interpret experiments. For a simple chemostat lacking cell recycle, a mass balance on cells gives:

$$\frac{dX}{dt} = (\mu - \frac{F}{V})X \qquad (1)$$

where X = cell concentration (cell/cm^3),

μ = specific growth rate (hr^{-1}),

F = medium flow rate (cm^3/hr),

V = bioreactor volume (cm^3), and

t = time (hr).

The factor F/V describes the dilution rate of the system, and is represented by the symbol D. At steady-state,

$$\frac{dX}{dt} = 0$$

so

$$\mu = D.$$

This is the principle upon which a chemostat operates. By selecting an appropriate dilution rate (D), the operator can directly control the growth rate of the cells. However, for mammalian cell culture, the relatively slow growth rate of the cells (doubling times > 12 hours) precludes high dilution rates in

order to prevent washing out of cells (when $D > \mu_{max}$). Cell recycle permits dilution of the system at much higher rates.

Early perfusion cultures for mammalian cells were described by Pirt and Callow (1964). Working with 100 ml culture vessels, they found that the steady-state cell density declined with increasing dilution rate, presenting data to show a steady decline in steady state cell densities in a chemostat as the dilution rate was increased from 0.4 to 0.9 volumes/day. They used the steady-state culture vessels to investigate the lot-to-lot variation in animal sera, the effect of pH, and cell washout kinetics. Semicontinuous perfusion was used by Sinclair (1966) to study the metabolism of mouse L cells in chemically defined medium. Like Pirt and Callow, Sinclair found a decrease in steady-state cell density with increasing perfusion rate. As the dilution rate was increased from 0.15 volume/day to 0.45 vol/day (apparent doubling times from 111 to 37 hours), steady-state cell densities fell from 2.0 to 0.4×10^6 cell/ml. He measured the residual concentrations of arginine, tyrosine, lactate, and glucose at different steady-states to examine the effect of the cell's growth rate on uptake rates.

The cell concentrations maintained at steady-state in these simple chemostats were typically below 2×10^6 cell/ml. This maximum cell density is related to the theoretical yield of cells from some limiting medium component. Pirt (1965) described a theory of continuous culture in which the cells consumed some substrate at a constant 'maintenance' rate to maintain cell functions, plus a variable rate to make new cell mass. A mass balance on substrate yields at steady state:

$$D(S_0 - S) = X\left(\frac{\mu}{Y_G} + m\right)$$

(2)

where S_0 = inlet substrate concentration (mole/l),

   S = substrate concentration in system (mole/l),

   Y_G = yield of cells on substrate (growth-related)

   (cells/mole substrate),

and m = maintenance requirement for substrate

   (mole/cell-hr).

Monod (1942) described a generalized relationship between limiting nutrient concentration and the cell's growth rate in terms of a saturable function:

$$\mu = \frac{\mu_{MAX}S}{K_S + S}$$

(3)

where μ_{MAX} = the maximum possible growth rate (hr^{-1}),

and K_S = the concentration of substrate giving

half-maximal growth (mole/l).

Under these conditions, μ is controlled by the availability of nutrients according to equation 3. Assuming a Monod-type dependency on the growth rate to the limiting substrate, Pirt solved for X, yielding:

$$X = \frac{DY_G}{mY_G + D} \left(S_0 - K_S\left(\frac{D}{\mu_{MAX} - D}\right)\right)$$

(4)

Equation 4 predicts that the cell concentration in a simple chemostat will fall with increasing dilution rate, decreasing to zero at $D = \mu_{MAX}$. The fundamental problem is that mammalian cells have an inherently slow growth rate. Typical doubling times run from 12 to 36 hours. Consequently, cell washout occurs at relatively low dilution rates. If the maintenance energy requirement is ignored, then the growth yield becomes the observed yield Y_{obs}, which reduces equation 4 to:

$$X = Y_{obs} \left(S_0 - K_S\left(\frac{D}{\mu_{MAX} - D}\right)\right)$$

2. Cell Recycle Systems

A technique which is effective in raising the cell concentrations and dilution rates in continuous culture is cell recycle. By recycling cells, fresh medium can dilute the bioreactor much faster than the cells are diluted. This provides the opportunity to grow cells at densities far higher than can be achieved by an ordinary chemostat. The separator acts as an internal partial cell recycle device. The separation efficiency, ε, is defined as the ratio of cell density exiting the bioreactor to the cell density within the bioreactor. ε, therefore, ranges in value from zero to one, with values closer to zero indicating improved retention. Since dead cells are smaller than live cells, and hence have a slower settling velocity, they are removed with a higher efficiency than are live cells. The separation efficiencies for total, viable and dead cells are designated ε_T, ε_V, and ε_D, respectively.

The differential equation for the growth and removal of the viable cells is:

$$\frac{d\,X_V}{dt} = (\mu - \alpha)\,X_V - \varepsilon_V\,D\,X_V \tag{5}$$

where X_V = viable cell density (cell/cm^3),

    μ = specific growth rate (hr^{-1}),

α = specific death rate (hr^{-1}),

ϵ_V = separation ratio for viable cells (dimensionless),

D = system dilution rate (hr^{-1}),

and t = time (hr).

The creation and removal of dead cells is described by:

$$\frac{d\,X_D}{dt} = \alpha\,X_V - \epsilon_D\,D\,X_D \qquad (6)$$

where X_D = dead cell concentration (cell/cm^3),

and ϵ_D = separation ratio for dead cells (dimensionless)

At steady-state, the concentrations of viable and dead cells reflect a balance between the growth and death of the viable cells and the removal rates for both kinds of cells. These removal rates, in turn, depend on the dilution rate of the system and the efficiencies of cell removal through the separator.

Since the diameter of cells decreases when the cells lose viability, their terminal settling velocity V_T also decreases. In the cell culture experiments described below, the efficiency of cell retention was separately determined for

31

viable and non-viable cells. These efficiencies are measured by using a vital stain (Trypan blue) and enumerating viable and dead cells both within the bioreactor and in the exit stream.

In order to recycle cells, some means must be found to separate the cells from the medium. This is much simpler for attached cells than for suspended cells. Merten (1987) has reviewed existing technologies for mammalian cell separation. Cells attached to a surface of the bioreactor remain in place when the liquid is removed. Cells grown on the surface of microcarriers, which are themselves suspended in liquid, were retained using a vertical settler by Butler *et al.* (1983). As the liquid in the bioreactor is removed through the vertical settler, the upward velocity of the liquid is less than the downward terminal settling velocity of the microcarriers. Consequently, the liquid stream emerging from the bioreactor is free of microcarriers, and the cells remain in the bioreactor. The advantages inherent in this kind of perfusion apparatus was made clear by the authors, who noted a four-fold increase in the maximum cell density attained, even though this was not a chemostat culture. The maximum cell density reported was about 9×10^6 cells/ml. Because of the limited surface area available in a microcarrier system, the cells must eventually stop dividing. Hence, even with perfusion, all microcarrier cultures (and, indeed, all attached cell cultures) are batch.

One of the first recycle perfusion systems for mammalian cells was the spin filter, described by Himmelfarb *et al.* (1969). They immersed a stainless steel mesh supporting a membrane filter in the culture vessel and rotated it at 200 to 300 RPM by bottom attached stir bars. As they withdrew medium from the interior of the filter, cells were excluded from the surface of the filter by

the centripetal forces imposed by the filter's rotation. The filter had a 3.0 μm pore size, which also served to exclude cells. By perfusing the bioreactor system at 5 to 6 volumes/day, they achieved steady-state cell densities of around 4 to 5×10^7. However, after two weeks, the filters always became clogged, ending the culture. Using a similar device in a 40 liter system, Tolbert *et al.* (1981) reported that the yield of cells from medium was three to four times higher in perfusion mode than in unfed batch mode. This increase in yield is a frequently observed advantage with continuous perfusion. Improvements recently reported in spin-filter technology by Avgerinos *et al.* (1990) permitted long-term culture (31 days) with viable cell densities of 6-7 $\times$ 10^7 cells/ml. These cells spontaneously formed huge clumps, 200 to 300 μm diameter. This large clump size allowed Avgerinos *et al.* to use a 100 μm filter, reducing the problems of clogging.

Clogging is a frequently observed difficulty inherent in spin filters technology. The fact that the filter is within the perfusion vessel precludes its replacement during the culture. External filters can be used to separate cells from the suspending medium, but this entails mechanically complex plumbing systems to remove the cells from the bioreactor, concentrate them, and return them to the reactor. Tolbert *et al.* (1988) recently described the use of such a device in a large-scale pharmaceutical production system. An external filtration unit was connected to a 100 liter bioreactor, which was perfused at 0.5 to 1 volume/day. Since the external filter unit could be aseptically replaced when needed, production runs averaged 90 days. The filtration unit consisted of a supported membrane filter with an agitator on the cell side to reduce membrane clogging.

Tangential flow filtration, in which the liquid to be filtered is caused to flow at a right angle to the membrane, has the advantage of reduced clogging. The tangentially flowing liquid continuously sweeps the membrane surface clean as the liquid passes across the membrane. Velez *et al.* (1989) used a 10 in^2 0.2 μm nylon membrane sandwiched between a channel plate and a filtrate plate. The 1.5 liter fermentor was perfused at 0.8 volumes/day and achieved 2.1×10^7 viable cells/ml. Unfortunately, the filtering system failed to remove any cells, even dead ones, so with time, the concentration (and fraction) of dead cells increased. A pump connected to the filter failed after nine days, terminating the culture. This failure illustrates the hazards connected with external cell recycle systems.

A centrifuge was used to separate cells by Hamamoto *et al.* (1989). They removed cells from their 3 liter culture and centrifuged them in small batches. After 30 minutes at $100 \times g$, the pelleted cells were resuspended in a small volume and returned to the bioreactor. By performing this operation repeatedly, they were able to achieve 10^7 hybridoma cells/ml with 2.1 vol/day perfusion. Cultures were maintained at steady-state in this condition for 30 days.

3. Sedimentation Separation

Perfusion mammalian cell systems have a common requirement for cell separation. When cells are grown to high density, the perfusion flow rate

34

must be proportionally high, often reaching 4 volumes per day or more. The problem to be solved in the design of efficient cell separators is how to separate the medium from the cells with a minimum loss of cell viability. In addition, the design of a cell separation system must provide for a steady removal of cells (both alive and dead) from the bioreactor in order to achieve a dynamic steady state.

Sedimentation has long been used to separate different cell types. A detailed review of the subject is provided by Pretlow and Pretlow (1982). The force field used to effect separation can be either gravitational or centrifugal. Bertoncello (1987) compared the cell separations achievable by either technique, but these are designed to separate different target cells amongst a complex biological tissue mix. Vertical tubes, tilted tubes, and funnels have been used to separate cells for mammalian cell bioreactors.

3.1. Vertical Tube Separators

Microcarrier-based bioreactor perfusion systems use a simple system to separate the cells. Since microcarriers are fairly large (typical microcarrier diameters average 165 microns, compared to a cell diameter of 12 microns), their settling velocity is orders of magnitude faster than that of cells. The settling velocity is fast enough that they can settle inside a vertical tube used to remove spent medium, provided that the tube is of sufficiently diameter for the medium flow rate. Butler *et al.* (1983) described a perfusion system for MDCK cells grown on microcarriers using a vertical tube to separate the microcarriers from the perfusate stream. They achieved 9×10^6 cells/ml

perfusing at 2.9 volumes/day. The vertical tube represents the simplest kind of internal sedimentation system.

The terminal velocity with which a particle in a viscous fluid will settle is based on a balance between gravitational accelerational forces and fluid viscous drag forces. One can calculate the terminal velocity with a simple formula if the velocity is very small. In such a flow regime, "creeping flow" effects predominate, and the terminal velocity is found by:

$$V_T = \frac{d_p^2 \Delta \rho g}{18 \mu}$$

(7)

where V_T = terminal velocity (cm/s),

   d_p = particle diameter (cm),

   $\Delta \rho$ = density difference (particle-fluid) (g/cm^3),

   g = gravitational acceleration (981 cm/s^2),

and μ = fluid viscosity (g/cm-s)

To calculate the terminal velocity of cells, we must make estimates of the cell's density and diameter, as well as the fluid viscosity and density. In the calculations to follow, I have assumed a cell diameter of 12 microns, a density difference of 0.05 g/cm^3, and a viscosity of 0.01 g/cm-s. Therefore, the settling velocity of a 12 micron cell is about 3.9×10^{-4} cm/s.

For laminar flow in a circular conduit, the fluid velocity field as a function of radius is given by the Hagen-Poiseuille equation:

$$V(r) = V_{max} \left(1 - \left(\frac{r}{R}\right)^2\right) \tag{8}$$

where $V(r)$ = fluid velocity as a function of radius (cm/s),

V_{max} = twice the average velocity (flow/area) (cm/s),

and R = the inner radius of the conduit (cm).

This equation describes a parabolic velocity distribution, wherein the velocity is maximum at the center and zero at the walls. Whether or not a particle will be retained in a vertical pipe depends on whether the maximum velocity at the center is greater or lesser than the particle's terminal settling velocity. All of those particles whose settling velocity is greater than V_{max} will be retained. However, not all particles whose settling velocity is less than V_{max} will be lost. If by random chance a small cell enters the vertical pipe *near the edge*, it may not rise if the *local* upwards fluid velocity is too small. Consequently, only a fraction of cells of a given size will be lost. We can calculate the fraction of cells which will be lost in a vertical pipe by first determining the radius at which the upwards fluid velocity equals the cell's terminal settling velocity:

37

$$r_c = \sqrt{1 - \frac{\pi R^2 V_T}{2 Q}}$$

(9)

where r_c = the critical radius for particle capture (cm) , and

Q = the volumetric flow rate (cm^3/s).

Then we calculate what fraction of the total flow occurs within an inner concentric cylinder of radius r_c:

$$Q_c = \int_0^{2\pi} \int_0^r V(r)\, r\, dr\, d\theta = \frac{4Q}{R^2}\left(\frac{r^2}{2} - \frac{r^4}{4R^2}\right)$$

(10)

When Q_c is divided by the total flow rate, we have the fraction of flow through the pipe which carries out cells:

$$\varepsilon = \frac{Q}{Q_c} = \frac{4}{R^2}\left(\frac{r^2}{2} - \frac{r^4}{4R^2}\right)$$

(11)

where ε = the fraction of cells lost out the pipe.

38

Substituting equation 9 into equation 11 and simplifying, we obtain the expression to estimate the retention of cells as a function of cell settling velocity, flow rate, and tube radius:

$$\varepsilon = 1 - \left(\frac{\pi R^2 V_T}{2 Q}\right)^2 = 1 - \left(\frac{V_T}{V_{max}}\right)^2 \tag{12}$$

3.2 Tilted Tube Separators.

A tilted pipe represents an improvement over a vertical one. Whereas the efficiency of separation in a vertical pipe for a given flow rate is only a function of the diameter of the pipe, a tilted pipe's efficiency can be improved either by increasing the diameter *or* the length of the pipe. A sufficiently long pipe can always clarify a suspension so long as the hydrodynamic flow regime is laminar. For microcarrier systems a tilted pipe can easily provide an absolute degree of microcarrier retention. Nahapetian *et al.* (1986) used a tilted tube sedimentation system to perfuse cultures of Vero cells on microcarriers. They achieved 3×10^7 cells/ml at a perfusion rate of 4 volumes/day. In practice, although internal tilted pipes are effective for the clarification of microcarrier suspensions, they are inadequate for the separation of cell suspensions, since the required length can exceed several meters.

To examine why this should be so, consider a particle suspended in fluid rising in a tube tilted at an angle θ from the vertical axis. The accelerational force due to gravity pulls the particle at an angle from the axis

of the center of the tube. There is a component of that force in the axial direction and a component in the radial direction. The axial component serves to retard the rise of the particle, whereas the radial component moves the particle steadily in the radial direction toward the bottom surface of the tube. The cross-flow velocity of the particle is constant, $V_T \sin(\theta)$. Knowing the diameter of the tube and the radial velocity, one can easily calculate the time taken for the particle to cross the tube of diameter δ:

$$\tau = \frac{\delta}{V_T \sin(\theta)} \tag{13}$$

where τ = the time for a particle to cross the tube (s),

and δ = the diameter of the tube (cm).

The net axial velocity is the difference between the the fluid axial velocity (taken from equation 8) and the axial component of the particle's terminal velocity, $V_T \cos(\theta)$. By combining these expressions into an integral form one can determine the length required to capture all particles of a given size:

$$L = \int_0^\tau \left[V_{max}\left(1 - \left(1 - \frac{2t}{\tau}\right)^2\right) - V_T \cos(\theta) \right] dt \tag{14}$$

where   L = the tube length needed to capture all particles.

This can be integrated to give the final expression for the length of tilted tube required to capture all particles of a given size:

$$L = \frac{2}{3} \delta \frac{V_{max}}{V_T \sin(\theta)} - \delta \cot(\theta) \tag{15}$$

Equation 15 permits the rational design of tilted tube settlers based on the hydrodynamics of single particle capture. When a suspension containing many particles, such as a cell culture broth, is to be clarified with a tilted tube, the actual capture efficiency is considerably improved over what equation 15 would predict. The efficiency of tilted tube settlers is greatly increased by what is known as the Boycott effect. The physician Alexander Boycott (1920) observed that "when ... blood is put to stand in narrow tubes, the corpuscles sediment a good deal faster if the tube is inclined than when it is vertical." The explanation for this effect is provided by Hill *et al.* (1977), who described enhanced sedimentation due to settling convection. As the particles collect on the lower surface of an inclined chamber, the local fluid density in the vicinity of the particles is increased. This increased density induces a convection current down the slope of the chamber, driving the particles to the bottom. At the same time, a clarified zone is created along the upper surface of the chamber. Due to the absence of particulates in the clarified zone,

the local fluid density is decreased, which induces an upward current of clarified fluid. Therefore, the presence of the particles in an inclined chamber induces convection currents which speed up the separation process.

3.3 Conical Separators

In an effort to internalize cell recycle, Sato et al. (1983) developed a cell sedimentation system based on a cone. They inserted a long, tapered cone into the perfusion vessel and removed liquid out the top as fresh medium was pumped into the vessel. Because of the cone's taper, its cross-sectional area increased with increasing height. Consequently, the velocity of the upward-flowing liquid decreased with increasing height. At some point in the cone, the liquid velocity is below the settling velocity of the cells, and they settle out onto the inner surface of the cone. The concentrated cells gently slide down the inner surface of the cone and are returned to the bulk of the culture. This system has the great advantage of achieving cell separation without moving parts. The cells are exposed to very gentle shear forces, and no external flow loops are needed. Unfortunately, in order to achieve adequate settling, the height of the conical section is up to ten times the height of the culture, thereby reducing the working volume within the fermentor to the bottom third. By perfusing the system at 2 volumes/day, their 500 ml vessel achieved 7×10^6 hybridoma cells/ml in serum-free medium. Tokashiki et al. (1988) placed the entire culture within the settling chamber. A culture vessel with a 1.2 liter volume was surrounded by a 90 cm^2 annular settling zone. Perfusion with 4 volumes/day yielded 10^7 cells/ml over 30 days of culture. Kitano et al.

(1986) developed an external cell precipitator for perfusion cultures. Like Sato's system, this device uses a tapered conical sedimentation chamber. However, this settler is situated above the culture vessel, with a long diptube reaching down to the liquid below. The cells migrate up the diptube with the removed perfusate and sediment on the walls of the cone. As the cells slide back down the cone, they enter the diptube. However, the concentrated cells are now all at the extreme inner wall surface of the diptube, and hence are able to slide past the upwards flowing medium to re-enter the culture vessel. The authors needed to add a water jacket to the settler to avoid convection currents from disturbing the sedimentation. They were able to maintain hybridoma cells at 4×10^6 viable cells/ml for 40 days with 0.7 volumes/day perfusion. Presumably, at faster perfusion rates the cells were washed out of the settler.

A common difficulty with simple conical cell separators lies in the fact that laminar flow in a diverging cone cannot be maintained. To understand the problems inherent with conical sedimentation systems, it is necessary to study the fluid dynamics of flow in a cone. Although diverging fluid flow in a wedge shaped region has been understood since Hamel (1916) published a solution, diverging fluid flow in a cone remains unmodelled. Langlois (1964) presented a dimensional analysis which shows that radial flow cannot be obtained in a cone. Eddy currents invariably appear in conical flow, and the position of these eddies depends on the flow rate: "...as the source gets stronger, the eddies are blasted farther and farther out from the origin." Consequently, as the perfusion rate is increased in a bioreactor system

equipped with a conical settler, the increasing scale of eddy currents disrupts the laminar flow upon which the separation critically depends.

3.4 Nested Conical Separators

To improve on the Sato design, I developed a cell separation system which utilizes a series of nested cones. By placing one cone inside another, I created a region between them consisting of an annular space which increases in cross-sectional area with increasing height. Thus, the principle of decreasing fluid velocity with increasing height is preserved. However, by nesting the cones, true laminar flow is possible, and an analytical solution to single particle capture has been developed. Figure I-1 shows the design of the nested cone cell separator.

Figure I-1.

Nested Cone Cell Separator
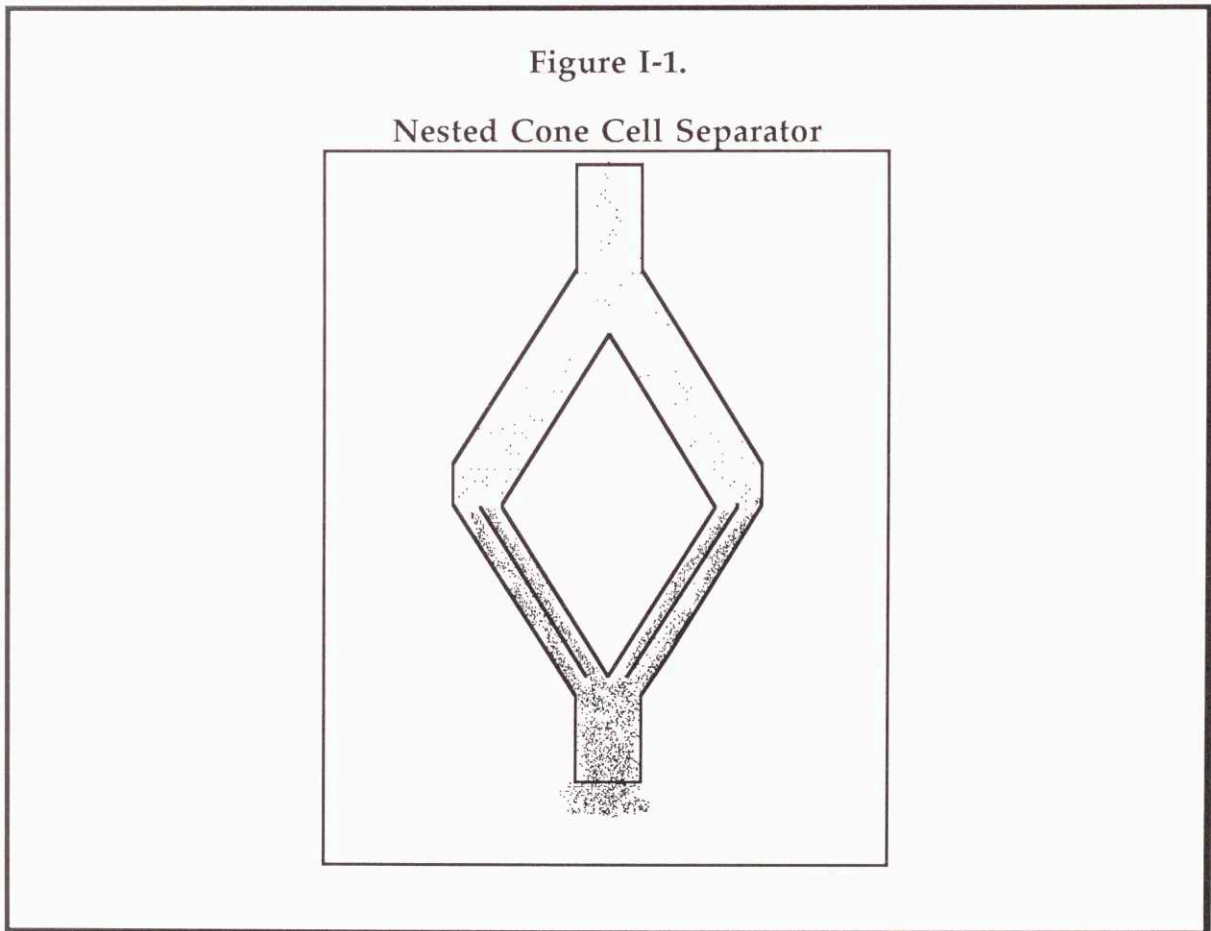
The analysis of particle capture dynamics in nested cone separators is possible if a number of simplifying assumptions are made. The theoretical fluid velocity profile between a pair of infinite planes is parabolic if the fluid is Newtonian and the flow regime is laminar. I assumed that in a nested cone separator, the fluid radial velocity distribution function is also parabolic. For this geometry the differential equation relating the position of a particle to its axial velocity is:

$$V_Z = \frac{dZ}{dt} = \frac{Q}{\pi \, \delta \, Z \, \sin(\theta)} \left[1 - (1 - \frac{2t}{\tau})^2 \right] - V_T \cos(\theta) \tag{16}$$

where V_Z = fluid velocity parallel to cone surface (cm/s),

δ = separation distance between parallel cones (cm),

and Z = distance from apex of cone (cm).

This nonlinear first-order differential equation has terms in Z and t, and is not readily separable. It was evaluated by numerical integration to assess the effects of changing the gap spacing δ, angle θ, flow rate Q, and particle size (since $V_T = f(d_p)$ via equation 7). The integration was performed using Euler's method:

46

$$Z(n+1) = Z(n) + \frac{dZ}{dt} \Delta t \tag{17}$$

where $Z(n) =$ z-axis position of particle at time n (cm),

and $Z(n+1) =$ z-axis position of particle at time n+1 (cm).

Since the velocity of a particle in the direction perpendicular to the flow is constant ($V_r = V_T \sin(\theta)$), the time taken for a particle to cross the gap δ is equal to τ:

$$\tau = \frac{\delta}{V_T} \sin(\theta) \tag{18}$$

One can integrate equation 17 using increments of time from t=0 to t=τ. By integrating both the axial and radial axes, one can determine the trajectories of particles between the parallel conical surfaces. Then, assuming that the velocity distribution in the radial axis is paraboloidal, equation 17 can be used to estimate, for a given cell size and flow rate, what fraction of cells can escape the separator. Figure I-2 shows the calculated values of epsilon for 11 micron cells at different perfusion rates when equation 17 was integrated numerically using a BASIC program (See Appendix I). A gap (δ) between conical surfaces of 0.5 cm, a bioreactor volume of 250 ml, and a half angle of 30° were used in the calculations.

Figure I-2.

Particle Capture Efficiencies for 11 Micron Cells in 250 ml Bioreactor
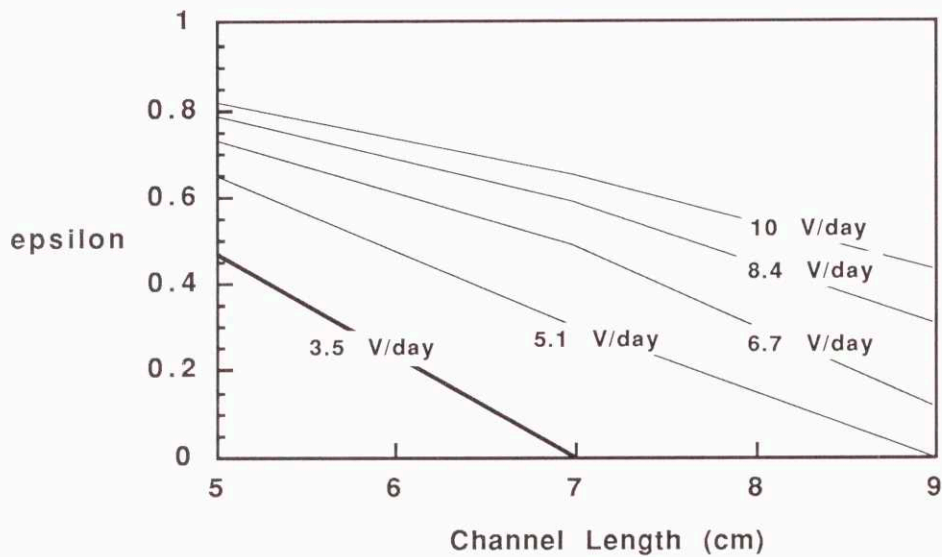
Figure I-2 shows that as the perfusion rate increases, a given separator (fixed L) will lose an increasing fraction of cells. Similar calculations for different size cells (Figure I-3) at 5.1 volume/day show that smaller cells will be preferentially removed from the system, while larger cells will be retained at even higher flow rates. Figure I-3 shows that a 9 cm long channel will retain all cells of 11 μ or greater, while losing a large fraction of cells whose diameter is 9 μ or less. Since a cell generally shrinks when it dies, a cell

48

separator operating under the conditions described above can be expected to show good viability. This kind of cell separator will remove dead cells preferentially, permitting long-term continuous operation without the buildup of dead cells which plagues so many alternative cell recycle systems.

These calculations assume a single channel device such as that shown in figure I-1. Additional cones can be constructed so as to create multiple parallel channels, significantly increasing the throughput of a given separator. Changing the angle θ that the sides of the conical section make with respect to the vertical has an interesting effect. As θ is changed from a small value (long narrow cone) to a high value (short squat cone), the required outer diameter of the separator remains constant. The length of the channel increases, but that effect is counterbalanced by the ever widening angle. The total surface area of the bioreactor headspace remains constant as θ varies. In actual practice, the Boycott effect will probably dominate angle considerations. The settled cells must slide down the lower surface of the separator in order to be returned to the culture.

Figure I-3.

Particle Capture Efficiencies for 5 Vol/day 250 ml Bioreactor
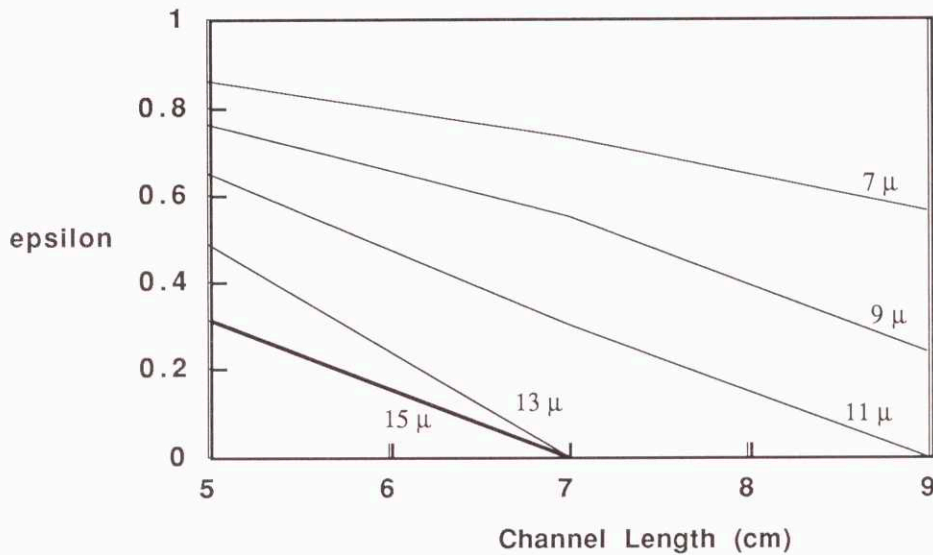
All these calculations apply only to very dilute cell suspensions. As the cell density increases, the Boycott effect described earlier plays an increasing role in determining particle capture efficiencies. Since the Boycott effect serves to augment sedimentation, the actual performance of nested cone separators is substantially better than figure I-2 would indicate. The effect of separator performance on steady-state cell concentrations is discussed in Section II-A.

Through the development of a variety of cell separation techniques, researchers have been able to perfuse mammalian cell cultures at rates adequate to support cell densities above 10^7 cells/ml. The cultures described were maintained at steady-state for periods of weeks, permitting the kind of metabolic studies that are required to understand the biochemical dynamics of cells at high density. It is through the use of these high density perfusion cultures to manipulate the cells' environment that we are able to separate the effects of stress due to nutritional limitation from stress due to waste product limitation and study each stress independently.

II. Experimental Techniques

A. Cells and Perfusion Culture System.

The Sp2/0 cell line, described by Köhler *et al.* (1976), is a murine-murine hybridoma which secretes no detectable antibody. Because of its non-secretion property, it is suitable for use as a fusion partner to create hybridomas and as a plasmid recipient to create transfectomas, since the resultant secreting clones must derive the antibody's specificity from the fusion partner or plasmid. I used for these experiments Sp2/0-based hybridoma cells which had been transfected with plasmids encoding for both heavy and light IgG chains, described by Sun *et al* (1986). The plasmids were constructed by combining murine genomic DNA fragments encoding heavy and light variable regions of a monoclonal antibody with a mammalian expression vector system containing human genomic DNA fragments coding for gamma 3 and kappa constant regions, generating chimeric antibodies of reduced immunogenicity in humans. In a preliminary clinical trial, these chimeric antibodies against gastrointestinal tumor antigens elicited an antibody response against the chimeric antibodies in only one patient out of ten (LoBuglio *et al.*, 1989), indicating the therapeutic potential of such a construct.

These Sp2/0 transfectoma cells grow in T-flasks or in small (100 ml) batch suspension cultures with a doubling time of about 18-20 hours. The peak antibody titer reached in such cultures is about 5 µg/ml, and the specific antibody productivity in batch cultures is about 0.2 pg IgG/cell-h. Cell stocks were subdivided three times per week in 75 cm^2 T-flasks using Dulbecco's

mimimal essential medium (DMEM, Gibco, Grand Island, NY) supplemented to a total glutamine concentration of 6 mM, 2 mM pyruvate, and 50 μM β-mercaptoethanol. I refer to this supplemented DMEM as DMEM*. Appendix 2 shows the complete formulation of the medium used to grow the cells. Because the cells tended to lose the capacity for IgG production over the period of several months, all perfusion experiments were performed using aliquots of cells freshly removed from the -120° C freezer.

The perfusion culture system used for these experiments was developed to achieve long-term steady-states with high viability and high cell density. Tyo and Thilly (1989) describe the performance of the system in some detail. The working volume of the bioreactors was 265 ml. Viable cell densities were typically in the range of $1 - 1.5 \times 10^7$ cells/ml. Figure II-1 shows the perfusion culture apparatus used. It incorporates a double-chambered nested cone cell separator. The internal gap in the separator was about 0.3 cm. The dimensions of the bioreactor are shown in Appendix 3. Fresh medium is pumped into the bioreactor via the medium inlet port. The waste outlet atop the separator removes a portion of the cells along with the culture broth. The entrance to the separator is a baffled Teflon section which also supports the magnetically coupled impellor. Aeration is provided by passing gas through a one meter section of expanded PTFE tubing (W. L. Gore & Associates, Elkton, MD).

The volume of the bioreactor is maintained constant by setting the waste outlet pump to a slightly higher flow rate than the inlet pump. Whenever the liquid level in the bioreactor falls below the level of the entrance to the separator, air bubbles, rather than liquid, are removed via the

separator. Although this arrangement permits adequate volume regulation, the occasional passage of an air bubble through the separator disrupts the laminar flow upon which separation depends. Thus, the outlet stream occasionally contains a temporarily elevated concentration of cells. Even though this disturbance does not interfere with the growth of the cells to high densities, it does sometimes interfere with the proper calculation of cell growth and death rates. This is because the determination of growth and death rates assumes proper knowledge of viable and dead cell densities *both* in the bioreactor and in the outlet stream.

Figure II-1.

Perfusion Culture Apparatus
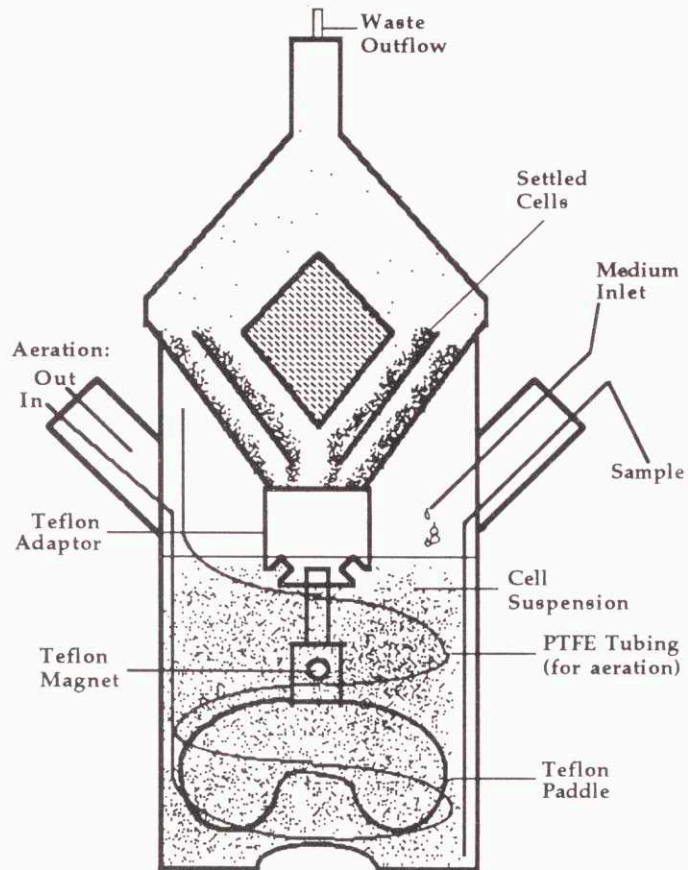
Perfusion culture experiments were initiated by inoculating the bioreactors with about 5×10^5 cells/ml taken from mid log-phase 100 ml suspension cultures. Within one or two days, as the cells began to grow, perfusion with fresh DMEM* (with 4% fetal bovine serum and without antibiotics) was begun at 1 volume/day. Depending on the experimental plan, the perfusion rate was steadily increased to a desired final value, and the cultures were allowed to achieve steady-state. After steady-state was maintained for several days, the perfusion rate or medium concentration was altered, and a new steady-state was maintained. This process was continued for up to 1,000 hours. Generally, duplicate culture vessels were used, although the 9 volumes/day with complete medium and 5 volumes/day with diluted medium experiments were conducted with single cultures.

Samples were taken from the bioreactor and outlet stream twice daily. The cell concentrations (viable and dead) were measured immediately. Cells were enumerated through the use of a Coulter counter (Coulter, Hialeah, FL) after appropriate dilution into saline solution. Cell size distributions were obtained with a Coulter counter by adjustment of the counting threshold. Particles with a size below the threshold setting are not counted. After performing a particle count at a particular threshold setting, the threshold was increased and the cells were re-counted. Three counts were made at each threshold setting and averaged. Differences in cell counts between successive settings represent the population of cells whose size falls between the two settings. The threshold settings were calibrated with monodisperse latex

spheres obtained from Coulter. Cell viabilities were determined with a hemacytometer following Trypan Blue staining. The samples were clarified by centrifugation and then stored at -20°C for later analysis.

B. Analytical Techniques

1) Enzymatic Assays

D-Glucose and L-Lactic Acid were determined using NADH-generating enzymatic reactions (Sigma, St. Louis, MO). Reaction products were measured at 340 nm using a Beckman spectrophotometer. Samples of authentic D-Glucose and L-lactic Acid (Sigma) were used to calibrate the assays. Immunoglobulin concentration data was kindly provided by C. Buser and J. Morrill. They used a sandwich-type enzyme linked immunosorbent assay (elisa) to measure IgG concentrations, calibrating with authentic samples of IgG (Jackson ImmunoResearch Labs, Inc., West Grove, PA).

2) Organic Acids

A Bio-Rad HPX-87H (Bio-Rad Laboratories, Richmond, CA) organic acid column was used to determine the concentrations of glucose, lactate, pyruvate, and pyrollidone carboxylic acid (PCA), a spontaneous breakdown product of glutamine. The column is packed with a sulfonated divinyl benzene-styrene copolymer resin and eluted in isocratic mode using 20 mM H_2SO_4 and 8% (v/v) CH_3CN. The elution buffer was run at 0.5 ml/min at room temperature. This HPLC column will interact with both ionized and hydrophobic regions of injected compounds. This separation depended on the polar/non-polar interactions of the compound between the mobile phase and the resin. Cations were irreversibly bound to the column. Consequently, since the separation was done at pH 1 to 3, all amino acids and many nucleotides remained bound to the column and were not detectable with this method.

Samples were first deproteinized by centrifugal ultrafiltration using Amicon Centrifree cartridges and ultrafiltration membranes with a cutoff of about 1000 daltons. Twenty μl of sample were injected. The output from the column was analyzed by a Hewlett-Packard Model 1090 diode array detector (DAD) coupled with a Hewlett-Packard system 9000 computer. Ultraviolet spectra from 190 to 300 nm wavelength were taken every 3.5 seconds and stored for later analysis. In this range of wavelengths, carbohydrates and organic acids are easily detected and quantified.

Figure II-2 shows a typical chromatogram produced by this technique. On it one can see peaks corresponding to salts, glucose, pyruvate, lactate, glycerol (derived from the deproteinizing membrane), and PCA. A few other peaks were identified at high wavelength (thymidine, uracil, uridine, and uric acid), but since they arise from the fetal bovine serum used as a medium supplement and seem not to be consumed by the cells, they were not pursued. Due to the 48 hour pre-incubation of the medium at 37° C to test for sterility, PCA levels in the medium entering the bioreactor were often as high as 2 to 3 mM, a concentration exceeded only by glucose and glutamine. The medium exiting the bioreactor had considerably lower PCA concentrations. Uptake rates for PCA were, therefore, quite substantial.

Figure II-2.

Organic Acid HPLC Chromatogram of Bioreactor Sample
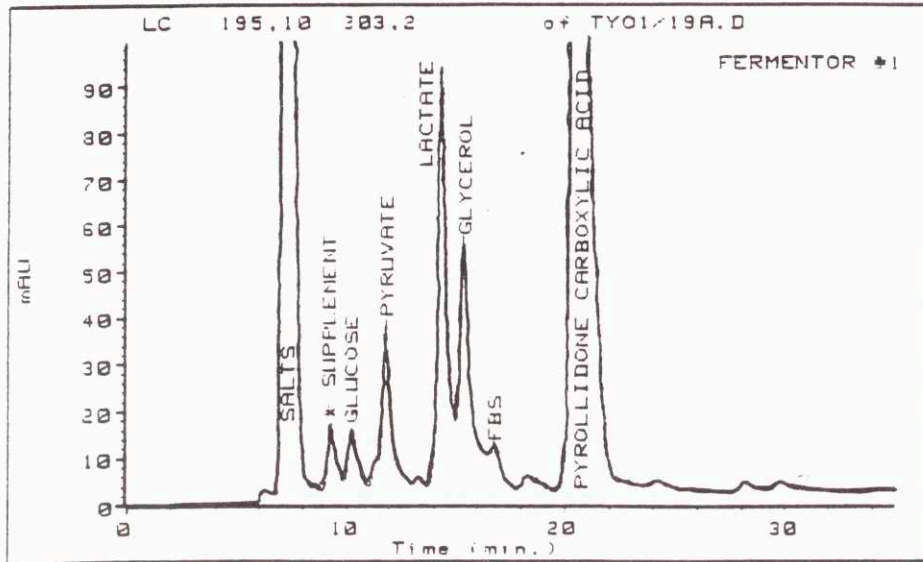
Data from chromatograms such as these were used to calculate concentrations of organic acid metabolites in the bioreactor samples and in the medium. To facilitate the calculation of concentrations, the early peak resulting from inorganic salts was used as an internal standard for the evaluation of injection volume, since its concentration was constant in the samples. Because the 20 μl injection syringe had excellent reproducibility, very little correction was usually necessary.

3) Organic Bases

To provide data in order to evaluate the metabolism of organic bases, I injected culture broth samples into a Bio-Rad HPX-87O Organic Base HPLC column. Like the organic acid column, this column is also packed with a divinyl benzene-styrene copolymer resin, but the organic base column is derivatized with a quaternary ammonium group. This permits separation of eluted compounds based on ionic and hydrophobic characteristics. Because I eluted the column with a solution of 0.25 M $(NH_4)_2SO_4$ at pH 6.0, acidic, neutral, and basic compounds were all recovered and analyzed on the HP 1050 diode array detector. This column served mainly to act as a check on the accuracy of other techniques, since there were no compounds detectable on this system which could not be measured with some other system. Figure II-3 shows a typical chromatogram obtained following the injection of 20 µl of deproteinized bioreactor sample. Lysine, glutamine, methionine, lactate, phenylalanine, PCA, and tyrosine all gave well-resolved peaks. Because the samples were injected automatically in auto-inject mode, correction for injector volume was unnecessary.

Figure II-3.

Organic Base HPLC Chromatogram of Bioreactor Sample
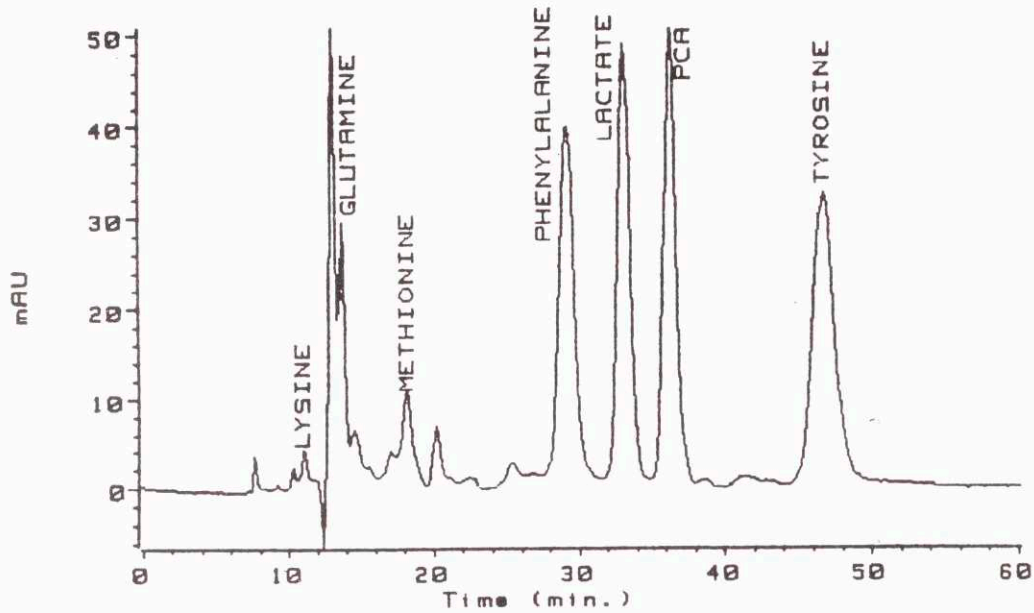
4) Amino Acids

Because of the central importance of amino acids in this research program, I used a technique specifically tailored to their analysis. In order to improve spectroscopic detection of amino acids, they are usually coupled covalently with a derivatizing agent. A wide variety of both pre- and post-column derivatization techniques are in use. I selected the technique of preinjection reaction with 4-N,N-dimethylaminobenzene-4'sulfonyl chloride (DABS-chloride) because the dabsylated amino acids formed are stable for

months when stored at -20° C. Consequently, one can derivatize many samples simultaneously with standarized conditions and analyze the reaction products later. The method of DABS-Cl was first reported by Chang *et al* (1983). The reactant, DABS-Cl, is shown in figure II-4.

Figure II-4.

Structure of DABS-Chloride

4-N,N-dimethylaminoazobenzene-4'sulfonyl chloride
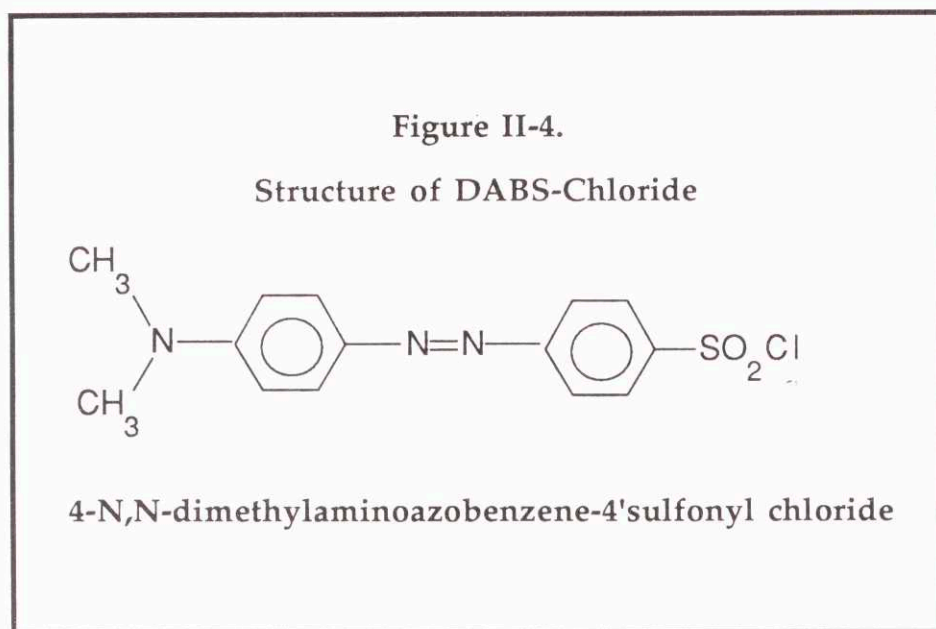
To prepare samples for injection, 20 µl of deproteinized sample was added to 70 µl of 200 mM NaHCO3 buffer (pH 9.0) and 10 µl of 1 mM ornithine (internal standard). To this mixture was added 100 µl of 15 mM DABS-Cl in acetone. The DABS immediately precipitated, but re-dissolved upon warming of the solution to 70° C. The solution was allowed to react for 15 minutes at that temperature in a sealed vial. The reaction was quenched by the addition of 0.3 ml of 40 mM pH 6.5 citrate buffer:Ethanol, 1:1 and then centrifuged for 5 minutes at 5000 RPM. The reaction products were either

injected immediately or stored at -20° C until needed. Included in each lot of reaction vials was one vial with amino acids standards. Each lot was calibrated using its own amino acid standard vial. 20 ml of the reacted samples was injected into a Beckman Ultrasphere™ (octadecylsilane bonded silica) column and eluted with a gradient of increasing CH_3CN and decreasing citrate buffer, pH 6.5, both containing 4% dimethylformamide. Slowly advancing the gradient over a period of 75 minutes gave good resolution of the amino acids.

The pattern of amino acid elution obtained using this technique is shown in figure II-5. Peaks were identified by injection of individual dabsylated amino acid standards. Peaks labeled with an asterisk arise from reaction products, and do not represent amino acids. Several amino acids eluted later in the chromatogram and are not shown on this figure.

Although all 20 proteinogenic amino acids were detectable with this technique, some peaks were resolved better than others. For instance, the methionine peak immediately preceded isoleucine. As the columns aged, the separation between these two peaks degraded. Since methionine was present in the fresh medium at 200 µM, while isoleucine was present at 800 µM, the larger isoleucine peak sometimes overlapped the methionine peak. When this occurred, the column was cleaned and regenerated, and the sample re-injected to give a clean methionine peak. Similarly, tryptophan, cystine, histidine, glutamate, and aspartate were determined with less accuracy than other amino acids because their concentrations (and hence peak sizes) were smaller.

Figure II-5.

HPLC Analysis of DABS-Amino Acids
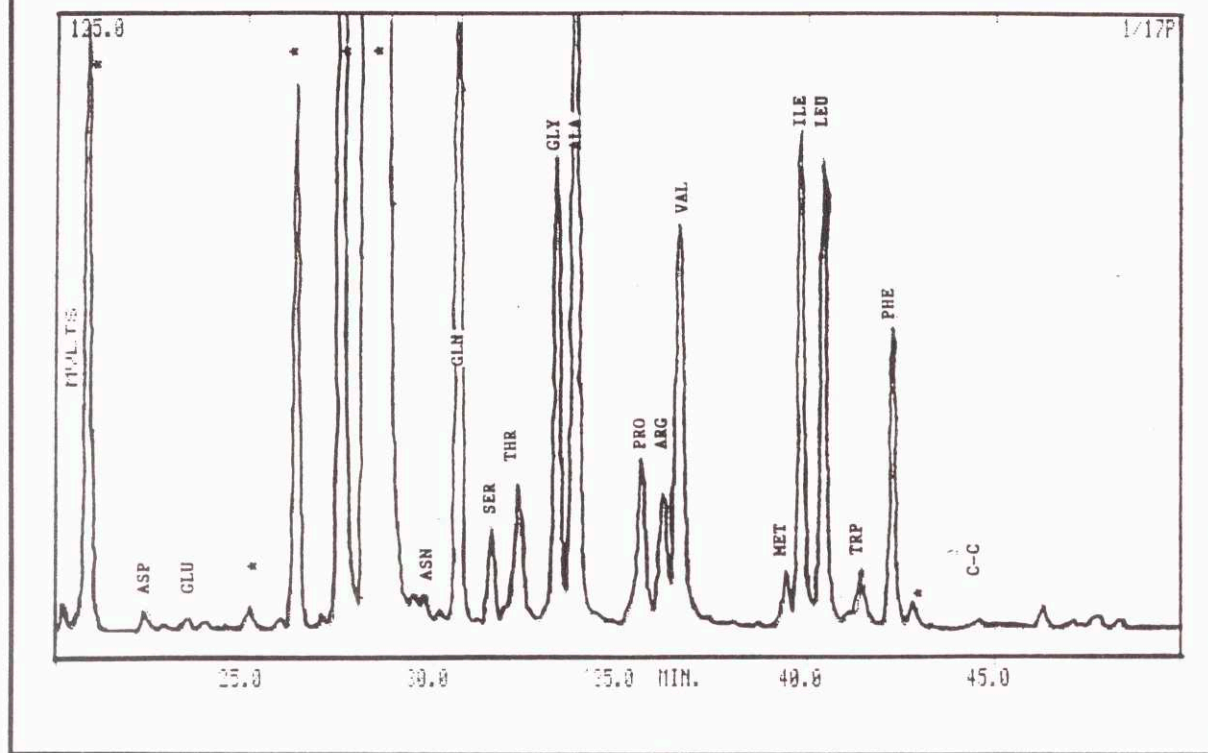
5) Linearity of Amino Acid Analysis

To examine the accuracy of the DABS-amino acid chromatographic system, I prepared standards of amino acids at 200 μM, 400 μM, and 800 μM (except glutamine, which was at 2 mM, 4 mM, and 8 mM). These standards, along with 200 μM ornithine as the internal standard, were reacted with DABS-Cl and separated with the reverse phase column as described earlier. Peak areas were calculated from the chromatograms and peak areas were normalized relative to the ornithine peak area. Figure II-6 shows the linearity

65

achieved with this technique for a typical amino acid, glycine. The line segment shown in this figures represents the linear regression line.

Figure II-6.

Linearity of Glycine Assay
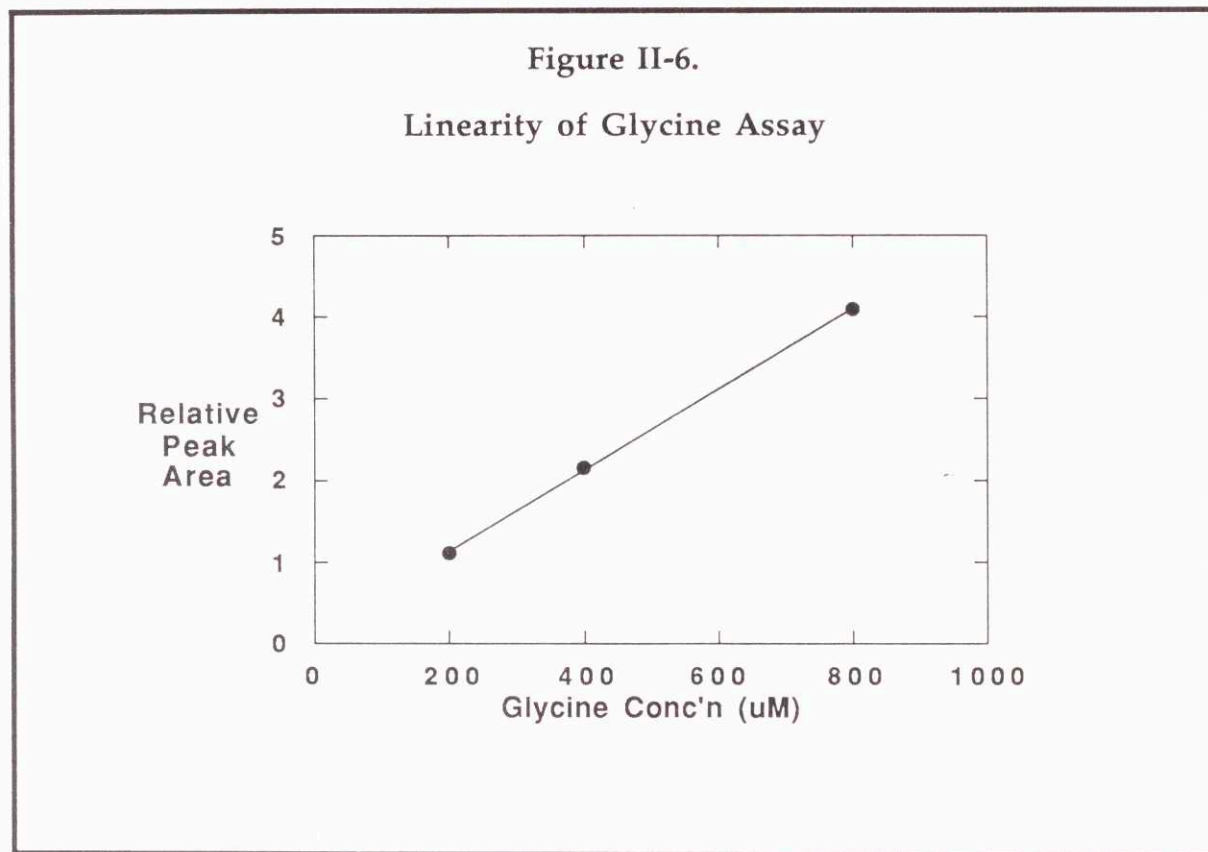
The linearity of all the amino acid peak areas was examined statistically using linear regression, and the results of that analysis are presented in Table II-1. For each amino acid, the regression's slope and intercept parameters are listed, expressed in terms of peak area relative to internal standard (which was constant). Also listed is the standard error of the estimate (S_{yx}), calculated from the calibration data according to the method of Downie and Heath (1983).

Table II-1.
Linearity of DABS-Amino Acid Peak Areas

Amino Acid	Slope Relative Peak Area	Intercept Relative Peak Area	Standard Error of the Estimate (µM)
Alanine	0.89	.22	24.6
Arginine	1.69	.06	28.8
Aspartate	0.54	.34	66.2
Asparagine	0.53	.37	55.9
Cysteine	0.56	-.06	28.6
Glutamate	0.51	.14	23.6
Glutamine	0.74	.11	19.4
Glycine	0.98	.15	8.4
Histidine	1.40	.39	5.9
Isoleucine	0.97	.11	11.0
Leucine	0.97	.10	3.3
Lysine	1.50	.30	10.2
Methionine	0.82	-.13	11.2
Phenylalanine	1.17	.08	24.8
Proline	1.08	.49	51.2
Serine	0.49	.26	36.2
Threonine	0.49	.07	12.7
Tryptophan	1.17	.04	0.8
Tyrosine	0.79	.31	35.0
Valine	1.08	.12	6.2

From table II-1 it can be seen that most amino acids gave excellent linearity over a broad range of concentrations. Some amino acids, like asparagine, gave higher y-intercept values. This was due to a slight loss in response at 800 µM concentration. Since asparagine, as well as several other amino acids, were present in samples at low concentrations, the calibration points at 200 and 400 µM were used for these amino acids to calculate concentrations from peak areas. The average standard error of the estimate for all amino acids was 23.2 µM. For amino acids at 400 µM, that translates to a 6% error, although the relative errors were higher for amino acids present at very low concentration like aspartate, glutamate, and asparagine.

6) Comparison of Different Assay Systems

To examine the accuracy of the organic acids and bases HPLC techniques, I first calculated the concentrations of lactic acid in all our injected samples as measured by the peak integrator using the area of the inorganic salts as an internal standard and the peak area of a standard solution of lactic acid as a reference area. I then compared these calculated lactate concentrations to the concentrations obtained earlier using the enzymatic assay. The results of these comparisons are shown in figure II-7. The overall accuracy shown in figure II-7 indicates that this technique has the capability of providing the kind of quantitative information needed to calculate specific rates of uptake and production of metabolites in the medium.

Figure II-7.

Comparison of Enzymatic and HPLC

Chromatographic Measurements of Lactic Acid
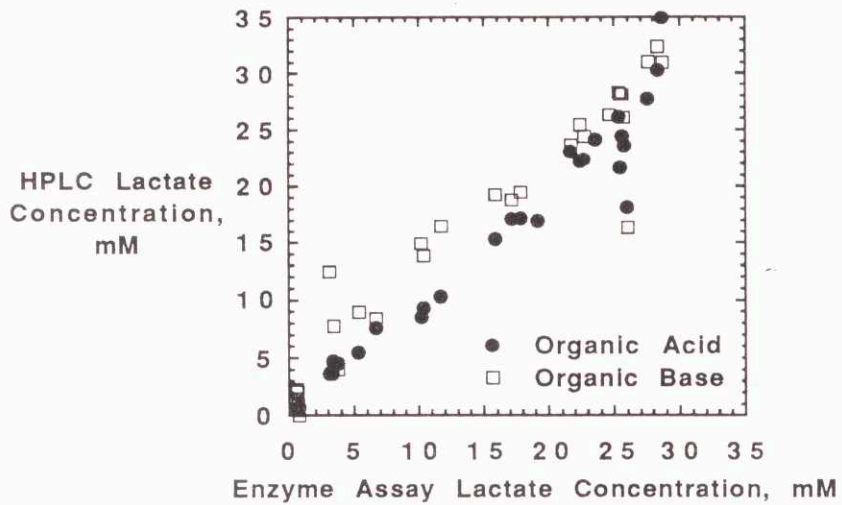
As an additional independent check on the accuracy of the different techniques used to determine other critical metabolite concentrations, I compared the concentrations determined by different systems for both glutamine and PCA. Glutamine measurements were made by the organic base HPLC system as well as the DABS-amino acid HPLC system. Although the peak for glutamine was close to those of some other amino acids in the

70

organic base system, its relatively high concentration made quantitative analysis easier. PCA, on the other hand, was well separated on both the organic acid and organic base columns. Because of its relatively high absorbance in the ultraviolet and the millimolar concentrations in which it was present, it gave a large, easily identified peak (see figures II-2 and II-3). Figure II-8 shows the relationship between glutamine concentrations determined in the DABS-amino acid and the organic base systems. Figure II-9 shows the PCA concentrations determined by the organic acid and organic base column systems.

Figure II-8.

Comparison of Glutamine Assay Techniques

Figure II-9.

Comparison of Pyrollidone Carboxylic Acid (PCA) Assay Techniques
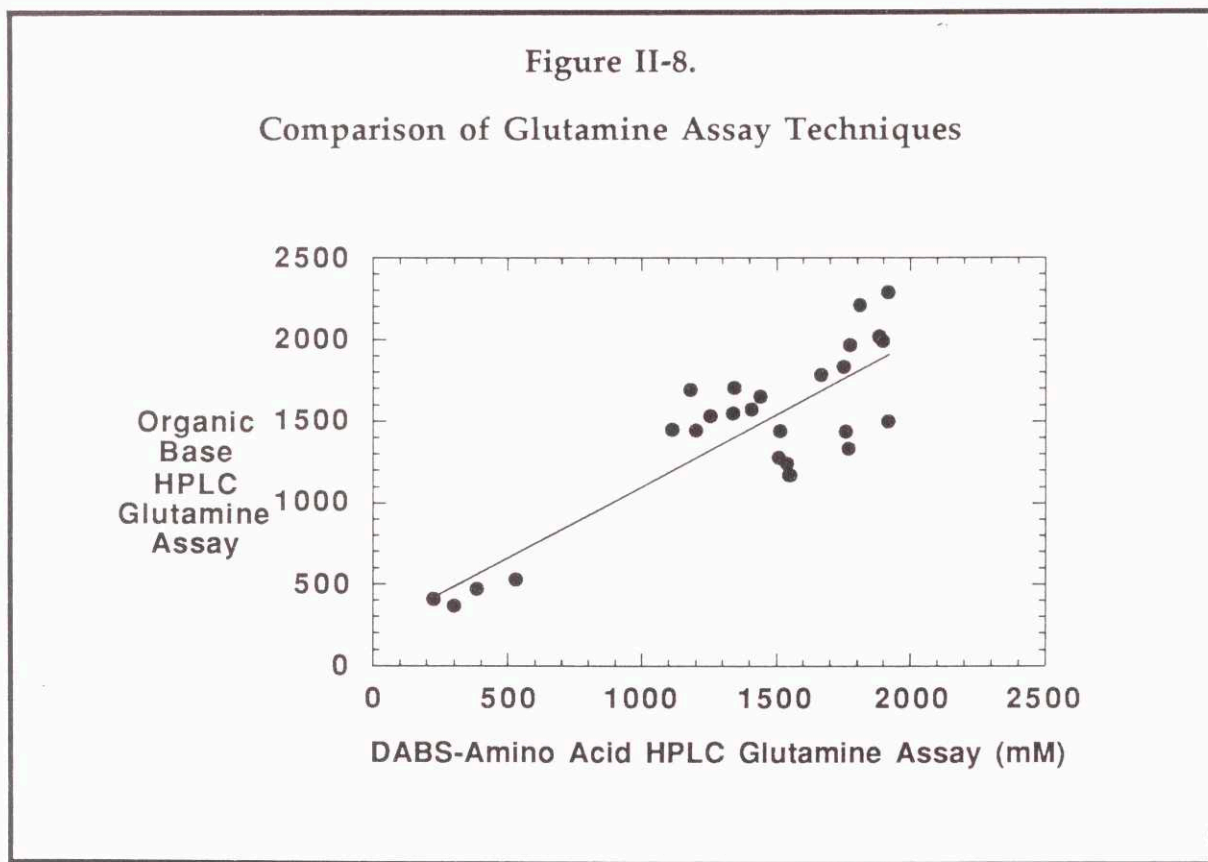
C. Mathematical Analysis

1. Growth and Death Rates

Equation 5 presented a mass balance on viable cells in a bioreactor with cell recycle, and equation 6 presented a similar mass balance on dead cells. At steady state equation 5 simplifies to:

$$\mu = \alpha + \varepsilon_V D \qquad (18)$$

Similarly, equation 6 simplifies at steady state to:

$$\frac{X_V}{X_D} = \frac{\varepsilon_D D}{\alpha} \qquad (19)$$

This expression states that the viability of the culture (represented as the ratio of viable to dead cells) is equal to the ratio of removal of dead cells to the specific death rate of the viable cells. The overall viability is increased by increasing the removal of dead cells and decreased by killing the live cells.

Substituting equation 18 into equation 19 and solving for μ gives:

$$\mu = \left(\frac{X_D}{X_V}\varepsilon_D - \varepsilon_V\right)D \tag{20}$$

By measuring X_D, X_V, ε_D, and ε_V at steady state, and setting D via the medium inlet pump, one can calculate the true growth rate using equation 20. However, the calculation of true growth and death rates at unsteady-state requires a formal solution to equations 5 and 6. From equation 5, we have

$$\int \frac{d\,X_V}{X_V(\mu - \alpha - \varepsilon_V D)} = \int dt \tag{21}$$

Integrating equation 21 gives:

$$\ln\left(\frac{X}{X_0}\right) = (\mu - \alpha - \varepsilon_V D)\,t \tag{22}$$

where X_0 = cell density at t = 0

Equation 22 can be solved for the apparent growth rate, μ_{app}, giving:

$$\mu_{app} = \frac{\ln(\frac{X}{X_0})}{\Delta t} + \varepsilon_V D$$

Equation 22 also can be solved for X to obtain the expression for the growth of cells in a recycle reactor:

$$X_V = X_{V0}\, e^{(\mu - \alpha - \varepsilon_V D)\, t} \tag{23}$$

Equation 22 does not by itself allow one to calculate μ and α. The net growth rate $(\mu - \alpha)$ can be determined in unsteady state conditions with equation 22, but to separate μ from α under this condition requires the solution of the differential equation for dead cells, equation 6:

$$\int \frac{d\,X_D}{\alpha\, X_V - \varepsilon_D\, D\, X_D} = \int dt \tag{24}$$

75

Substituting equation 23 into 24 for X_V, integrating, and solving for α gives:

$$\alpha = \frac{B(X_D - X_{D_0} e^{(-\varepsilon_D Dt)})}{(e^{Bt} - 1) X_{V_0} e^{(-\varepsilon_D Dt)}}$$

(25)

where $\quad B = \mu - \alpha - D(\varepsilon_V + \varepsilon_D)$

and $\quad X_{D0} \quad$ = dead cell concentration at time = 0

$$(cell/cm^3)$$

Using equation 25 we can determine the unsteady-state death rate, which in turn can be used to determine the true unsteady-state growth rate :

$$\mu = \mu_{app} - \alpha$$

(26)

These equations were applied to the unsteady-state data during the early transient period when the cell density increased 20-fold. As mentioned earlier, bubbles passing through the cell separator could disturb the laminar flow and cause a temporary increase in the cell density exiting the cell separator. Whenever a sample was taken recently following a "bubble event,"

equations 25 and 26 gave unreliable estimates of μ and α. In these cases the simpler equations for steady-state and data smoothing were applied.

2. Metabolite Uptake and Product Formation Rates

As cells grow in a bioreactor system, they consume nutritional substrates and produce waste metabolites. In addition, the transfectoma cells I was using produce monoclonal antibody. The basic assumption in the mass balances to follow is that each cell consumes and excretes at the same rate. The per cell (specific) rate measurements are calculated for the culture as a whole. In actuality, there may very well be a heterogeneous distribution of metabolic rates. Heterogeneousness in monoclonal antibody production in these same cells has been observed (C. Buser, J. Morrill, and L. Tsuruda, unpublished observations).

A mass balance on a material consumed by the cells gives:

$$\frac{dS}{dt} = D(S_i - S) - q_S X_v \tag{27}$$

where S_i = inlet substrate concentration (mole/liter),

and q_S = specific substrate uptake rate (mole/cell-hr).

At steady state, equation 25 simplifies to:

$$q_S = \frac{D(S_i - S)}{X_V}$$

(28)

At unsteady state, equation 27 must be integrated and the resulting expression for S solved for q_S to estimate the specific productivity. The integral form of equation 27 is:

$$\int \frac{dS}{D(S_i - S) - q_S X_V} = \int dt$$

This equation can be integrated and solved for qs to yield:

$$q_S = \frac{(\mu - \varepsilon_V D + D)(S - S_0 e^{-Dt} - S_i(1 - e^{-Dt}))}{X_{V_0} e^{-Dt}(1 - e^{(\mu - \varepsilon_V D + D)t})}$$

(29)

78

In actual practice, equation 29 is very sensitive to 'noise' in the form of measurement error. The fundamental difficulty is that unsteady state specific rates are calculated from many time derivatives. Thus, a small error in the measurement of a parameter from one determination to another creates a much larger error in the estimate of the *difference* of these two numbers. Moreover, several parameters must be measured repeatedly in order to evaluate equation 29: the flow rate, the substrate concentration, the cell density and percent viability, both within the bioreactor and at the outlet of the separator. In order to avoid unrealistic estimates of q_S due to an accumulation of small errors, a simpler approach was taken. It was assumed that during the time interval under consideration, the effective cell density was the log-mean cell density:

$$\overline{X_{LM}} = \frac{X - X_0}{\ln(\frac{X}{X_0})}$$

(30)

The volumetric uptake rate is defined by:

$$Q_S = q_S \overline{X_{V_{LM}}}$$

(31)

where $\overline{X}_{V\ LM}$ = log-mean viable cell density

(cell/cm^3)

This expression is substituted for q_PX to give a simplified version of equation 27:

$$\frac{dS}{dt} = D(S_i - S) - Q_S \tag{32}$$

where $\quad Q_S$ = volumetric substrate uptake rate (mole/liter-h)

This expression can be integrated with respect to time and solved for Q_S to yield:

$$Q_S = \frac{e^{(-Dt)}D(S_i - S) - D(S_i - S_0)}{e^{(-Dt)} - 1} \tag{33}$$

In practice, equation 33 was used to evaluate the volumetric productivity, and then equation 31 was used to evaluate the specific productivity. In addition, to further reduce the undue influence of scatter in the data, cell densities, metabolite concentrations, and flow rates were all subjected to a three point floating average routine prior to rate calculations. Although this smoothing routine may reduce the sensitivity to short-term changes in the specific rates, it provides a necessarily smooth database to evaluate specific rates with real physical meaning.

Productivity was calculated with an identical routine. The inlet product concentrations (if any) along with the smoothed product concentration data were used in equation 33 to estimate a volumetric productivity, which was in turn used (with the log-mean viable cell density) to estimate the specific rates of production during transient unsteady-state conditions. At steady state, equation 33 reduces to equation 28.

III. Experimental Results

A. Cell Separation

1. Cell Removal Rates

The nested conical cell separator permits perfusion of suspension cell cultures with dilution rates substantially higher than has been reported for other cell separation systems. This is because of the high efficiency of cell retention and selective removal of dead cells attained by the nested conical cell separator. Because this cell separator operates on a principle of gravitational sedimentation, the terminal settling velocity V_T of the cells is a critical parameter. Once the design of a separator has been determined, the only critical operating parameter which can be directly manipulated is the liquid flow rate through the system. Equation 16 (Section II) described the velocity of a particle in a nested conical separator in terms of the flow rate Q and the terminal velocity V_T. Although one cannot readily control the diameter of an individual cell, the population of cells which is obtained in this type of bioreactor is profoundly affected by the flow rate.

To illustrate this concept, consider the losses of viable cells from a nested conical separator under conditions of varying flow rate. The exact dimensions of the separator used are presented in Appendix 3. The values for epsilon were calculated by determining the viable cell densities exiting the separator and within the bioreactor. The ratio of these two cell densities is the value of epsilon. Figure III-1 shows that the loss of viable cells is strongly

dependent on the flow rate. The data were fitted to an exponential regression, and the resulting equation is shown above the graph. Using this regression equation to solve for Q when ε is equal to 1 (no separation), one predicts that the separator would fail totally at a flow rate of 210 ml/h, at which flow rate all the viable cells would leave the bioreactor. Of course, the non-viable cells, being smaller in size (and hence with a slower settling velocity), are removed from the system in much greater proportions.

Figure III-1.

Viable Cell Loss as a Function of Flow Rate

$$\varepsilon = .000816 * e^{\wedge}(.034\ Q)$$
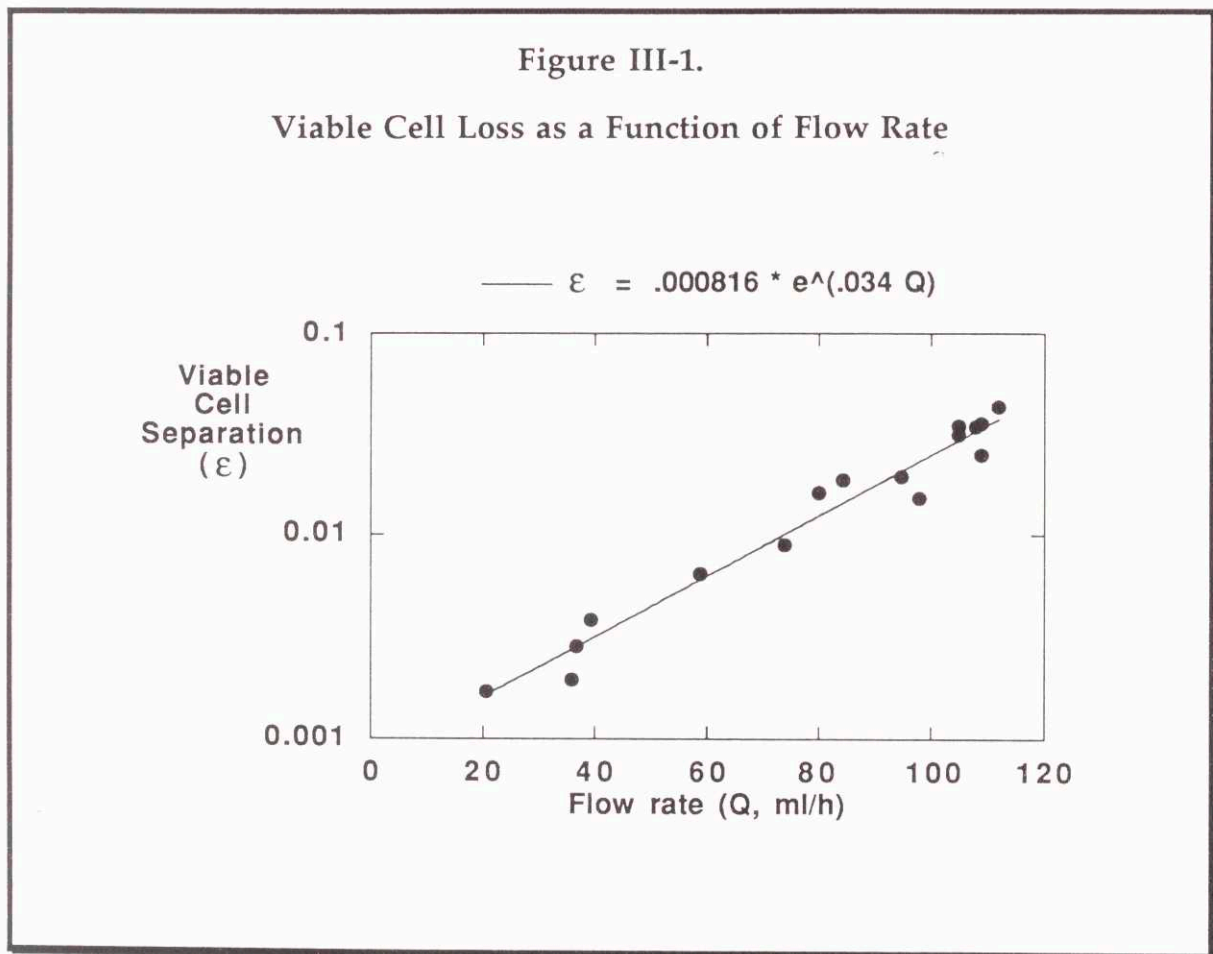
The losses of cells from the separator are strongly affected by the size of the cells. This is the mechanism by which smaller, non-viable cells are selectively removed from the bioreactor. The effect of cell size on separator losses was examined by determining the cell size frequency distribution for cells within the bioreactor and cells exiting the separator. Figure III-2 presents the results of such a size analysis performed on a bioreactor perfused at 10 volumes/day. A gaussian distribution function fits both cell populations. The curves in figure III-2 are the gaussian functions fitted to each population by nonlinear regression analysis. The population of cells within the bioreactor have sizes centered on 11.8 microns, while the cells exiting the bioreactor have a much smaller central size, 10.4 microns.

Figure III-2.

Cell Size Frequency Distributions in Bioreactor and Separator
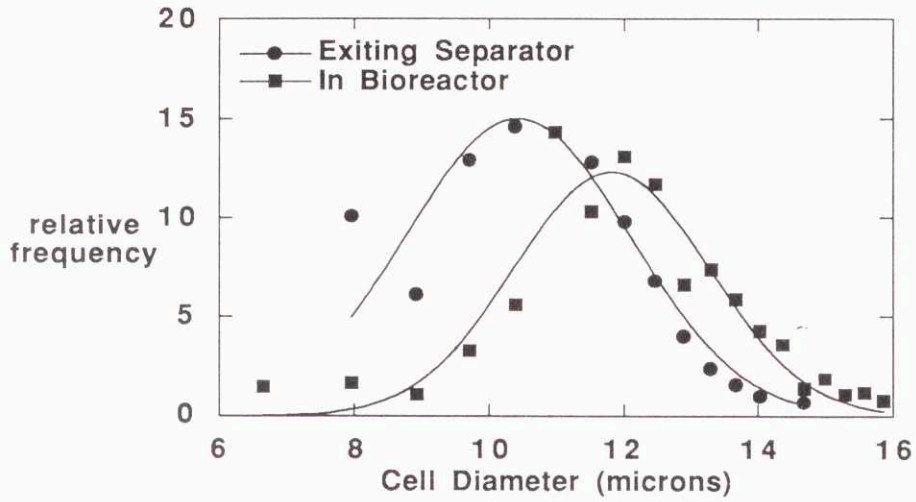
The cell size data used to produce figure III-2 was further analyzed to determine values of epsilon for each individual cell diameter. For each cell diameter, the ratio of cell density exiting the bioreactor to cell density within the bioreactor (ϵ) was calculated. This was done for samples taken of cell cultures perfused at 3 and at 9 volumes per day. Figure III-3 shows the effect of cell size on separator losses at different perfusion rates. At 9 volumes/day, cells larger than 10 microns diameter are nearly totally retained, while smaller cells are effectively removed. At 3 volumes/day perfusion, cells as small as 8 microns are retained. Only the smallest cells can be removed from the system at this perfusion rate.

Figure III-3.

Cell Losses as a Function of Cell Diameter at Different Flow Rates
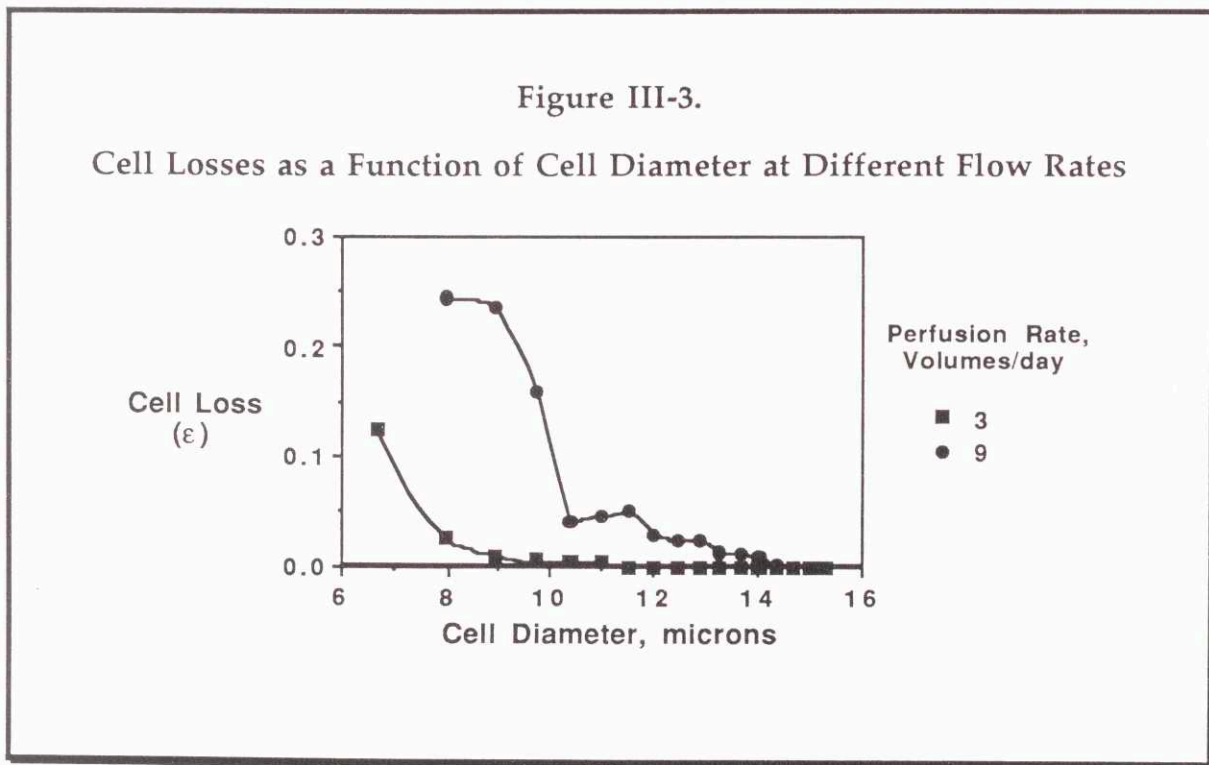
2. Cell Size Distributions

Figure III-3 showed that smaller cells are preferentially removed from the bioreactor. The selective removal of smaller cells has a profound effect on the resulting cell size distributions in the bioreactor. To see why this should be so, consider the effect of flow rate on cell removal. At higher flow rates, all the smaller cells are effectively removed, while at lower flow rates a greater proportion of small cells are permitted to remain in the bioreactor. Figure III-4 shows the cell size distributions within the bioreactor for cultures perfused at 3 and 9 volumes/day. Gaussian frequency distribution functions were calculated for each population by nonlinear regression, and the resulting curves are shown. The cell population in the culture perfused at 3 volumes/day has a maximum at a cell diameter of only 7.8 microns, while the cells in the culture perfused at 9 volumes/day have a maximum at a diameter of 12.1 microns. Simply by changing the perfusion rate, it is possible to alter the size distribution of cells in the culture. Since the size distribution of a culture is dependent on the age distribution of its constituent cells, we are seeing an alteration in the age distributions of these cultures. Thus, it can be seen that the unique design of the nested conical cell separator provides a new tool to manipulate the populations of cells grown in bioreactors.

Figure III-4.

The Effect of Perfusion Rate on Cell Size Distributions
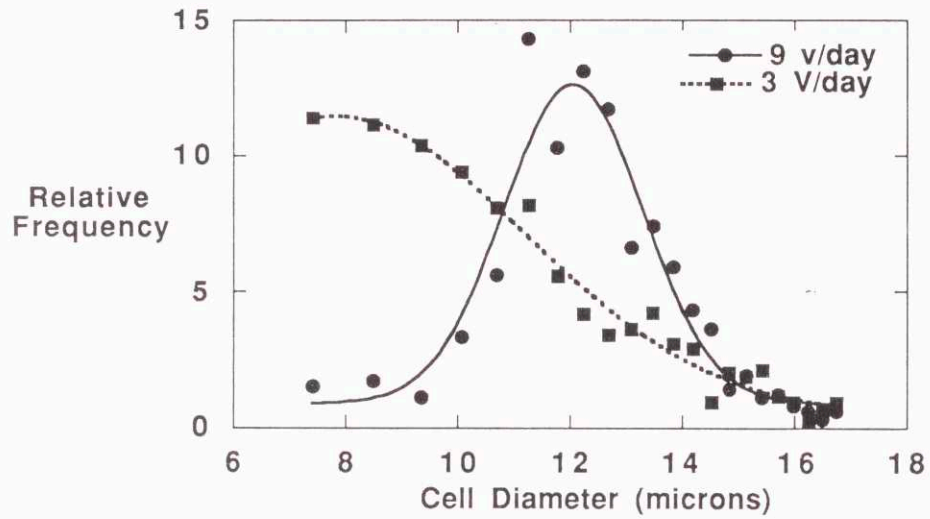
B. Transient Phenomena

A series of perfusion cultures was run to study the effects of nutritional and waste product limitations on the patterns of metabolic activities exhibited by monoclonal antibody secreting cells at high cell density under steady state conditions. Since I wished to examine the behavior of these cells at high density (defined as greater than 10^7 viable cells/cm^3), a period of about two weeks of exponential cell growth was required to attain the desired cell density. During this time of growth, the culture was sampled frequently, usually twice daily. These samples were subjected to the same kinds of metabolite assays that the samples taken from the high density steady states were. The information obtained during the transitional period from low density ($< 10^6$ cells/cm^3) provided some startling clues regarding the regulation of cellular metabolism.

Data from a total of five different cultures were used in the metabolic studies. Three of these cultures were run simultaneously. These three cultures were brought to steady state with a dilution rate of about 3 volumes/day. Maintenance of steady state was judged by a constancy of cell density for 4 consecutive days. Subsequently, the perfusion rates were raised to about 5 volumes/day and held at that value until a new steady state was obtained. After about four weeks, one culture (#1) became contaminated and was taken down. The remaining cultures were used for further metabolic studies, including the stepwise dilution of the medium with buffered saline to investigate the effects of nutritional limitation.

1. Cell Growth

Three 250 ml cultures were inoculated at about 5×10^5 cells/ml using cells taken from mid-log phase batch cultures. Perfusion was begun about 24 hours later at one volume/day and gradually increased to 3 volumes/day as the cells grew. The bioreactors were gassed through microporous teflon tubing with a mixture containing 20% O_2, 5% CO_2, 75% N_2 until cell densities exceeded 10^7 viable cells/ml, when the gas mixture was changed to 40% O_2/60% N_2. It had been shown previously that the growth of these particular cells are not inhibited by 40% O_2 (Oller *et al.*, 1989). The shift to higher oxygen content was done to ensure that the growth of the cells was not oxygen-limited. To prevent dehydration of the medium, all the incoming gas was passed through a water column at 37°C. The bioreactors were maintained in a 37°C room in the dark (except for sampling).

After inoculation, the cells grew steadily, increasing in cell density exponentially until 10^7 cells/ml was exceeded. At that time, the cells apparently ceased growth. However, since the cells constantly were being removed from the bioreactors by the separator, this cessation in observed growth simply reflected a dynamic balance between growth of new cells and their removal from the system. Actually, the cells were maintaining a doubling time of about 28 hours. Figure III-5 shows the growth of the cells during the three simultaneous perfusion cultures. The reproducibility of the system can be readily noted by the similarity in the growth curves.

Figure III-5

Growth of Cells in Perfusion Bioreactor System
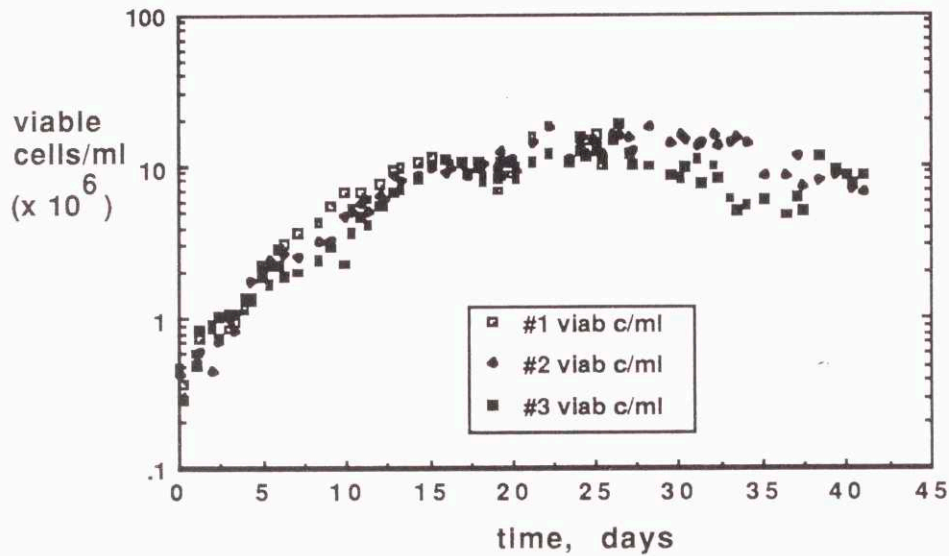
One of these three cultures, "culture #1", was analyzed in great detail. An examination of the metabolic rates during the transient phase as the cell density increased from 5×10^5 to $>10^7$ cells/ml reveals a wealth of information the concerning cellular response to conditions of varying cell density. Due to unavoidable scatter in the primary data, the cell density, viability, flow rate, and metabolite concentration data were all subjected to a three-point floating averaging routine prior to rate calculations.

The cell density and medium flow rates for culture #1 are shown in figure III-6. As the cells grew, the medium flow rate was increased until the dilution rate was slightly over 3 volumes/day. The system was allowed to arrive at steady state. At about day 17, the medium flow rate was increased to about 5 volumes/day, and a new steady state was reached. The results in this section describe the events during the transition from low cell density to high density (days 0 - 16). During the transition from low to high cell densities, the doubling time increased from 21 to 41 hours.

Figure III-6.

Cell Density and Medium Flow Rate During Transient Growth Phase
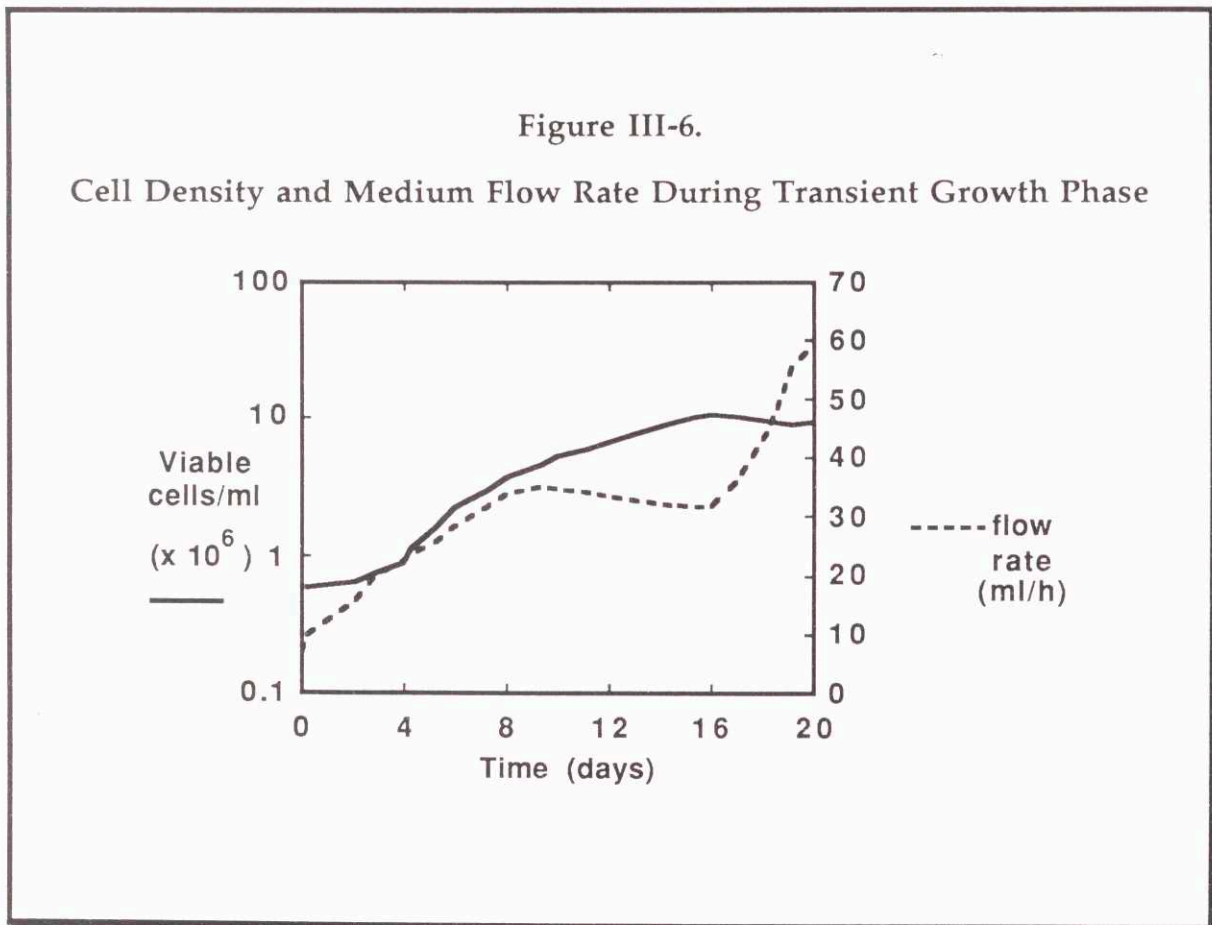
2. Immunoglobulin Production

The cells used in these studies were selected for examination because they secrete a product of interest: monoclonal antibodies. This particular line of transfectoma cells produces relatively low amounts of antibody in culture, compared to hybridoma cells. When these cells were grown in batch cultures, the maximum specific productivity they exhibited was about 0.25 pg IgG/cell-hr. The cells' IgG productivity declines over the period of months as they are maintained in culture (J. Morrill and C. Buser, unpublished observations). However, over the period of two or three weeks, there is no drastic loss of specific IgG productivity for cells maintained in low density batch cultures.

Cells grown to high density in perfusion cultures exhibited a quantitatively different behavior than cells grown at low density. Figure III-7 presents the specific IgG productivity of culture #1 as the cell density increased from 5×10^5 to over 10^7 cells/ml. The productivity declined from a high of 0.25 pg/cell-h to less than 0.01 pg/cell-h. The sections to follow will show that many metabolic changes were observed during this same period. This down-regulation in IgG productivity is just one out of many profound alterations in cellular activities which accompany the transition to high density culture.

Figure III-7.

Immunoglobulin Productivity During Transient Growth Phase
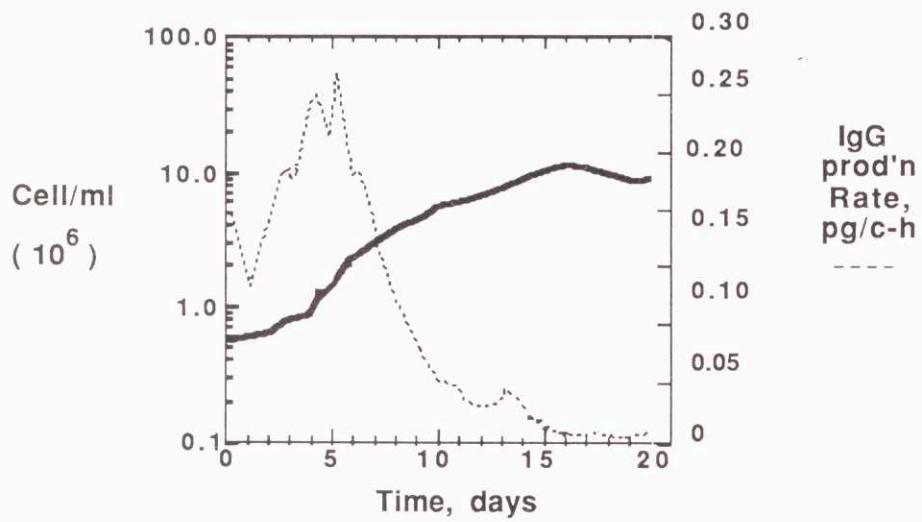
3. Glycolysis

The anaerobic process of energy generation through glycolysis is one of the best understood metabolic pathways. Glucose is converted to pyruvate with the generation of 2 high energy ATP molecules and two electrons per glucose molecule metabolized. The pair of electrons removed from the glucose molecule in the form of NADH is not passed to oxygen by tumor cells in vitro. Instead, lactate dehydrogenase uses the electrons to reduce the pyruvate, generating lactate. The bulk of this lactate is excreted by the cells into the medium.

Glucose and lactate concentrations during the transitional phase are shown on figure III-8. As the cells grew, the glucose level fell from about 20 mM to about 8-10 mM. The input medium contained about 25 mM glucose. Lactate levels rose from 5 mM to around 25 mM.

Figure III-8.

Glucose and Lactate Concentrations During Transient Growth Phase
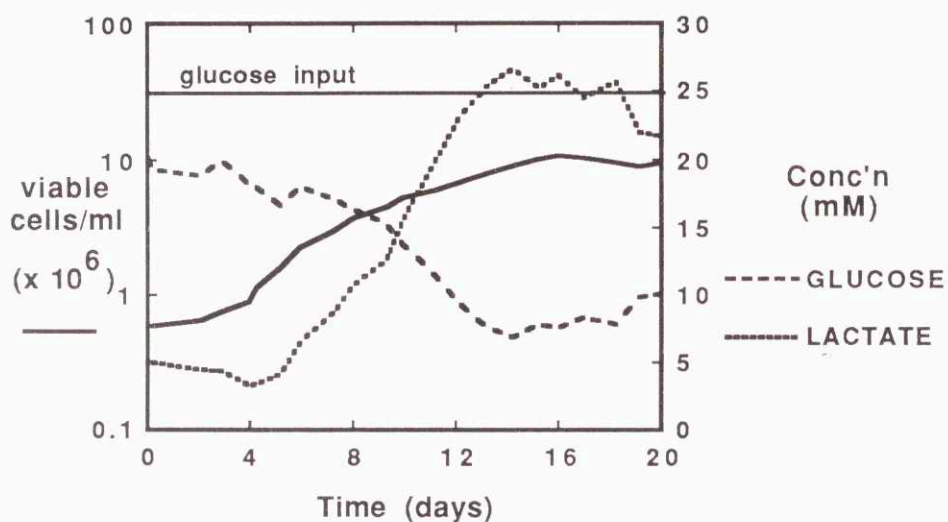
The specific rates of glucose uptake and lactate production are presented in figure III-9. Although there was a fluctuation in rates around day 16, for most of the transient phase the specific glucose and lactate rates remained fairly constant at about 200 and 400 fmol/cell-h, respectively. Moreover, the ratio of these rates holds very close to the theoretical glycolytic yield of 2 moles lactate per mole glucose.

Figure III-9.

Glucose Uptake and Lactate Production Rates During Transient Growth Phase
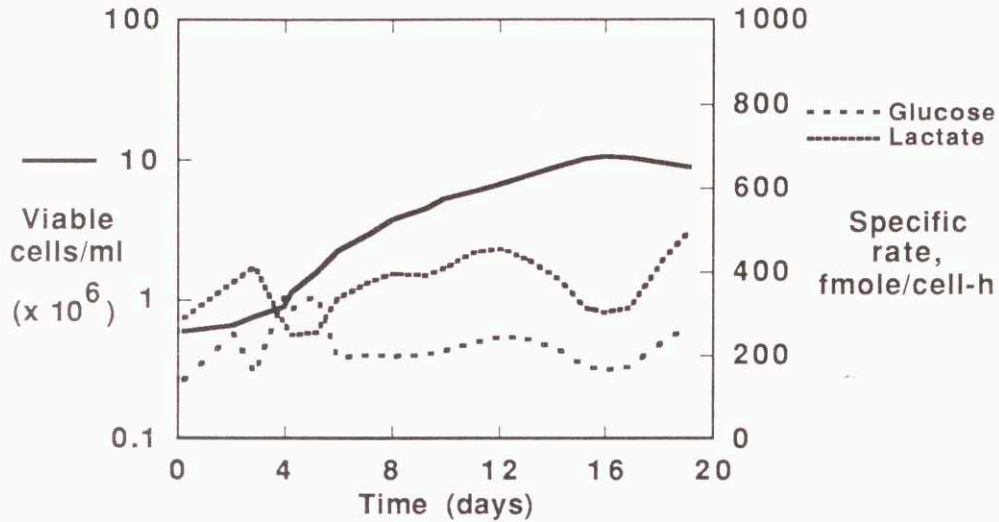
A hallmark of glycolysis is the stoichiometric conversion of glucose to lactate. A 100% yield of lactate from glucose (2 moles lactate per mole glucose) represents complete conversion. Figure III-10 shows the conversion yield from glucose to lactate during the transient growth phase. Following some fluctuations in yield during the first few days, when the perfusion rate was being adjusted, the conversion yield remained constant at about 95-100%. This tight stoichiometric coupling between glucose uptake and lactate production suggests that the glucose and lactate rates observed are true

glycolytic rates. This permits the calculation of glycolytic ATP generation rates on the basis of two moles ATP per mole glucose consumed. This calculation is presented in section III-B-6.

Figure III-10

Glucose to Lactate Conversion Yield During Transient Growth Phase
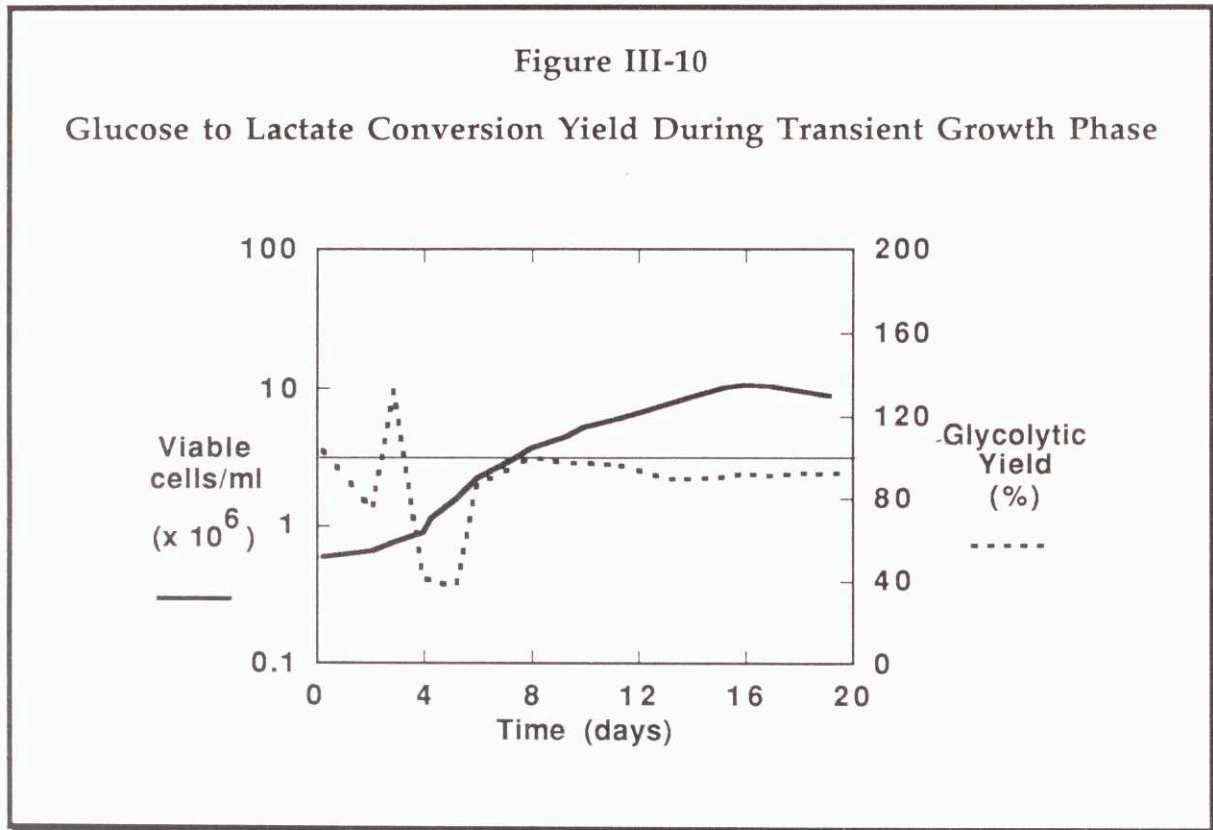
4. Organic Acids

A variety of organic acids were detected by the organic acid HPLC system used. Three organic acids together accounted for more than 90% of the total optical absorption at 210 nm: pyruvate, lactate, and pyrrolidone carboxylic acid (PCA). Pyruvate is a nutrient supplied in the medium. It helps to buffer the redox potential as the cells produce lactate, and it can serve as a source of energy and carbon skeletons for biosynthesis. Lactate is the endproduct of glycolysis. PCA arises from the spontaneous breakdown of glutamine. Its structure is shown in figure III-11.

Figure III-11.

The Structure of Pyrollidone Carboxylic Acid
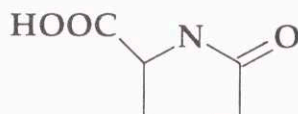
Pyrrolidone Carboxylic Acid
(PCA)

PCA, also known as pyroglutamic acid, can be prepared in the laboratory by autoclaving glutamine in solution. It has long been realized that glutamine is unstable in aqueous solutions. Tritsch and Moore (1962) reported reaction rates for solutions of glutamine in PBS (phosphate-buffered saline). Ozturk and Palsson (1990) recently reported glutamine decomposition rates in a variety of cell culture media which imply that a substantial fraction of the glutamine originally present in cell culture medium may degrade by the time the medium is fed to the cells, depending on storage pH and temperature.

In the culture system used in these experiments, antibiotics were never used. To make any possible contamination in fresh medium reservoirs apparent prior to use, and thereby reduce the chances for contamination of the bioreactors, medium reservoirs were held at 37°C for at least 48 hours. Several contaminated reservoirs were discovered in this way, thereby saving the cultures. The undesired side effect of this pre-incubation was glutamine degradation to PCA.

Both the organic acid and organic base columns cleanly resolved PCA. Concentrations calculated using both HPLC systems on the basis of normalized peak areas agreed fairly well (see figure II-12). PCA concentrations in the inlet medium were around 3 mM. The original medium glutamine concentration was 6 mM, but samples taken from nearly empty fresh medium reservoirs contained only 3 mM glutamine. The PCA concentration neatly accounts for the loss of glutamine.

PCA concentrations in samples of culture broth revealed a surprising decrease in PCA concentrations relative to the medium. Figure III-12 shows the PCA and pyruvate concentrations measured in culture #1 during the transitional period. It shows that the cells decreased the pyruvate concentration by about 0.5 mM, while they decreased the PCA concentration by over 1 mM. Neither compound came close to exhaustion.

Figure III-12.

PCA and Pyruvate Concentrations During Transient Growth Phase
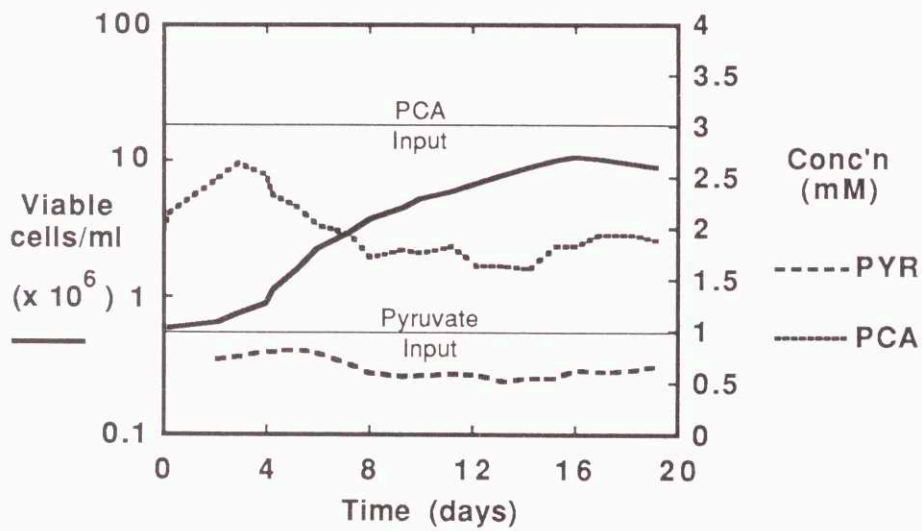
The PCA concentration data indicate that the increase in cell density was accompanied by a decrease in the PCA uptake rate. Figure III-13 shows that the specific PCA uptake rate fell from 60 fmol/cell-h to under 20 fmol/cell-h during the transitional period. The specific PCA uptake rate profile parallels the specific IgG production profile. In the sections to follow, it will be shown that most of the specific rates observed (with the notable exception of glycolysis) show this same dramatic decline during the ascent to high cell density.

Figure III-13.

Specific PCA Uptake Rate During Transient Growth Phase
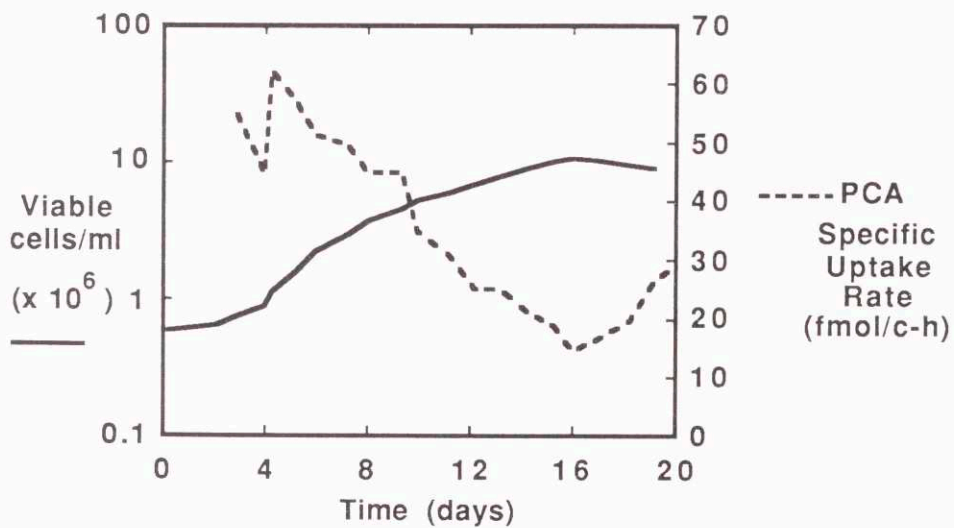
The metabolic fate of the PCA which the cells ingest is a matter for some speculation, since studies of its metabolic role in cell culture are very limited. Several studies in mammals have been made of the fate of exogenous PCA administered orally to rabbits and mice (Lange and Carey, 1966) and intravenously to humans (Chmielewska *et al.*, 1967). PCA is widely found in plant and animal tissues, and up to 2.5% of the water-soluble material present in the stratum corneum of human skin is PCA (Pascher, 1956). Van Der Werf and Meister (1975), in their review of PCA metabolism, reported that they had incubated kidney slices with ^{14}C-PCA and found radioactivity in glutamate, glutamine, aspartate, and glycine.

In cell culture, the effects of glutamine breakdown which have been described in the literature consist primarily of the loss of glutamine and the accumulation of its toxic decomposition product, ammonium ion. Relatively little has been reported concerning glutamine's other breakdown product, PCA. Baechtel *et al.* (1976) examined the effect of exogenously added PCA on BALB/c splenocyte blastogenesis and reported PCA to be without effect in concentrations up to 5 mM. Kitos and Waymouth (1967) studied mouse L cells grown in the presence of ^{14}C labeled PCA and found no evidence of incorporation.

The enzymology of PCA metabolism was reviewed by Abraham and Podell (1981) and by Meister (1974). PCA is a part of the γ-glutamyl cycle, in which glutathione is synthesized from glutamate, cysteine, and glycine. In a membrane-bound enzyme complex, the glutathione then covalently bonds

via a transpeptidation reaction to an extracellular amino to form a γ-glutamyl amino acid. This is translocated to an intracellular position, and the γ-glutamyl amino acid is cleaved to yield free amino acid plus PCA. The PCA formed is then converted to glutamate in an ATP-dependent reaction catalyzed by 5-oxoprolinase. The glutamate is then free to begin another round of glutathione synthesis. That this cycle is actually important in amino acid transport is shown by the work of Viña *et al.* (1990), who showed that inhibition of the activity of γ–glutamyl transpeptidase by acivicin decreased amino acid uptake by 53% in human keratinocytes in culture. Viña *et al.* (1989) showed evidence that PCA itself may signal amino acid uptake in cells.

Whether or not the PCA consumed by the cells in my experimental system is involved in the regulation of amino acid transport is not discernable from the data. However, since the cells ingested PCA at rates exceeded only by glutamine and glucose, it seems likely that PCA plays a substantial role in amino acid metabolism at the substrate level. The ubiquitous presence of 5-oxoprolinase, which converts PCA to glutamate, points to PCA's following the path of glutamine in the glutaminolytic pathway. Since ATP is required to convert PCA to glutamate, the ATP yield from the oxidation of PCA is slightly less that the ATP yield from glutamine. The details of ATP rate calculations based on PCA uptake are presented in section III-B-6.

The pyruvate specific uptake rate profile is shown in figure III-14. The uptake rate declined somewhat during the transient growth phase, but not greatly. The uptake rate declined from a high of about 2.5 fmol/cell-h to a low of about 1.5 fmole/cell-h.

Figure III-14.

Specific Pyruvate Uptake Rate During Transient Growth Phase
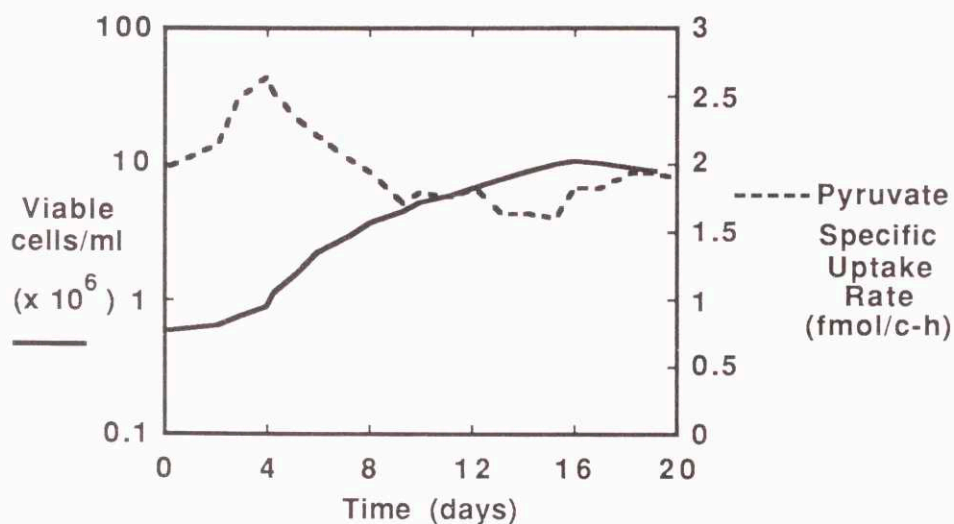
5. Amino Acids

Amino acids play a central role in cellular metabolism. Not only do they serve as building blocks for protein biosynthesis, but also they function as energy sources, lipid precursors, and nucleotide precursors. Analyzing the effects of different environments on amino acid metabolic rates was a primary goal of this research project.

The DABS-Cl/reverse phase HPLC technique used in these studies proved a reliable method for determining most amino acids. Only histidine failed to give reliable concentration data. Unfortunately, both the organic base and the organic acid columns used for metabolite analysis retained histidine, so I was unable to obtain quantitative histidine data. However, since histidine is a relatively minor component of cell proteins, its omission should not seriously jeopardize the overall amino acid metabolic analysis.

The data have been grouped for presentation in this section based on relationships in biochemical pathways wherever possible. For each group of amino acids, the amino acid concentrations will be presented first, followed by the specific rates of uptake or formation.

Figure III-15 shows the concentration profiles of glutamine and alanine during the transitional growth period. Note that the input glutamine level was actually 3 mM. The original medium formulation had 6 mM glutamine, but as discussed earlier, half of that had decomposed prior to the culture. Figure III-15 shows that the cells never consumed more than half the

glutamine. The alanine concentration hovered around 1.2 mM, making it the second most concentrated organic waste product (after lactate).

Figure III-15.

Glutamine and Alanine Concentration Profiles During Transient Growth Phase
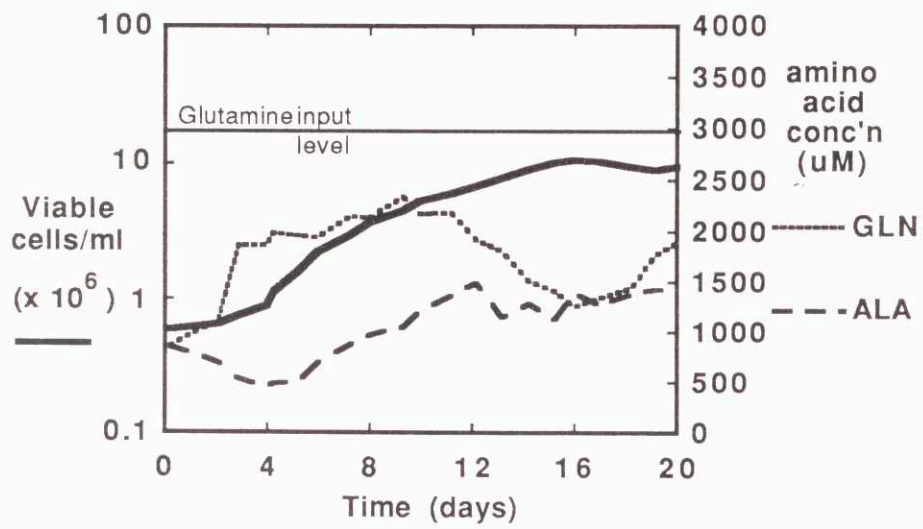
Figure III-16 shows the specific rates of glutamine uptake and alanine production during the transient growth phase. Both rates follow the same pattern of decline as the cell density increased, falling from about 60 fmol/cell-h to 20 fmol/cell-h. The metabolic rates for these two amino acids are higher than those for any other amino acids. Since alanine is an endproduct of glutamine metabolism, it is expected that the two rates should maintain a constant ratio. Figure III-16 shows that the two rates actually are nearly identical during this transitional period. That indicates that there was nearly stoichiometric conversion of glutamine to alanine. This permits the calculation of ATP generation rates during this period (section III-B-6.)

Figure III-16.

Specific Glutamine and Alanine Rates During Transient Growth Phase
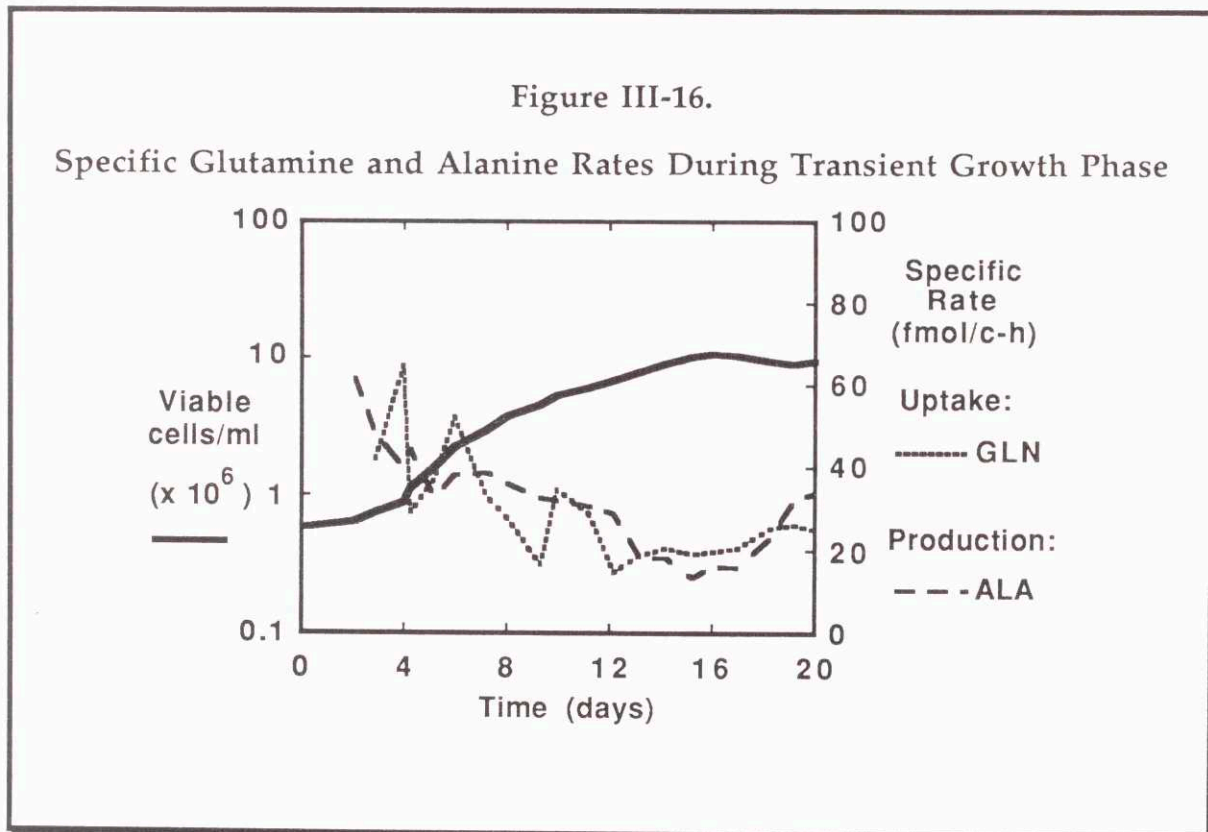
Figure III-17 shows the concentration profiles of the branched-chain amino acids, valine, leucine, and isoleucine. The concentrations of these amino acids actually neared the input concentration as the cells grew to high density. At a cell density of 10^7 cells/ml, less than 20% of these amino acids supplied in the feed medium was used by the cells.

Figure III-17
Branched-Chain Amino Acid Concentration Profiles
During Transient Growth Phase
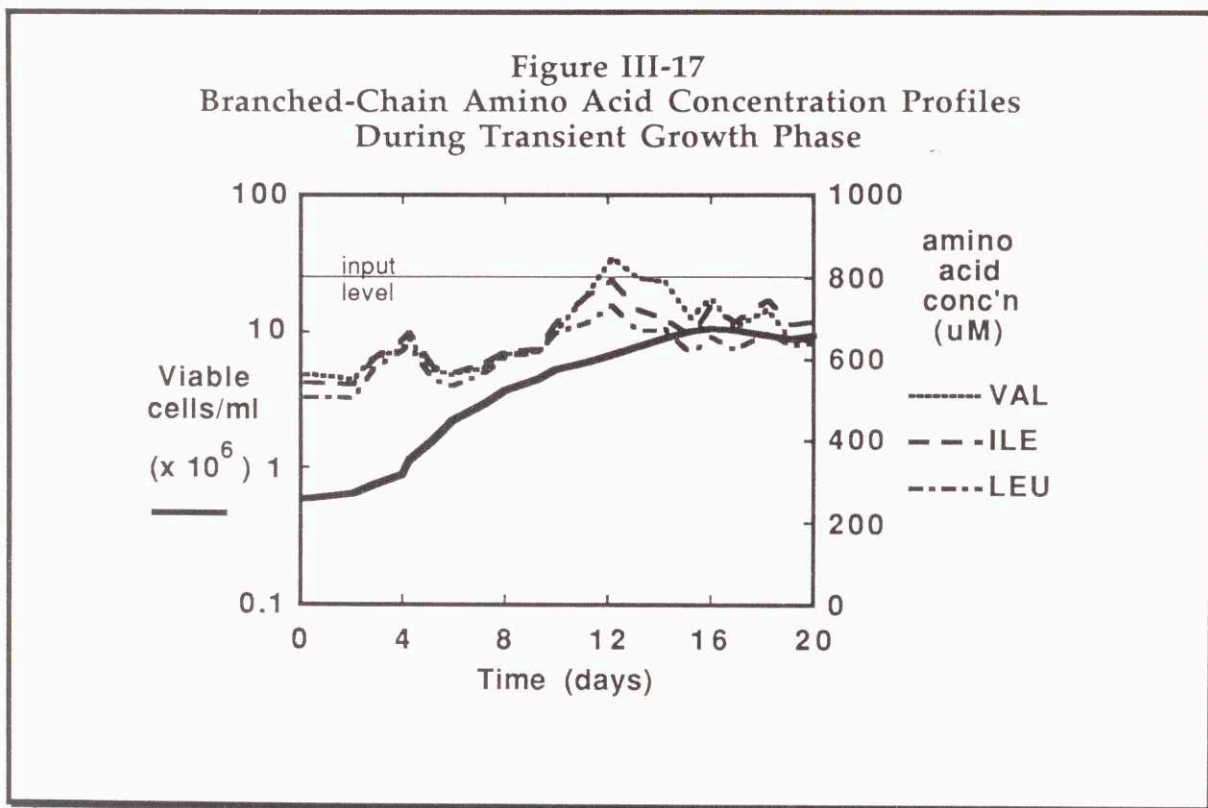
Figure III-18 shows the specific uptake rates for the branched-chain amino acids valine, isoleucine, and leucine during the transition to high cell density. The uptake rates of these three amino acids fell dramatically, plummeting from an initial value of 25-30 fmol/cell-h to 1-2 fmol/cell-h. This represents a decline of over 90% in the uptake rates of these essential amino acids.

Figure III-18

Specific Branched-Chain Amino Acid Uptake Rates During Transient Growth Phase
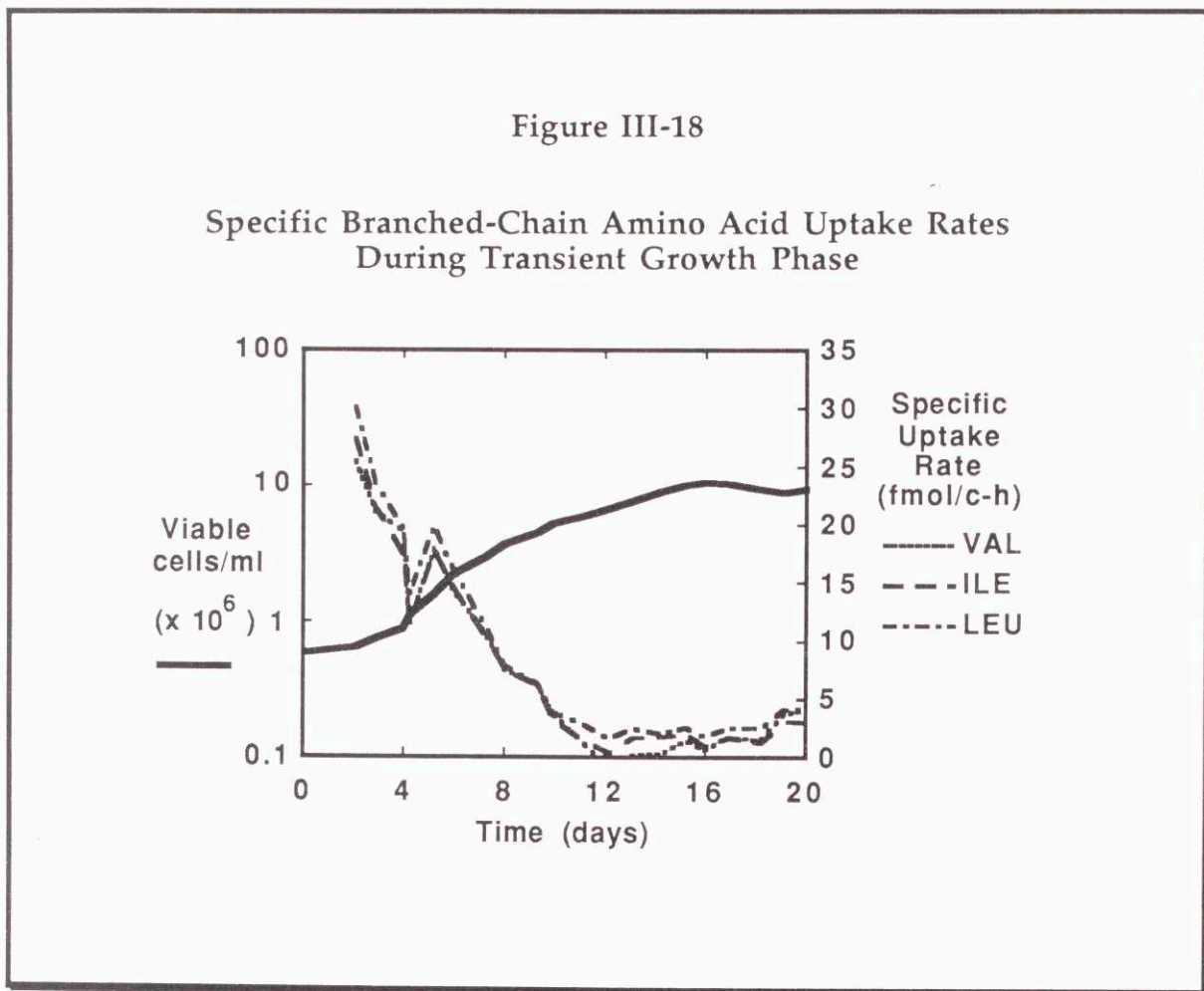
Figure III-19 shows phenylalanine, and tyrosine concentration profiles for culture #1 during the approach to high cell density. These amino acids enter the bioreactor at about 400 µM. The phenylalanine and tyrosine concentrations in culture broth samples eventually became experimentally indistinguishable from the fresh medium samples.

Figure III-19.

Phenylalanine and Tyrosine Concentration Profiles During Transient Growth Phase
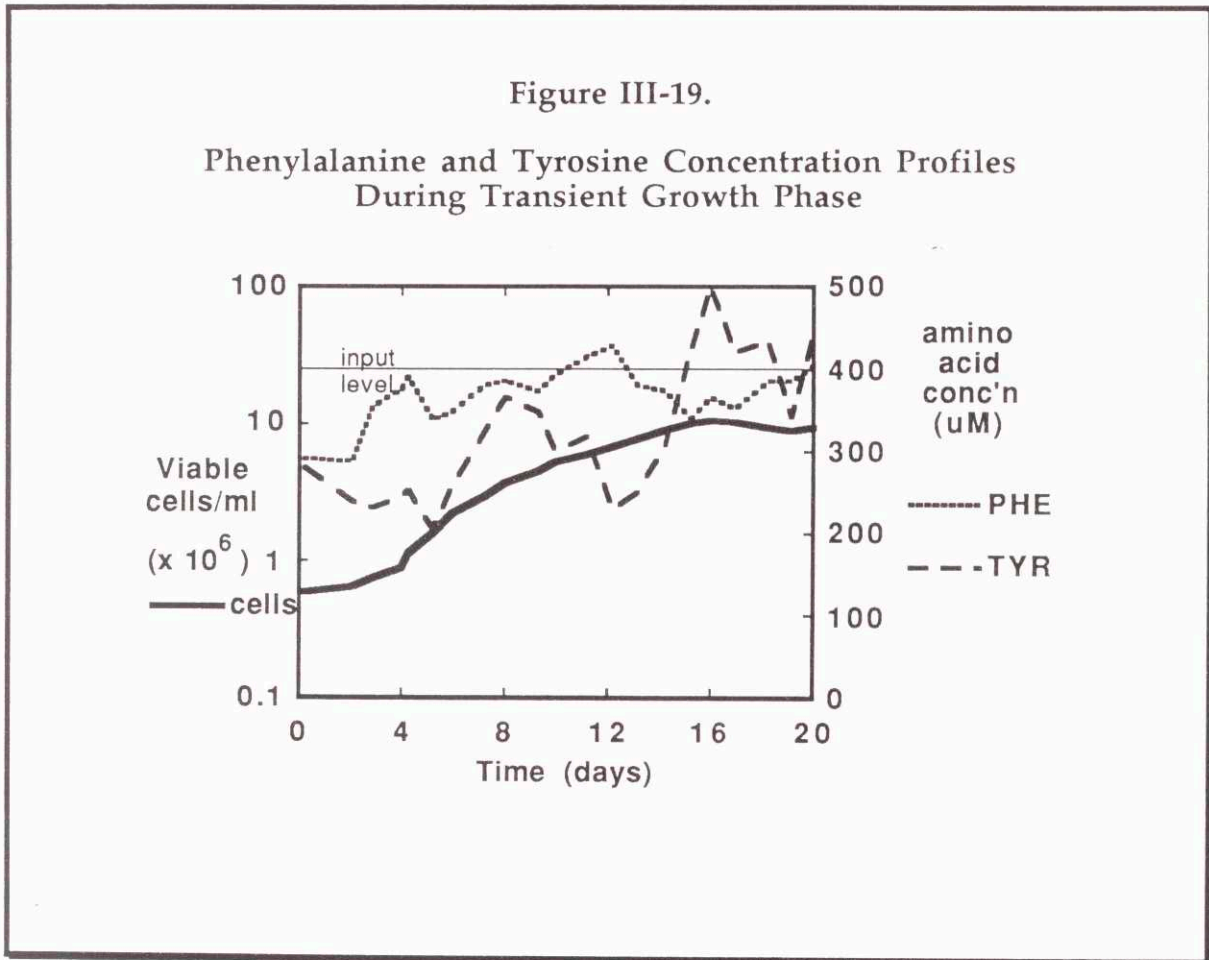
The specific rates of phenylalanine and tyrosine uptake during the transient growth phase are shown on figure III-20. The specific phenylalanine and tyrosine rates fell from a high of 10 and 25 fmol/cell-h, respectively, to less than 2 fmol/cell hr during the transient.

Figure III-20.

Specific Phenylalanine and Tyrosine Uptake Rates
During Transient Growth Phase
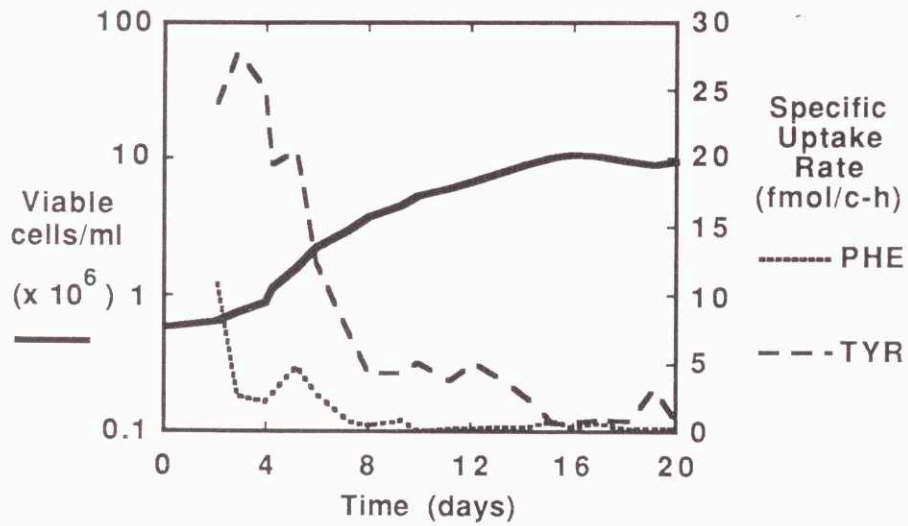
Threonine and lysine are essential amino acids supplied at 800 µM in fresh medium. Figure III-21 shows the concentration profiles for threonine and lysine in culture #1 during the transition to high cell density. As the cells increased in density, these amino acid concentrations also increased. Since there is no biosynthetic pathway for these amino acids in mammalian cells, the uptake rates must have been falling.

Figure III-21

**Threonine and Lysine Concentration Profiles
During Transient Growth Phase**

113
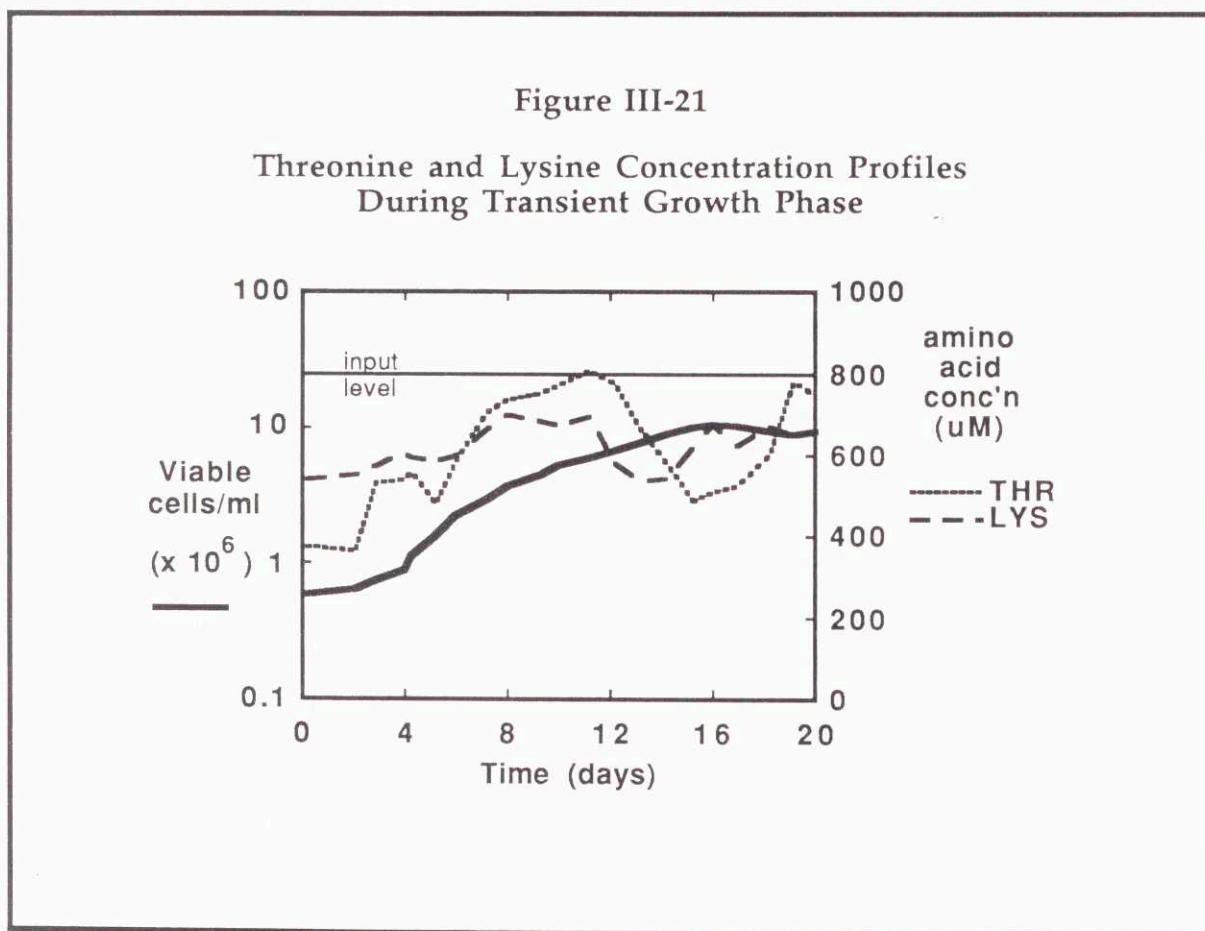
The specific uptake rates for threonine and lysine during the growth phase are presented in figure III-22. The uptake rates of these amino acids declined during cell growth, too. The uptake rates of threonine and lysine fell from initial values of approximately 40 and 15 fmol/cell-h to less than 2 fmol/cell-h. Moreover, it can be seen on figure III-22 that the shift to very low uptake rates for these two amino acids was complete when the cell density was about 4×10^6 cells/ml, a considerably lower cell density than was correlated with the down-regulation in the other amino acid uptake rates.

Figure III-22.

Specific Threonine and Lysine Uptake Rates During Transient Growth Phase
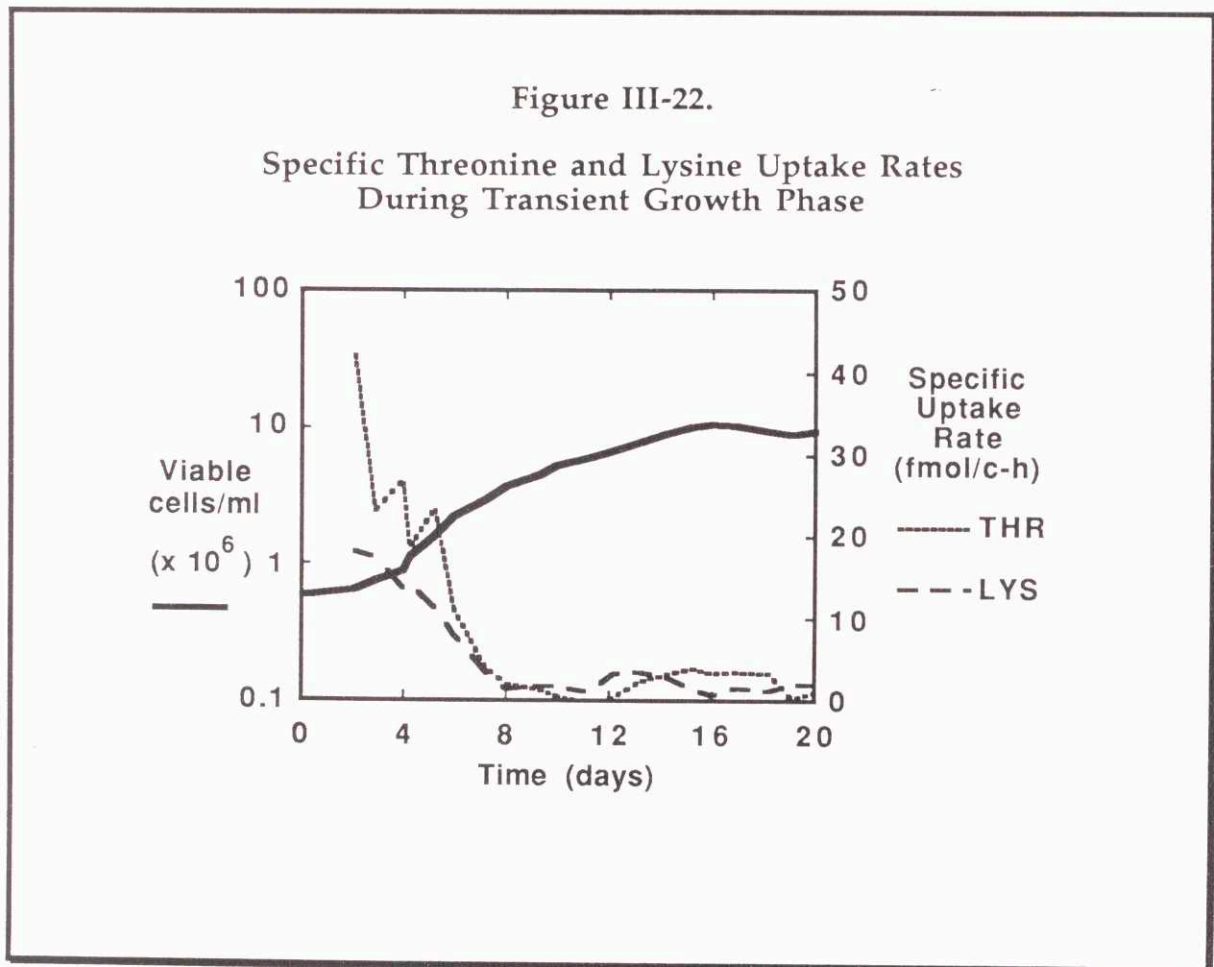
The acidic amino acids aspartate and glutamate are not supplied in the medium, but glutamate is present in significant amounts in serum. Both of these amino acids play important roles in intermediary metabolism, functioning as precursors to several other amino acids as well as to nucleotides. These cells apparently are able to regulate their membrane permeability for the acidic amino acids to the extent that the acidic amino acids do not accumulate in the medium to any great extent. Figure III-23 shows the concentration profiles for aspartate and glutamate during the transitional phase for culture #1.

Figure III-23

Aspartate and Glutamate Concentration Profiles During Transient Growth Phase
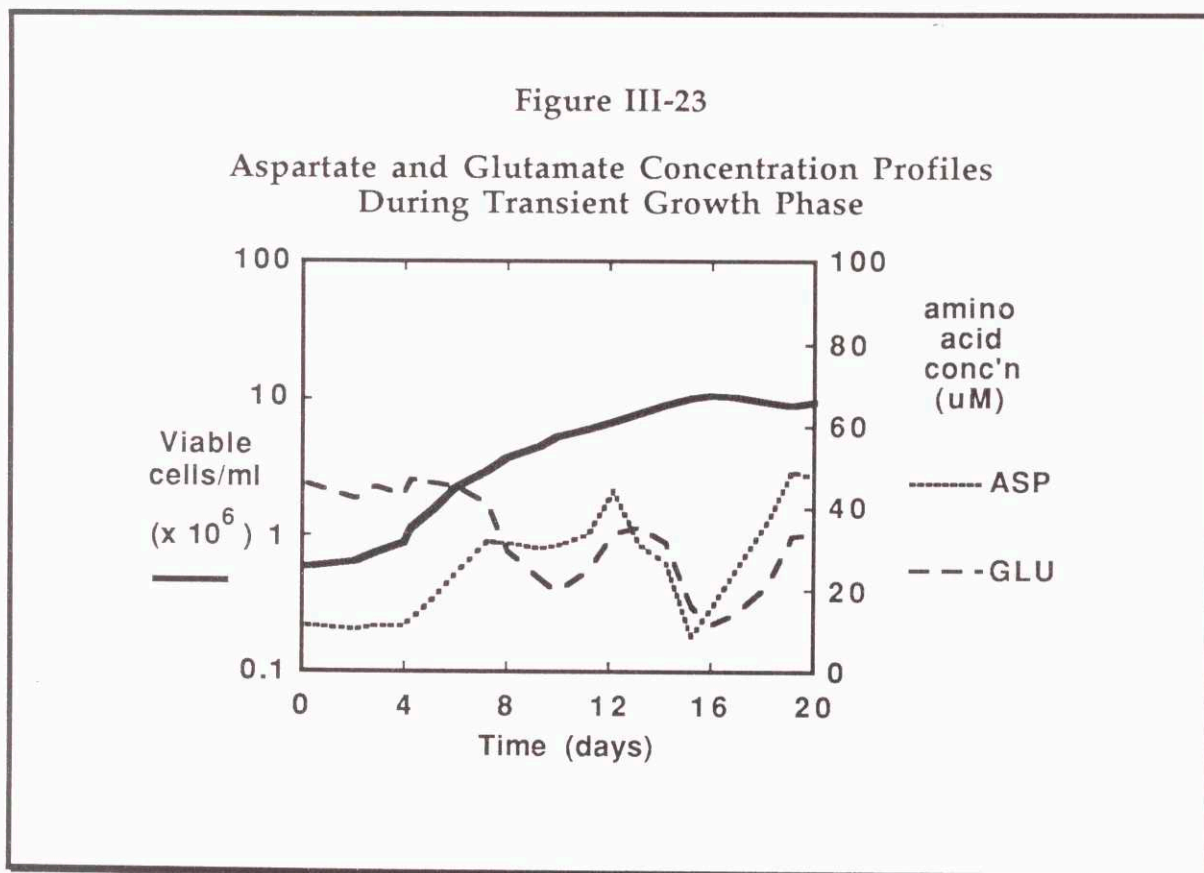
Since glutamate and aspartate were already present in the serum used to supplement the medium, the baseline concentrations of these two amino acids were not zero, but instead 10-20 μM. Therefore, the low concentrations found in samples of culture broth are difficult to distinguish from the original feed concentrations. Since the calculation of uptake rates is based on the difference between inlet and broth concentrations, rate measurements for these amino acids, presented in figure III-24, are very rough estimates. Since the overall magnitude of uptake/production rates are very low for these acidic amino acids, less than ±1 fmol/cell-h, they account for a very small fraction of net amino acid transport.

Figure III-24.

Specific Aspartate and Glutamate Rates During Transient Growth Phase
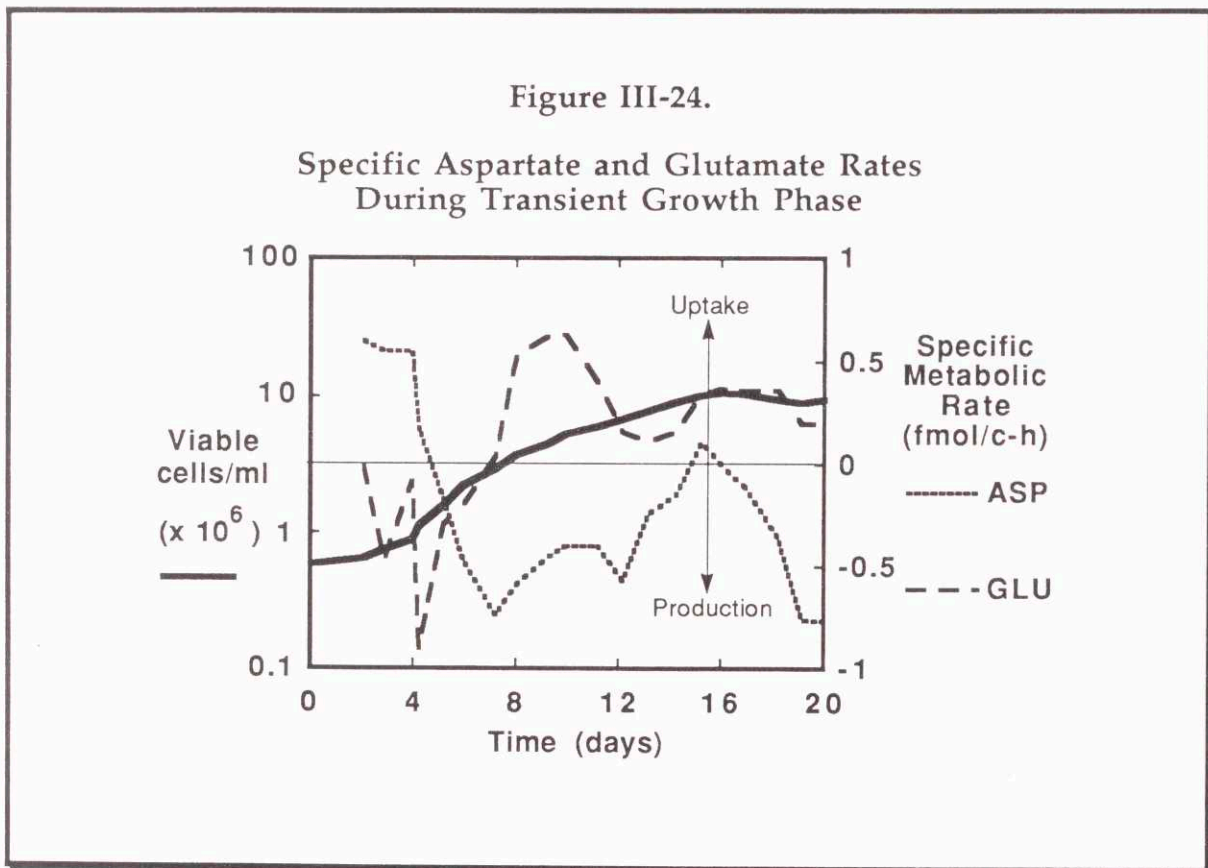
Proline and asparagine are omitted from the medium because they are easily synthesized by the cells from glutamate and aspartate, respectively. Glycine is supplied at an initial concentration of 400 μM. Figure III-25 shows the proline, asparagine, and glycine concentration profiles for culture #1 during the transient growth phase. It is apparent that all three amino acids are released into the medium by the cells.

Figure III-25.

Asparagine, Glycine, and Proline Concentration Profiles During Transient Growth Phase
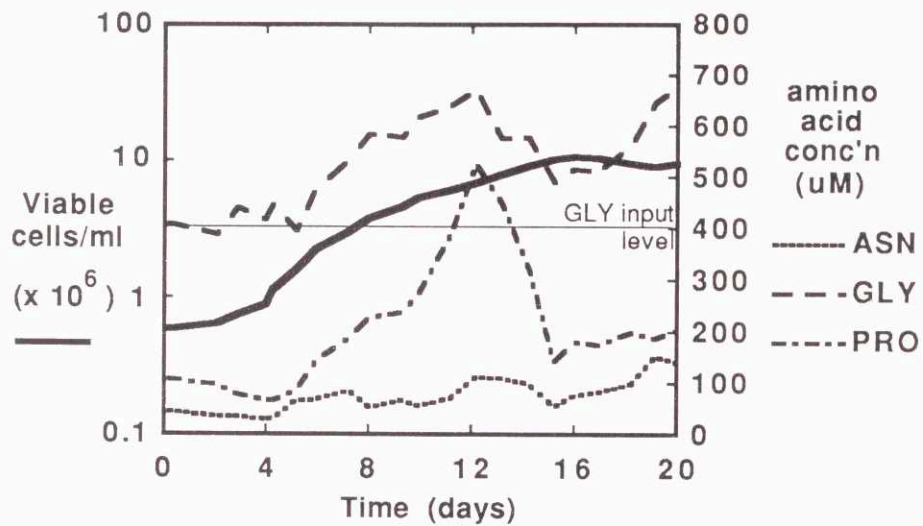
The specific asparagine, glycine and proline formation rates during culture #1's transient phase are presented in figure III-26. All three production rates reach minimal levels on day 15, when the cell density reaches 10^7 cells/ml. It is clear that amino acid production is also down-regulated concurrently with the approach to high cell density.

Figure III-26.

Specific Asparagine, Glycine, and Proline Production Rates During Transient Growth Phase

118
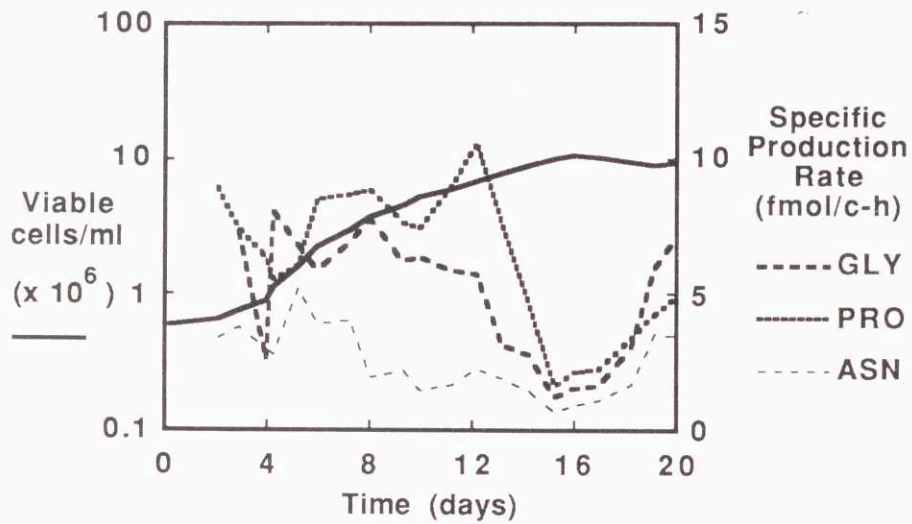
Arginine, methionine, and cystine are originally present in the fresh medium at 400, 200, and 200 μM, respectively. Inlet medium samples taken from a spent medium reservoir contained only about 250 μM arginine. It is not known whether this discrepancy arises from error in formulation or reflects breakdown of arginine. Lambert and Pirt showed that, under certain conditions, arginine is unstable in cell culture media, declining in concentration by 11% over 6 days at 37°C. Methionine and cystine were difficult to quantitatively analyze in the DABS-amino acid reverse phase HPLC system because the peaks associated with them were small and sometimes merged with nearby peaks. Figure III-27 shows the concentrations of arginine, methionine, and cystine found in culture #1 during the transitional period.

Figure III-27.

Arginine, Methionine, and Cystine Concentration Profiles During Transient Growth Phase
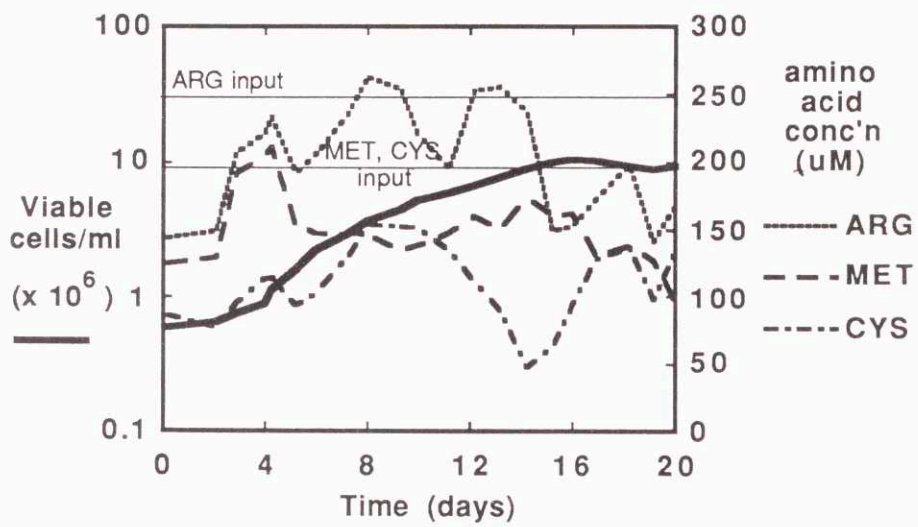
The specific uptake rates of arginine, methionine and cystine are shown in figure III-28. These rates fall from an early high of about 5 fmol/cell–h to about 1 fmol/cell-h as the cells reached a density above 10^7 cells/ml. As noted earlier, the assays of methionine and cystine suffered from considerable scatter, accounting for the spread in the calculated rates. When the cell density exceeded 10^7 cells/ml, however, the uptake rates of these amino acids did not contribute much to the total amino acid uptake rate.

Figure III-28.

Specific Arginine, Methionine, and Cystine Uptake Rates During Transient Growth Phase
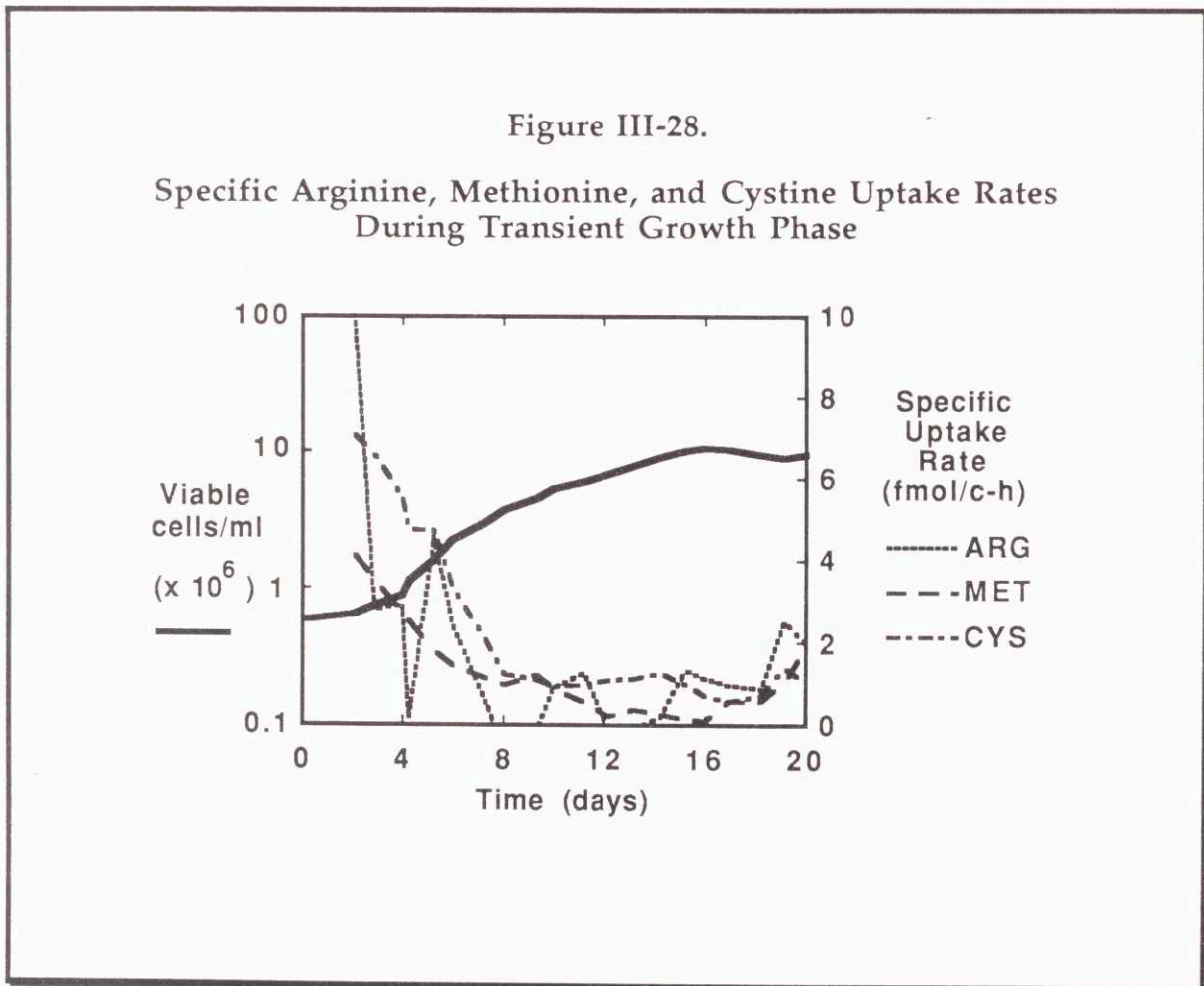
Serine and tryptophan are supplied in the medium at 400 and 78 μM, respectively. Serine, in addition to providing building blocks for protein synthesis, is an important source of single carbon units for nucleotide biosynthesis. After a carbon atom is extracted from serine by serine hydroxymethyltransferase, the remaining carbon skeleton is released as glycine. Although tryptophan can serve as a precursor to nicotinamide in the liver, it functions primarily as a protein constituent in transfectoma cell culture, especially since nicotinamide is already present in the medium. Figure III-29 shows the serine and tryptophan concentration profiles during the transient phase.

Figure III-29.

Serine and Tryptophan Concentration Profiles During Transient Growth Phase
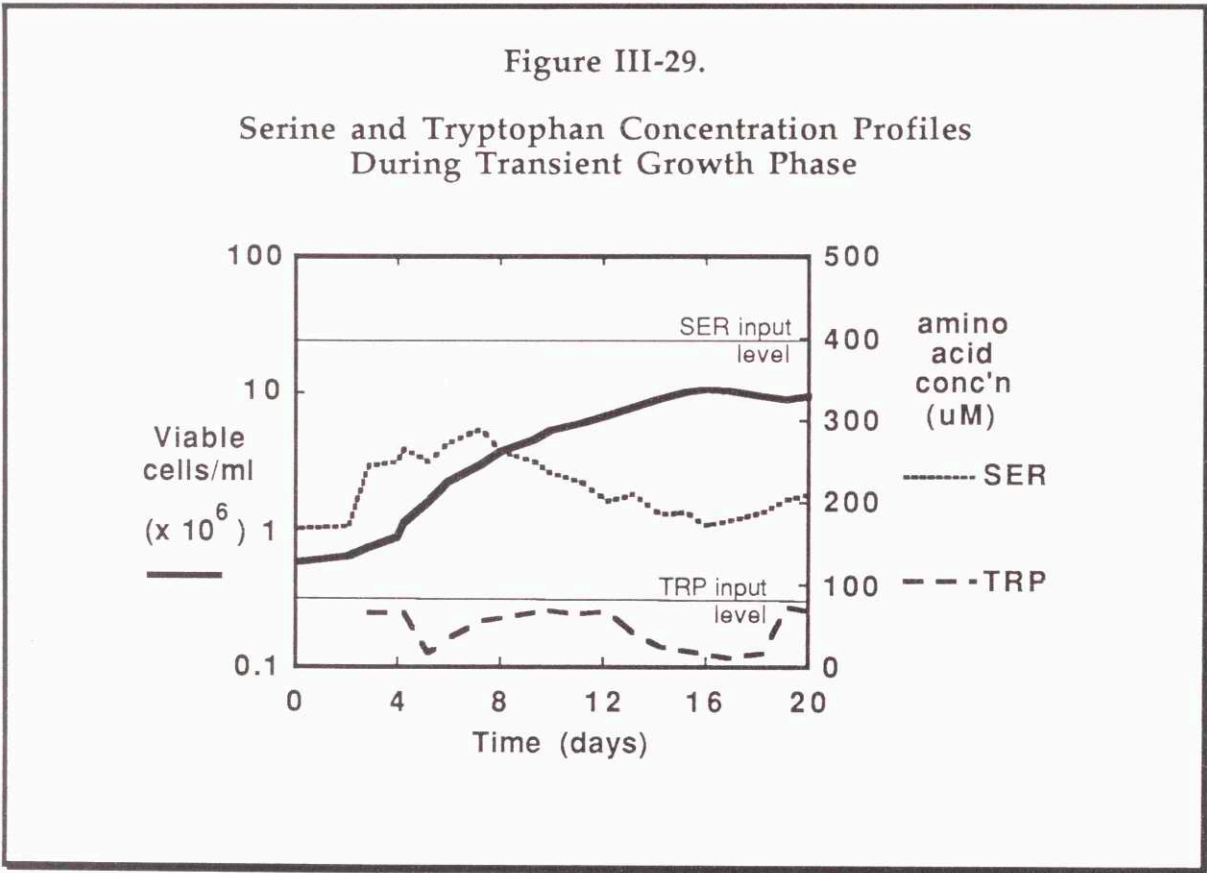
The specific uptake rates for serine and tryptophan during the growth transient are shown in figure III-30. As the cell density increased, both uptake rates declined, though to different extents. While the tryptophan uptake rate fell to 1 fmol/cell-h, the serine uptake continued at 2-3 fmol/cell-h. Possibly this difference reflects the serine requirement for generating the single carbon units used in nucleotide biosynthesis.

Figure III-30.

Specific Serine and Tryptophan Uptake Rates During Transient Growth Phase

Viable cells/ml (x 10^6)

Specific Uptake Rate (fmol/c-h)

-----SER

——— TRP

Time (days)
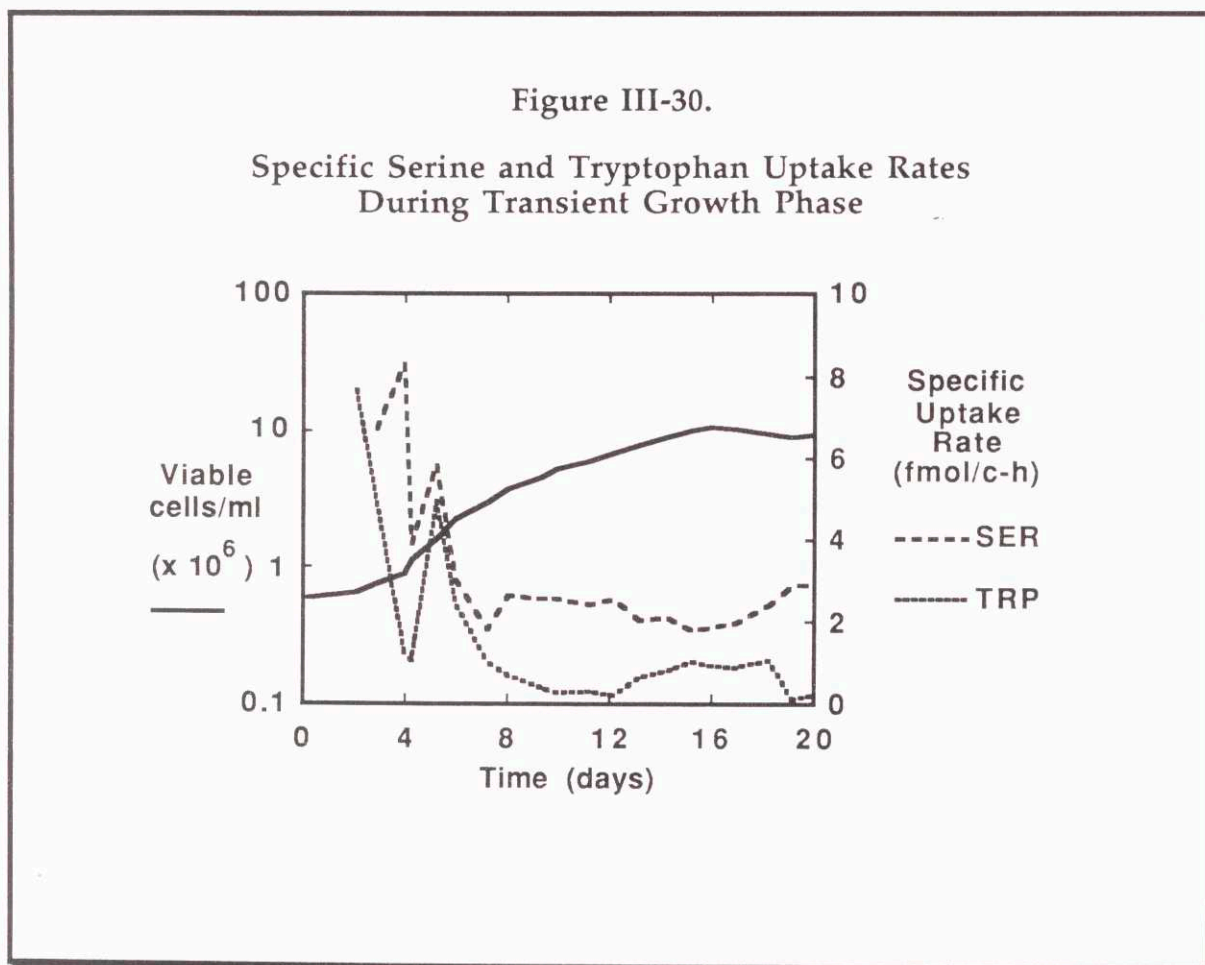
Although some differences between individual amino acids were seen with regard to their patterns of uptake or production, most of the specific rates followed a similar pattern. This pattern can best be seen by summing the total values of the specific rates of amino acid uptake plus formation. This procedure generates a parameter which is indicative of the total amino acid transport across the cell membranes. Since PCA, the breakdown product of glutamine, is consumed at a high rate by the cells, and is probably utilized by the cells as glutamate (see ATP Generation, next section), it has been included in the total amino acid transport calculation.

Figure III-31 presents the calculated *total* amino acid uptake rate (in which, for instance, the rate of alanine production is added to the rate of glutamine uptake) for the cells in culture #1 during the transitional growth phase. PCA accounts for about 20% of the total amino acid transport. The total amino acid uptake falls from an early value of 300 fmol/cell-h to a low of about 75 fmol/cell-h, representing a 75% decline in specific amino acid transport as the cells increased in density from 5×10^5 to 10^7 cells/ml. Despite this great decline in amino acid metabolism, the cells continued to grow exponentially during this entire period. The calculated growth rate of the cells did decline during the transient. During the early transient period, at a cell density of 1.6×10^6 cells/ml, the doubling time was about 21 hours. When the cell density reached a steady-state value of 10^7 cells/ml, the calculated growth rate was about 41 hours. However, this approximate 50% decline in growth rate cannot alone account for the observed decline in the total specific amino acid uptake rate, especially in light of the fact that the uptake rates of several essential amino acids declined by more than 90% (see figure III-18).

124

The late increase in total specific amino acid uptake rate which began at day 17 is coincident with the increase in medium flow rate from 3 to 5 volumes/day. Presumably, the sudden increase in nutrients, decrease in waste products, and (temporary) decrease in cell density contributed to this stimulation of metabolic rates.

Finally, it must be understood that the decrease in amino acid metabolism seen in figure III-31 is **not** the result of nutrient exhaustion. The concentration profiles of the carbohydrate and amino acid nutrients show that as the cells increased in number, decreasing rates of metabolism prevented depletion of nutrients. Thus, the pattern of down-regulation seen with these metabolites reflects a more fundamental change in the cells behavior.

Figure III-31.

Total Specific Amino Acid Transport Rate
During Transient Growth Phase
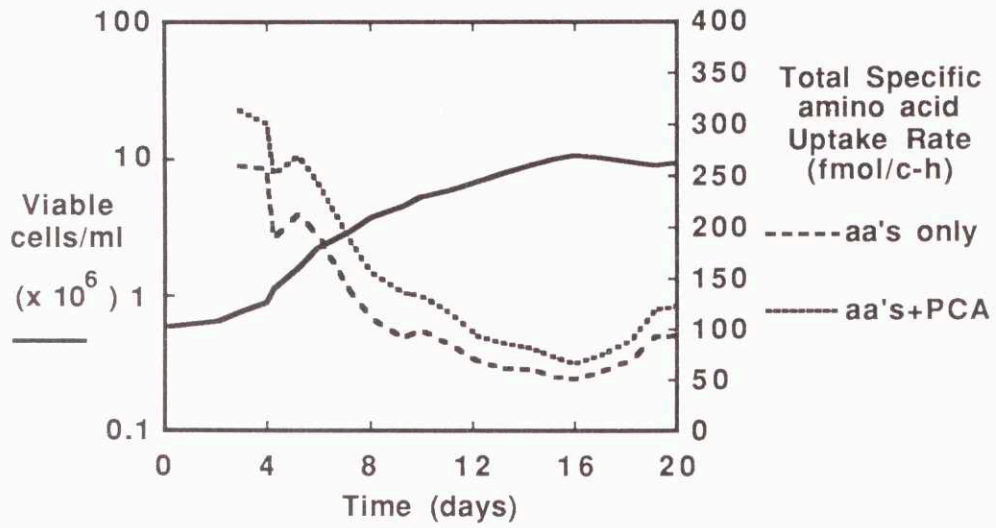
6. ATP Generation

The estimated ATP generation rate is valid only if several simplifying assumptions are made concerning ATP yield from glycolysis and glutaminolysis. Glycolytic ATP generation generates 2 moles of ATP for each mole of ATP converted to lactate. The rate of glycolysis can be estimated by either of two ways: measuring the glucose uptake rate or the lactate production rate. Either means has its shortcomings. Glucose is converted to substrates other than lactate in the production of nucleotides, glycoproteins and glycolipids. Therefore, the observed glucose uptake rate includes the glucose used for glycolysis as well as glucose used for biosynthesis. Lactate, on the other hand, can be produced by many other pathways, especially the partial oxidation of amino acids. Glutamine oxidation, in particular, can produce pyruvate. Much of this pyruvate is converted to alanine, a portion of which may be reduced to lactate. The partial conversion of glutamine to lactate has been observed in other experimental systems (Lanks and Li, 1988, Zielke *et al*, 1980, Lanks *et al*, 1986). Zielke's group found that about 10% of the glutamine which was utilized by human diploid fibroblasts appeared as lactate. Despite these alternative pathways for glucose utilization and lactate formation, in the cultures examined here the bulk of the lactate which appears in the medium is derived from glucose via glycolysis. Even if 10% of the glutamine consumption resulted in lactate formation, that would still account for less than 2% of the lactate which was formed. Similarly, the magnitude of the glucose uptake rate, approximately 200 fmol/cell-h, is far greater than the biosynthetic demand for glucose, based on the carbohydrate content of cells.

In order to estimate the ATP yield from glycolysis, I used the average of the glucose uptake rate and the lactate production rate to estimate the glycolytic rate. Glycolytic ATP generation was then calculated as:

$$1/2 \text{ (Glucose Uptake Rate + Lactate Prod'n Rate/2)} \times 2 = \text{ATP Rate}$$

Glutaminolysis, the partial oxidation of glutamine, is considerably more difficult to quantitate from input/output rates than glycolysis. The sequence of reactions in glutaminolysis leading to alanine formation is:

glutamine → glutamate

glutamate → 2-oxoglutarate

2-oxoglutarate → succinate

succinate → fumarate

fumarate → malate

malate → pyruvate

pyruvate → alanine
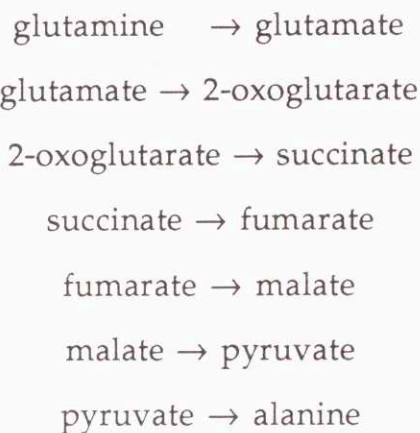
Two problems, in particular, interfere with simple glutaminolytic calculations based on glutamine and alanine rates. First, the exact distribution of endproducts actually formed from glutamine is quite uncertain. Glutamine has been shown to be converted to the organic acids lactate, pyruvate, 2-oxoglutarate, citrate, fumarate, malate, and succinate, as well as the amino acids alanine, aspartate, glutamate, proline, and asparagine. Many of these metabolites are subsequently utilized for biosynthetic processes and are thus not excreted. Pyrimidine biosynthesis, in particular, creates a significant

demand for aspartate. Aspartate, in turn, is made from oxalacetate, which might generate three more ATP's per glutamine than alanine production does (see below). Protein synthesis, of course, creates a demand for all these amino acids. Consequently, although it is technically straightforward to calculate the rates of glutamine uptake and rates of glutamine metabolite formation, one cannot determine exactly the total spectrum of endproducts made from glutamine from these rates alone.

The other major difficulty with glutaminolytic rate calculations derives from the multiplicity of metabolic pathways connecting glutamine to its endproducts. Even if one knew exactly the metabolic fate of 100% of the glutamine consumed by the cells, the ratios of alternative pathways leading to those endproducts would not be certain. For instance, parallel pathways exist to connect glutamate $\rightarrow$ oxoglutarate. In one pathway, transamination, the amino group of glutamate is passed to a keto acid. The other reaction is oxidative deamination catalyzed by mitochondrial glutamate dehydrogenase, in which the amino group is released as NH_4^+. This reaction generates NADH, which could yield 3 ATP's . Another uncertainty lies in the fate of the NADPH generated by the action of cytoplasmic malic enzyme, catalyzing the reaction malate $\rightarrow$ pyruvate. Much of the NADPH produced by malic enzyme is used for cytoplasmic reducing power for biosynthesis. Although transhydrogenases exist for interconverting NADPH and NADH, it is uncertain to what extent the cells actually use the NADPH generated by malic enzyme to reduce oxygen and thereby produce ATP.

Several assumptions must be made in order to calculate ATP yields from glutaminolysis. For the calculations to follow, I assumed that alanine is

the immediate endproduct of all glutaminolytic metabolism. I assumed that mitochondrial transamination generates the oxoglutarate from glutamate. I assumed that the NADPH produced by malic enzyme is used exclusively for biosynthetic reductions, not ATP generation. Finally, I assumed that all the PCA entering the cells is converted to glutamate (with the cleavage of one ATP per PCA) and hence enters the glutaminolytic pathway at a position one ATP down. For a justification of this assumption, see section III-2-4.

Based on these assumptions, the portions of the glutaminolytic pathway which yield ATP are:

2-oxoglutarate → succinate (+ NADH + GTP)   (=4 ATP)

succinate → fumarate (+ FADH$_2$)   (= 2 ATP)

TOTAL: 6 ATP
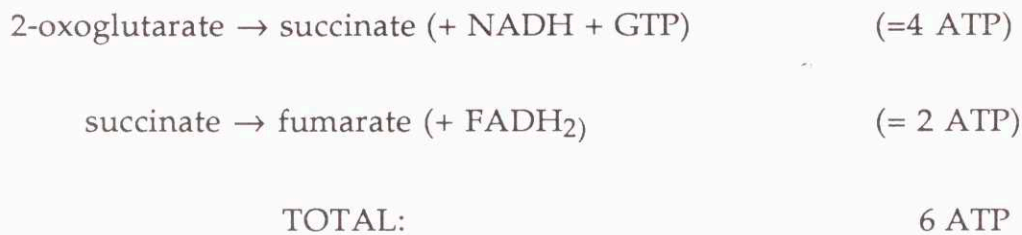
Summarizing, the formula used to calculate cellular ATP generation rates is:

ATP Rate   = Glycolytic Energy Rate + Glutaminolytic Energy Rate

ATP Rate   = (Glucose Uptake Rate + Lactate Prod'n Rate÷2) +

(6 × Glutamine Uptake Rate + 5 × PCA Uptake Rate)

This calculation was performed on the metabolite rate data for culture #1 during the transient growth phase. The results of these calculations are presented in figure III-32. Calculated ATP generation rates declined from about 1000 fmol/cell-h to about 500 fmol/cell-h as the cells grew to 10^7 cells/ml. Unlike the patterns seen in amino acid metabolic rates, energy generation declined only 50% during the transient growth phase. Like amino acid transport rates, ATP generation rates rebounded sharply on day 17, when the medium flow rate was increased from 3 to 5 volumes/day.

Figure III-32.

ATP Generation Rates During Transient Growth Phase
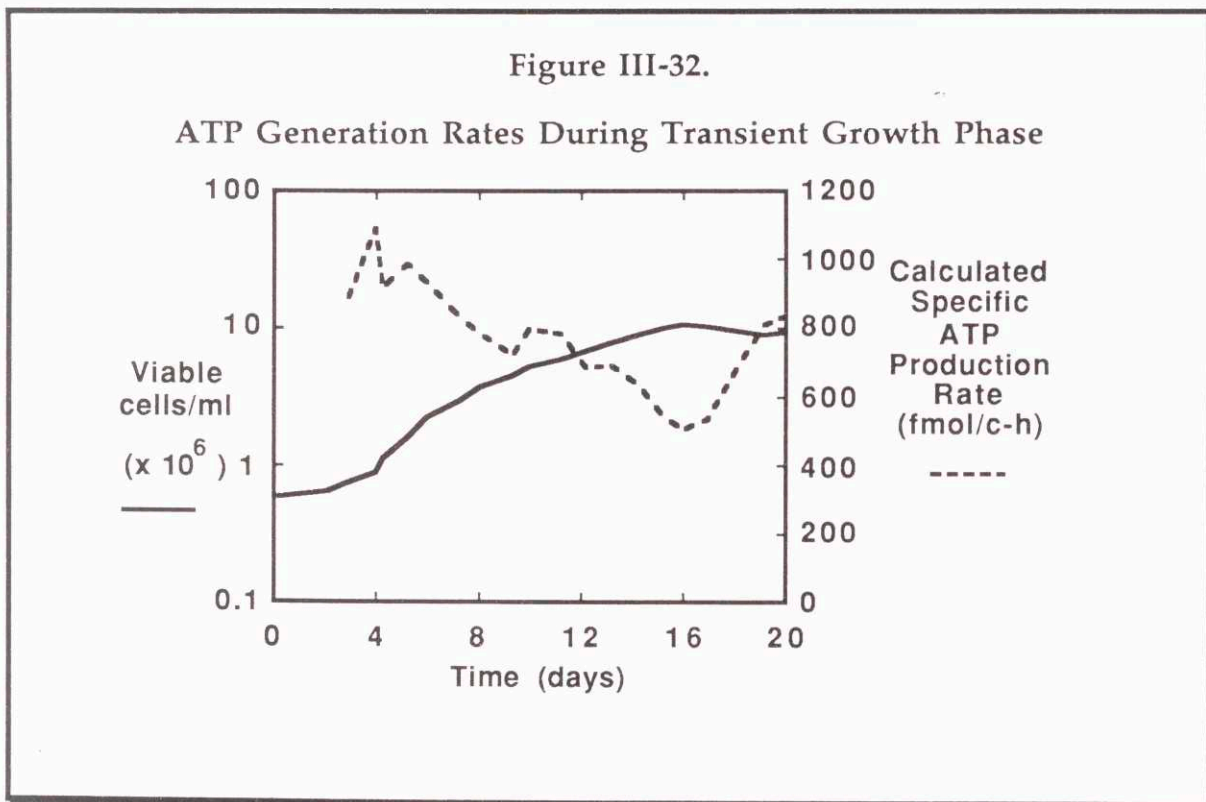
7. Redox Potential

The redox potential of a system is a measure of the potential for electrons to participate in oxidation-reduction reactions. In an oxidation-reduction reaction, electrons are passed from an electron donor to an electron acceptor. The Nernst equation relates the observed redox potential to the standard reduction potential of a given redox couple and the concentration ratio of the electron donor and acceptor species:

$$E_h = E_0' + \frac{RT}{nF} \ln\left[\frac{\text{electron acceptor}}{\text{electron donor}}\right]$$

(34)

where E_h = observed redox potential of redox couple (mV),

E_0' = standard potential of redox couple (mV),

R = gas constant (8.31 joule/°K-mole),

and F = Faraday constant (96,406 joule/volt)

The redox potential of a redox couple can be determined in a solution by measuring the concentration of each member of that pair and then applying the Nernst equation. In a complex solution containing many redox couples, equilibrium of redox potential for all couples cannot be achieved unless there exists a means of passing electrons from one redox couple to

another. Although this electron transfer will happen spontaneously, the rate of spontaneous electron transfer is very slow. This precludes near-equilibrium conditions from occurring in a dynamically changing system. Biological systems have evolved several means of rapidly transferring electrons between redox couples. The most commonly studied of these systems involves the participation of pyrimidine nucleotides and their dehydrogenases.

The pyrimidine nucleotide which is most commonly involved in catabolic processes is nicotinamide adenine dinucleotide (NAD^+) and its reduced form, NADH. Since many of the NAD^+-linked dehydrogenases have a high level of activity in the cell, the redox potential of many redox couples are at near-equilibrium. Consequently, if one is able to calculate the concentrations of both species in any one redox couple in a cell, the redox potentials of all linked couples can be determined. Knowing the intracellular redox potential, one can calculate the ratio of $[NAD^+]/[NADH]$. This ratio has special biological significance, for many allosteric enzymes at critical points in metabolic pathways have binding sites for NAD^+ or NADH to exert control over enzyme activity.

The cell has two segregated compartments with regard to $[NAD^+]/[NADH]$ ratios: cytoplasmic and mitochondrial. The $[NAD^+]/[NADH]$ ratios differ substantially between these components. Williamson *et al.* (1966) examined the localization of the NAD^+ linked enzymes lactate dehydrogenase and β-hydroxybutyrate dehydrogenase. Lactate dehydrogenase is a cytoplasmic enzyme with the high levels of activity necessary to ensure that lactate and pyruvate are always in equilibrium with cytoplasmic

[NAD$^+$]/[NADH]. β-hydroxybutyrate dehydrogenase is localized to the mitochondrial cristae, and has sufficient activity to bring β-hydroxybutyrate and acetoacetate in equilibrium with mitochondrial [NAD$^+$]/[NADH]. Williamson *et al.* reported that a potential difference of about 60 mV exists between the redox potential of the cytoplasm and the mitochondria, based on different redox potentials of the lactate and the β-hydroxybutyrate redox couples. This potential difference helps to drive electrons (in the form of reduced substrates) into the mitochondria for subsequent passage to oxygen.

In vivo, redox potentials are maintained within a fairly narrow range. Brunengraber *et al.*(1973) perfused rat livers and measured [lactate]/[pyruvate] ratios that ranged between 6 to 8, corresponding to cytoplasmic redox potentials from -238 to -242 mV. In vitro, [lactate]/[pyruvate] ratios can vary wildly. As glucose is converted to lactate via glycolysis, lactate levels can accumulate to levels far higher than those seen in vivo. Typical human plasma contains 0.7 to 1.8 mM lactate, while lactate concentrations can exceed 30 mM in vitro. Imamura *et al.* (1982) showed that MDCK cells reach [lactate]/[pyruvate] ratios which exceed 1000 after just 4 days in culture with glucose as the carbohydrate source. They showed that substitution of the glucose to a non-glycolytic carbohydrate source maintained a physiological redox potential in the cytoplasm. Siano and Mutharasan (1991) recently described a fiber optic probe they developed to determine relative changes in NADH fluorescence in a hybridoma bioreactor. They correlated changes in NADH levels with changes in dissolved oxygen concentrations in perfusion bioreactors operated at densities up to 18.1×10^6 viable cells/ml. Pulses of

glucose and glutamine into nutrient-depleted cultures also gave rise to changes in NADH fluorescence.

In the cultures used in the experiments described in this work, lactate concentrations occasionally exceeded 25 mM. pH control was maintained despite this lactate level through adjustment of the gas flow rate through the aeration tubing. Although the toxicity of lactate in cell cultures is mediated mainly from its effects on pH, the high [lactate]/[pyruvate] ratio encountered in these experiments might have additional effects on cell metabolism. Figure III-33 presents the redox potential calculated from the [lactate]/[pyruvate] ratio for culture #1 during the transient growth phase. From day 8 onwards, the [lactate]/[pyruvate] ratio exceeded the physiological range. The redox potential reached a maximum of -265 mV on day 14, as the cell density reached 10^7 cells/ml.

Figure III-33.

Redox Potential During Transient Growth Phase
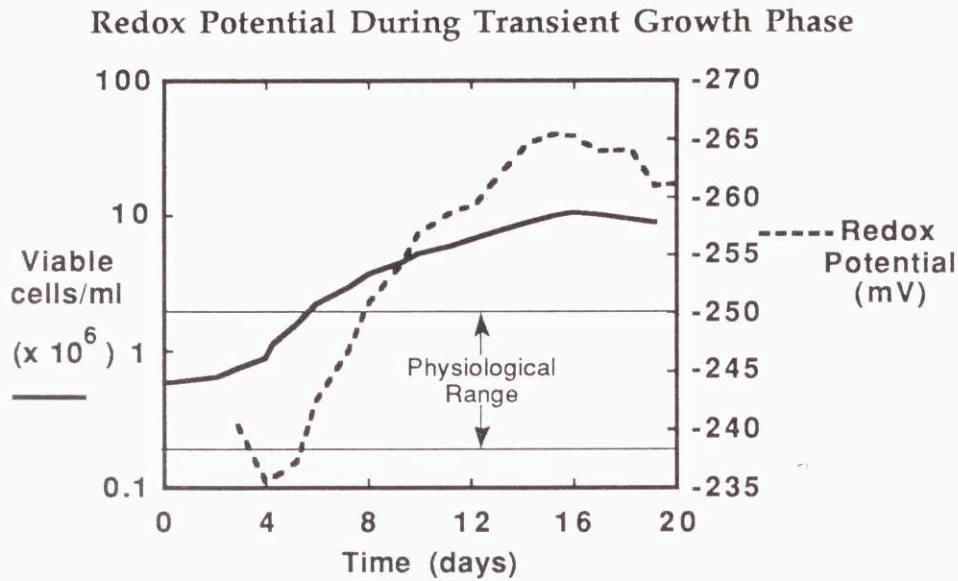
During the transition to high cell density, many of the metabolic rates changed dramatically. Amino acid uptake, PCA uptake, ATP production and IgG production all fell as the cell density increased. Although many of these simultaneous alterations *could* have been purely coincidental, it is noteworthy that the redox potential, known to be a major control parameter in many biochemical pathways, also changed during this time period. The nutrient concentration data showed that there was no exhaustion in nutrients. Dissolved oxygen levels were maintained in physiological ranges by gassing with enriched oxygen through the porous tubing, and the pH was

136

kept in control by manipulating the gas flow rate through the tubing. Consequently, the alteration in metabolic patterns observed during the transition must reflect some effect of waste products.

Figure III-34 examines the relationship between redox potential and IgG productivity. A strong correlation exists between these two parameters. Of course, the presence of a high degree of correlation between two parameters does not prove causation.

Figure III-34

**Specific IgG Productivity vs. Redox Potential
During Transient Growth Phase**

In the same manner, figure III-35 presents the correlation of total amino acid transport with redox potential. PCA uptake rates were included in this analysis because PCA can be converted easily to glutamate and thus represents a significant source of amino acids. The correlation between amino acid transport and redox potential is even stronger than that between IgG production and redox potential. The same caution regarding inferring causality exists with regard to specific amino acid transport. Nevertheless, the high degree of correlation between these two parameters, along with the fact

that redox potential is a fundamental control parameter, gives strength to the hypothesis that the reduction in cellular metabolic rates is an effect of alterations in redox potential to nonphysiological values.

Figure III-35.

Total Specific Amino Acid Transport vs. Redox Potential During Transient Growth Phase
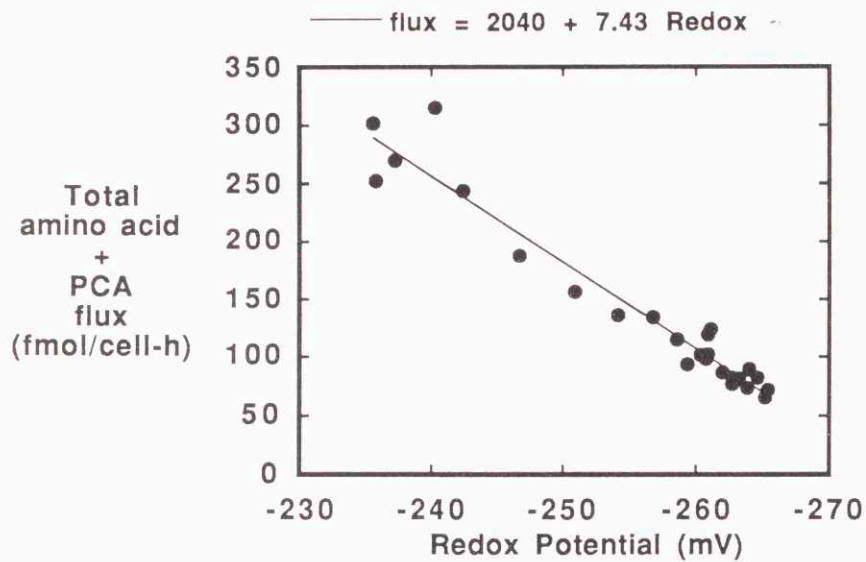
C. Steady State Phenomena

An objective of this research project was to examine the ways in which transfectoma cells can alter their patterns of nutrient uptake and waste formation in response to limitations in the food supply and/or excessive waste concentrations. The perfusion cultures described earlier were established to maintain the cells at high density at steady state in a variety of conditions. At each steady state, samples of cells and medium were collected and stored for later processing. Steady state was considered achieved when the cell density remained constant for 4 days at a constant flow rate. Data from two independent experiments was averaged to determine metabolic parameters with perfusion at 3 and 5 volumes/day with whole medium. Data for perfusion with whole medium at 9 volumes/day and diluted medium at 5 volumes/day were obtained from single cultures.

1. Environmental Conditions

The effects of two different environmental stresses were examined during the course of the experiments: excessive waste concentrations and insufficient nutrient concentrations. Through the use of the perfusion bioreactor, concentrations of nutrients and wastes were independently manipulated. *Nutrients* were limited by diluting the perfusion medium with buffered saline solution. This condition was imposed on a culture which had already achieved steady state with normal strength medium. By gradually diluting the medium over the course of several days, the cells were prevented

from drastically depleting some essential nutrient and causing undue stresses on the system. Similarly, the condition of excessive *wastes* was imposed by initiating a culture and perfusing with complete medium at three volumes/day and then simply allowing the cells to increase exponentially until conditions reached steady state. By allowing the culture to gradually approach this stressful condition, the loss of the culture due to a sudden massive accumulation of wastes poisoning the cells was averted.

Table III-1 shows a summary of the environmental conditions to which the cells were exposed as a result of the manipulations described above. The **transient** condition existed as the cells were in the fifth and sixth days of the culture, when the cell density was low. **Steady state** conditions show the result of increasing the perfusion rate ($3 \rightarrow 9$ volumes/day), as well as diluting the medium.

The viable cell density increased considerably with an increase in the dilution rate from 3 to 5 volumes/day, and a slight cell density increase accompanied an further increase in dilution rate to 9 volumes/day. This phenomenon occurred despite increasing losses of cells from the separator with increasing flow rates. Because cell loss out the separator, ε, increases with increasing perfusion rate, this particular bioreactor system has a maximum theoretical viable cell density. Improvements in the separator's cell retention characteristics could increase this maximum cell density considerably. Perfusion with medium diluted 50% with buffered saline caused a decline in the viable cell density of 43%, as compared to perfusion with whole medium at the same rate (5 volumes/day).

Cell viability, as measured by Trypan Blue exclusion, varied with the conditions in the bioreactor. It was highest during the early transient period. At steady state, the viability depended strongly on the perfusion rate. At 9 volumes/day, the viability approached that seen during the early transient phase. As the perfusion rate decreases, viability also decreases. This was not caused by any particular effect of the perfusion rate on death rates (see table III-2), but rather by the differential removal rates of live and dead cells.

Table III-1.

Environmental Conditions in the Perfusion Bioreactor

	Viable Cell/ml ($\times 10^6$)	Viability (%)	qp IgG fg/c-h	Glucose mM	Lactate mM	Gln mM	Redox Value mV
A: Transient Early Growth Phase (5-6 day) 2 Vol/day	1.6	83	230	18	6	2.0	-241
B: SteadyState 3 Vol/day	9.8	63	9.5	8	27	1.3	-266
5 Vol/day	14.0	72	1.6	10	24	1.8	-265
9 Vol/day	15.6	81	N/A	14	21	2.5	-266
5 Vol/day (Diluted 1:1 with saline)	8.0	58	7.7	1.2	21	0.3	-265

N/A = Not Applicable (Cells had irreversibly drifted to non-production prior to culture

The IgG productivity, measured as femtograms IgG produced per cell per hour, decreased precipitously as the system achieved high cell density steady states. Due to difficulties in accurately measuring IgG concentrations below one microgram/ml, differences in IgG productivity between the steady states are not significant. The IgG productivity was not measured at 9 volumes/day because the cells used for that culture had drifted to a non-producing phenotype during the several months that the cells were maintained in T-flasks prior to the experiment. This type of long-term loss of productivity in hybridoma cells was also reported by Schmid *et al.* (1990) and by Frame and Hu (1990a). Producing cells were subcloned from master stocks and frozen at -130° by L. Tsuruda following the discovery of phenotypic drift. Subcloned cells were thawed immediately prior to the initiation of all subsequent experiments.

A detailed study in the mechanism of the drop in IgG productivity as cells reach high density is the subject of ongoing doctoral research by C. Buser and J. Morrill. They have found that the near total shutdown in IgG productivity as the cells reach high density ($> 5 \times 10^6$ cells/ml) is reversible. They observed that cells removed from the bioreactor at high density and grown in batch cultures at low density (10^5 to 10^6 cells/ml) exhibit normal levels of IgG productivity, about 0.25 pg/cell-h. C. Buser has shown that the cells in the high density state have 30-50% of the "normal" intracellular concentration of IgG mRNA, while IgG secretion levels are >1% of normal. Using fluorescent immunostaining techniques, J. Morrill has shown that cells

143

in the high density state have almost no intracellular IgG molecules. These facts lead to the conclusion that this density dependent down-regulation of IgG synthesis is mediated by a block in translation, not transcription or post-translational processing.

During the early transient phase, glucose and glutamine levels were high, and the lactate concentration was low. The redox potential, -241 mV, was within the normal physiological range of -238 to -250 mV. At all steady states the lactate concentration was quite high, reaching a peak of 27 mM with 3 volumes/day perfusion. Increasing the perfusion rate increased the glucose and glutamine and decreased the lactate levels, as expected. However, the increased waste removal rate at high perfusion rates was partially offset by the higher cell density, which produced a higher level of waste production. A tripling of the perfusion rate, therefore, produced only a 22% decline in lactate levels.

Perfusion with diluted medium created conditions with low levels of nutrients. Under these conditions, the cells consumed over 90% of the glucose and over 80% of the glutamine supplied in the medium. The glutamine concentration fell to just 300 μM, and glucose fell to 1.2 mM. At high cell density steady state, redox potentials were consistently about -265 mV, well outside the normal physiological range.

2. Growth and Death Rates

The calculated values for cell growth and death rates are presented in table III-2. These rates were calculated using equations 22, 25, and 26 (section II-C-1). In order to determine true growth rates, the death rate and the apparent growth rate must first be estimated. These parameters require nine laboratory measurements each (cell densities and viabilities in bioreactor and in outlet stream for two time points, plus flow rate), so they are very susceptible to experimental error. In addition, the calculations involve differences between successive measurements, so small errors become magnified in the process. A practical difficulty arose in these measurements, because the system is designed periodically to allow the passage of an air bubble through the separator in order to maintain the culture at constant volume. Whenever this occurred, the cell density, both alive and dead, in the outlet stream would be temporarily elevated because of the disturbance in the settler imposed by the rapidly moving, large bubble. Thus, inadvertent overestimations of the production rates of dead and live cells were sometimes made. Although considerable efforts were made to avoid sampling the system soon after such a disturbance, it was occasionally unavoidable. The use of three point running averages, plus averaging data for two independent cultures served to reduce the magnitude of error in the determination of growth and death rates. Nevertheless, the values given in table III-2 should be interpreted with caution in light of these considerations.

Table III-2

Growth and Death Rates in the Perfusion Bioreactor

	Viable Cell/ml (×10⁶)	Apparent Growth rate (hr^{-1})	Death Rate (hr^{-1})	True Growth Rate (hr^{-1})	Doubling Time (hr)
A: Transient Early Growth Phase (5-6 day) 2 Vol/day	1.6	.037	.004	.033	21
B: Steady States 3 Vol/day	9.8	.029	.013	.016	42
5 Vol/day	14.0	.053	.021	.031	22
9 Vol/day	15.6	.037	.013	.024	29
5 Vol/day (Diluted 1:1 with saline)	8.0	.048	.021	.027	26

The doubling time during the early growth phase was about 21 hours, nearly the maximum growth rate seen for these cells. Death rates during this phase were very low. The death rates at all high density states were substantially higher than during the low density early transient. Perfusion at only 3 volumes/day, a high waste level condition, increased the doubling time to just over 40 hours. Relieving this environmental stress by increasing the perfusion rate gave doubling times under 30 hours. Dilution of the medium with saline produced only a modest decrease of the calculated growth rate and no apparent change in the death rate.

3. Amino Acids

Table III-3 presents the specific amino acid uptake rates which were measured in the perfusion bioreactor during the early transient (days 5-6) and at each of the steady states. Negative values denote net production. The totals are the sum of the absolute values of uptake, showing total transport (uptake + formation).

The values for cellular amino acid content were adapted from Mohberg and Johnson (1963). They used acid hydrolysis of murine L-929 fibroblast cell proteins to yield free amino acids, which were then measured on a Beckman amino acid analyzer. This process destroys several amino acids, so methionine, cystine, and tryptophan were assayed separately. Acid hydrolysis also converts glutamine to glutamate, and asparagine to aspartate. Glutamine and asparagine cell contents in table III-3 were estimated by assuming that half of the post-hydrolysis glutamate was derived from glutamine. A similar assumption was used to estimate the asparagine content of L-cells.

It is clear from a comparison of the cellular amino acid composition with uptake rates that a great deal of amino acid metabolism is occurring within the cells. Some amino acids, especially glutamine, are consumed ar rates far in excess of the requirements for protein synthesis, while other amino acids, such as alanine, proline, and glycine, are produced in such excess by the cells that they are excreted. The uptake and production rates are higher during the early transient phase than at any steady state. This is a restatement of section III-B (Transient Phenomena), which showed a rapid decline in amino acid rates during the early transitional period.

147

Table III-3

Specific Amino Acid Uptake Rates in the Perfusion Bioreactor

Amino Acid	Cell Content mole%	Early Transient fmol/c-h	3 Vol/day fmol/c-h	5 Vol/day fmol/c-h	9 Vol/day fmol/c-h	5 Vol/day (Diluted) fmol/c-h
Alanine	6.3	-36	-15	-21	-30	-19
Arginine	14	2.6	0.84	0.67	0.04	1.8
Aspartate	3.6	-0.46	-0.17	-0.38	-0.71	-0.83
Asparagine	3.6	-4.4	-1.2	-1.3	-0.81	-1.06
Cystine	1.4	3.4	0.23	0.35	ND	ND
Glutamate	4.7	-.15	0.31	.03	-0.45	-0.68
Glutamine	4.7	41	17	27	38	32
Glycine	5.9	-4.3	-1.8	-2.5	-3.2	-2.5
Histidine	5.2	ND	ND	ND	ND	ND
Isoleucine	3.6	14	1.6	2.8	5.6	5.5
Leucine	7.2	16	2.8	2.8	3.4	7.5
Lysine	12	7.5	0.34	2.8	6.8	ND
Methionine	1.9	1.5	0.72	1.4	1.3	1.4
Phenylalanine	3.5	2.8	0.42	0.86	3.0	1.1
Proline	4.1	-7.8	-2.2	-2.1	-6.4	-6.9
Serine	4.9	3.6	2.6	3.2	4.4	3.5
Threonine	4.3	12.8	1.5	2.8	5.5	2.3
Tryptophan	1.2	2.8	ND	1.5	0.72	ND
Tyrosine	2.7	13.4	0.69	0.50	4.2	4.3
Valine	5.0	14	1.6	2.0	8.2	4.6
Totals	100%	188	51	76	123	95

ND = Not Determined

The effect of metabolic waste accumulation on amino acid metabolism can be seen by comparing steady states achieved with 3, 5, and 9 volumes/day perfusion. 3 volumes/day represents the condition of waste-limited culture, while 5 and 9 volumes/day represent states of increasing relief from waste inhibition. Table III-1 showed that as the perfusion rate was increased, the viable cell density also increased. Consequently, the waste accumulation, as evidenced by the lactate levels, was only partially relieved by increasing perfusion rate. Nevertheless, table III-3 shows that this relief from waste limitation was sufficient to stimulate amino acid metabolism to a significant degree. Total amino acid transport (= uptake + production) increased by 140% as the perfusion rate was increased from 3 to 9 volumes/day. The effect of increasing perfusion rate on the uptake rates of individual amino acids was variable. Leucine uptake increased by only 21%, while valine uptake increased by over 400%. These differences must reflect different metabolic fates of these amino acids. Those amino acids whose rates of uptake or production were very low, such as arginine, aspartate, and glutamate, show little or no sensitivity to the perfusion rates. Since these amino acids are synthesized as needed by the cells in well-regulated pathways, it is unsurprising that there would be no perfusion rate effect.

Perfusion with saline-diluted medium at 5 volumes/day, creating a state of nutritional limitation, stimulated total amino acid transport by 25%, as compared to perfusion with 5 volumes/day using complete medium. Again, there was variation between individual amino acid rates with regard to their sensitivity to nutrient limitation. Alanine, asparagine, glutamine, glycine, methionine, serine, phenylalanine, and threonine rates were only

149

slightly affected by nutritional limitation, while arginine, aspartate, isoleucine, leucine, proline, tyrosine, and valine rates were stimulated. The glutamine uptake rate could not have been much higher than observed, however, because the cells consumed most of the glutamine in the diluted medium.

4. Organic Acids

Table III-4 shows the organic acid uptake rates at different steady states and during the early transient phase. Pyruvate uptake rates were higher during the transient phase than at 3 volumes/day steady state, but relieving waste limitation by increasing the perfusion rate resulted in substantial increases in pyruvate uptake, so that at 9 volumes/day, the pyruvate uptake rate was slightly higher than it had been during the low cell density transient phase. Nutritional limitation, on the other hand, produced a dramatic decline in pyruvate uptake rates. Compared to perfusion at 5 volumes/day with whole medium, perfusion with diluted medium at 5 volumes/day decreased pyruvate uptake by over 70%.

PCA uptake rates responded similarly to pyruvate uptake rates to conditions of waste limitation. The low cell density transient phase was characterized by high rates of PCA uptake. Relieving this waste limitation via perfusion at 9 volumes/day increased the PCA uptake rate by over 200%, nearly restoring the low cell density rate. In contrast to the inhibiting effects of

nutrient limitation on pyruvate uptake, PCA uptake was unaffected by nutrient limitation.

Table III-4

Specific Organic Acid Uptake Rates in Perfusion Culture

Organic Acid	Early Transient fmol/c-h	Steady States			
		3 Vol/day fmol/c-h	5 Vol/day fmol/c-h	9 Vol/day fmol/c-h	5 Vol/day (Diluted) fmol/c-h
Pyruvate	12	3.9	4.5	14.3	1.3
PCA	52	10.8	14	33	14

5. ATP Generation

Table III-5 presents the glycolytic and glutaminolytic rate data for the early low cell density transient phase and for steady state high cell density conditions. The calculated specific ATP generation rates are also presented. The specific ATP rates were calculated using the formula presented in section III-B-6, based on 2 moles ATP per glucose $\rightarrow$ 2 lactate, + 6 moles per glutamine + 5 moles per PCA.

Table III-5.

Specific ATP Generation Rates in Perfusion Bioreactor (fmol/cell-h)

	Glucose Uptake Rate	Lactate Prod'n Rate	PCA Uptake Rate	Gln Uptake Rate	Ala Prod'n Rate	ATP Prod'n Rate
A: Transient Early Growth Phase (5-6 day) 2 Vol/day	247	323	52	41	36	916
B: Steady State						
3 Vol/day	187	341	11	17	16	513
5 Vol/day	204	381	14	27	21	627
9 Vol/day	265	529	33	38	30	923
5 Vol/day (Diluted 1:1 with saline)	278	549	14	32	19	818

Glycolytic rates are not especially elevated during the transient phase, while the PCA and glutamine uptake rates and the alanine production rate are highest during the transient phase. Only 45% of the ATP produced during the transient phase is derived from glycolysis.

The effect of waste limitation on ATP generation can be seen by a comparison of ATP generation rates during perfusion with whole medium at 3, 5 ,and 9 volumes/day. As the perfusion rate was increased, waste metabolite inhibition of ATP generation is relieved. The ATP generation rate is 80% higher at 9 volumes/day. Also, even though glycolytic rates increased by 48%, glutaminolytic ATP production increased by 150% as the perfusion rate was increased from 3 to 9 volumes/day. Consequently, the fraction of ATP generated by glycolysis decreased from 70% to only 57 % as the perfusion rate increased from 3 to 9 volumes/day. Nevertheless, the fraction of ATP derived from glycolysis was higher at all high density steady states than during the early transient phase.

The effects of nutrient limitation on ATP generation can be seen by comparing the two 5 volume/day conditions. Despite the fact that the cells were exposed to decreased concentrations of nutrients while being perfused with diluted medium, overall ATP generation increased by 30%. Glycolytic ATP generation increased by 40%, but glutaminolytic ATP generation increased by only 30%. Both of these figures represent nearly the maximum extent to which the cells could increase ATP generation, because the shift to diluted medium caused a 42% drop in viable cell density, and the remaining cells consumed nearly all the glucose and glutamine which was available.

6. Glycolytic and Glutaminolytic Efficiencies

An examination of conversion yields provides a means of evaluating the effects of different environments on the regulation of energy-yielding pathways. As glucose is consumed, a portion is used to generate biosynthetic raw material, some is passed through the pentose phosphate pathway to generate cytoplasmic reducing equivalents, and some is converted to lactate via glycolysis to generate energy in the form of ATP. If all the glucose were to be converted to lactate, then two moles of lactate would be formed for each mole of glucose consumed. This is defined as 100% glycolytic efficiency. Similarly, as glutamine is consumed, a portion is used directly in protein synthesis, some is converted to other amino acids for protein and nucleotide synthesis, and some of the excess amino acids derived from glutaminolysis represent metabolic endproducts and are excreted. Since PCA can be converted into glutamate, which is itself the first metabolite of glutaminolysis, it feeds into this same pathway. Consequently, to calculate the efficiency of glutaminolysis, one must consider the ratio of endproducts formed (in this case alanine) to nutrients consumed (glutamine + PCA). Table III-6 presents the calculated efficiencies for glycolysis and glutaminolysis for early transient and steady state conditions in the perfusion bioreactor.

Table III-6.

Glycolytic and Glutaminolytic Efficiencies in the Perfusion Bioreactor

	Glycolytic Efficiency (Percent)	Glutaminolytic Efficiency (percent)
A: Transient Early Growth Phase (5-6 day) 2 Vol/day	65	39
B: Steady States 3 Vol/day 5 Vol/day 9 Vol/day	91 93 100	57 51 42
5 Vol/day (Diluted 1:1 with saline)	99	41

In the early transient phase, when the cells were at low density, both glutaminolytic and glycolytic efficiencies were relatively low. One can surmise from this that the cells were utilizing glucose, glutamine, and PCA primarily in pathways other that glycolysis and glutaminolysis. At high cell density steady states, glycolytic efficiencies were relatively unaffected by the environment, remaining in the range of 91 - 100%. In contrast, glutaminolytic conversion efficiencies were influenced by the environment. Waste

limitation tended to increase glutaminolytic efficiency. As this limitation was relieved by increasing the perfusion rate, the glutaminolytic efficiency decreased from 57% to 42%. Interestingly, inducing nutritional limitation by perfusion at 5 volumes/day with diluted medium also reduced the glutaminolytic efficiency from 51% to 41%. Presumably these differences reflect alterations in the balance of endproducts formed from glutamine in response to nutritional- or waste-induced stresses.

IV. Discussion

A. Nested Conical Separator Performance

The successful long-term operation of the bioreactors was critically dependent on their ability to separate the cells from the culture medium. Perfusion cultures were used to maintain cells at steady-state for metabolic rate determinations. Simple chemostats can maintain these cells at densities around 10^6 cells/cm^3, but cell recycle is necessary to reach much higher densities. In conventional chemostats, the cell density normally declines with increasing perfusion rates (Pirt and Callow, 1964). The problem with most mammalian cell recycle systems currently in use is that they are usually too efficient at retaining cells, including dead cells. The viability declines as dead cells accumulate in the bioreactors. The nested conical separator was able to avoid the accumulation of dead cells by a simple process of differential sedimentation.

Since dead cells are smaller than live cells, they sediment more slowly in an accelerational field. Sedimentation to retain cells in a bioreactor system has the benefit of performing a 'garbage collection' on the system, since the dead cells are preferentially removed. That is why the viability in the bioreactors was over 80% in the 9 volumes/day culture and remained above 50% under all conditions.

Many other cell separation systems suffer from a pronounced tendency toward accumulation of dead cells. Martin *et al.* (1987) described substantial cell line dependence on spin-filter separator performance. Some hybridoma cell lines they tested were unable to grow at all with the rotating-filter separator. Crossflow microfiltration to separate animal cells can result in a sustained decline in cell viability. Maiorella *et al* (1991) recently analyzed the killing of hybridoma cells in a variety of tangential crossflow separation filters and related the rate of killing to the wall shear rate in the filter unit. Shear rates above about 3000 sec^{-1} rapidly killed cells. They also examined cell death due to the pumps used to move the cells to external filters. Tip speeds above 250 cm/sec led to a rapid loss of viability. For these reasons, external cell separators have consistently given rise to low viabilities. Even some sedimentation separators fail to maintain a high viability. Kitano *et al.* (1986) described the steady loss of viability with their conical cell precipitator. The percentage of viable cells in their system declined to about 25% after 40 days. Probably this loss in viability was related to the external position of the separator. Because of the long diptube connecting the separator to the culture, cells must spend inordinate lengths of time in the separator system away from the uniform environment within the culture vessel.

There are other perfusion systems which have successfully operated at high viabilities and high densities. The ring-neck settler device of Tokashiki *et al.* (1988) maintained mouse-human hybridoma cells at 10^7 cells/ml with 70% to 80% viability over 28 days. Using the same separation system, Takazawa and Tokashiki (1989) obtained 1.1×10^7 hybridoma cells/ml with a viability of about 80%. Sato *et al.* (1983), in their internal cone-type

158

sedimentation column system, maintained a steady 95% viability as their Namalva (human lymphoblastoid) cells grew to 7×10^6 cells/ml. However, since they were perfusing the system at a maximum dilution rate of only 1.6 volumes/day, they were unable to keep up with the cells' demand for glucose. After just 11 days, the glucose level had fallen to less than 0.3 mM. Even some very carefully designed tangential flow systems can achieve high viabilities. Velez *et al.* (1989) operated their external filtration system so as to achieve 3×10^7 cells/ml at about 80% viability. After about 10 days the filtration system clogged, requiring its replacement.

The percent viability of cells obtained in the nested conical bioreactor system was dependent on the flow rate. At low flow rates, the output is 6-fold enriched in dead cells, as compared to the contents of the bioreactor. At 9 volumes/day, the enrichment ratio is 8.8. Table III-1 showed that the percent viability increased from 63% to 81% as the perfusion rate was increased from 3 to 9 volumes/day. Consequently, it can be concluded that the viability increase is caused primarily by the increased removal rate of dead cells from the bioreactor at high perfusion rates, rather than by any effect of the perfusion rate on death rates.

Another particular feature of the nested conical separator is its ability to influence the size distribution of the cells in the culture. Since small cells are preferentially removed, especially at high perfusion rates, the resultant cell population within the bioreactor is relatively enriched for large-diameter cells. Figure I-3 showed theoretical capture efficiencies for different sizes of particles as a function of channel length. At any given channel length, particles of a larger diameter have a lower value of epsilon and hence are

better retained. Figure III-2 showed the different cell size distributions in the bioreactor and exiting the separator. The differences in population distributions were greatest at the extremes of size. The smallest cells, which represented a small fraction of the cells in the bioreactor, are a much greater fraction of cells in the outlet stream. Large cells, on the other hand, are relatively underrepresented in the output stream. The segregation of populations by the separator is amplified at higher flow rates. The effect that this had on the resulting size distribution within the bioreactor was presented by figure III-4, which showed that the most frequent cell diameter at a perfusion rate of 9 volumes/day was about 12 microns, while at 3 volumes/day, the cell population peaked at about 8 microns.

As a mammalian cell undergoes a growth cycle from mitosis to mitosis, its volume changes twofold. Therefore, as the cells in an asynchronous exponentially growing culture undergo mitotic division, there is an twofold exponential age distribution function, with an associated twofold exponential size distribution function. There also exists some distribution function, presumably gaussian, for the size of **all** cells just having completed mitosis. These distribution functions combine to describe the overall age and size distributions in a culture. If a process, such as differential sedimentation, selectively removes a particular size class of cells, then it will also perform a differential age selection on the culture, preferentially removing just-divided (and hence smaller) cells. All sedimentation cell separators inadvertently remove younger cells. At present, there is no information in the literature to allow informed prediction on the effects of altering the age distribution in a culture. If the rate of antibody secretion is a

function of a cell's position in the mitotic cycle, then the use of sedimentation cell separation will have pronounced effects on the observed productivity. Suzuki and Ollis (1989) developed a cell cycle model for antibody production which they used to explain perfusion culture behavior. These effects can be either positive or negative, depending on the which position in the mitotic cycle has maximal antibody production.

Finally, in the operation of the nested conical cell separator, the perfusion rate has a pronounced effect on viable cell density. Table III-1 showed that the maximum viable cell density was achieved at the maximum perfusion rate, 9 volumes/day. The maximum cell density possible with this system has not yet been determined, but it is clear that as the perfusion rate is increased beyond 9 volumes/day, eventually the losses of cells through the separator will cause a decrease in cell density. The environment of the cells at this operating point will be very much different than at 9 volumes/day, because the increased flow rate will cause a further reduction in waste metabolites. As the perfusion rate approaches that which causes cell washout, the environment of the cells will approach fresh medium as a limit.

B. Pyrrolidone Carboxylic Acid as a Nutrient

Pyrrolidone carboxylic acid (PCA, also known as pyroglutamic acid, pGlu, and 5-oxoproline) arises spontaneously in cell culture media as a result of the breakdown of glutamine. In the literature, it has been generally disregarded as a nutrient. Glutamine breakdown has been widely investigated, but this interest has been driven by concerns about the resultant loss of glutamine as a nutrient and the accompanying production of the other byproduct, toxic ammonia (Glacken *et al.*, 1986; Ozturk and Palsson, 1990; Dalili *et al.*, 1990).

PCA exists widely in vivo. Many proteins and peptides have PCA residues at their amino terminal. For instance, the tripeptide TRF (thyrotropin releasing factor) consists of PCA-His-Pro. Baglioni (1970) found a murine monoclonal antibody with a PCA amino terminal. Stott and Munro (1972) then reported that up to 70% of intracellular mouse-myeloma IgG heavy chains they examined had N-terminal PCA. In their excellent review of PCA in proteins, Abraham and Podell (1981) describe experiments which show that the PCA which is found on the N-terminal positions of these proteins arises either by cyclization of N-terminal glutamate, or by cyclization of glutamyl-tRNA to a PCA-tRNA complex, followed by its incorporation into protein chains.

Several investigators have examined whether exogenous PCA could be incorporated into N-terminal PCA residues. Kitos and Waymouth (1966) added labelled PCA into culture medium containing L-929 murine fibroblasts. After 4 days, nearly all the radioactivity remained in the medium in the form

of PCA. Moav and Harris (1967) showed that exogenous PCA was not incorporated by rabbit lymph node cells into immunoglobulin heavy chains which were known to have N-terminal PCA. On the other hand, Rush and Starr (1970) showed that a "decyclase" enzyme activity in human myeloma cells permitted exogenous PCA to be converted into a form which could subsequently be incorporated into proteins. This publication represents the only reported instance to date of exogenous PCA utilization as an amino acid by cells in culture. Most likely this decyclase activity is the enzyme 5-oxoprolinase, which uses ATP to cleave PCA to glutamate as part of the γ-glutamyl cycle (described in section III-B-4). Interestingly, Rush and Starr showed that certain murine plasmacytomas they assayed simultaneously lacked the decyclase activity and were unable to incorporate exogenous PCA into proteins which were known to have N-terminal PCA.

This critical finding may explain the inability of certain cell lines to utilize PCA as a nutrient. 5-oxoprolinase is an enzyme of the γ-glutamyl cycle, which acts in amino acid transport to move amino acid units into the cell. Glutathione is synthesized from glycine, cysteine, and glutamate. Glutathione is exported by many cells, where it is free to react with extracellular amino acids. Following the formation of a γ-glutamyl amino acid, the complex is moved to an intracellular position by the enzyme γ-glutamyl transpeptidase. However, that this system plays a significant role in amino acid transport is not universally accepted, and it has been shown not to function in some cell lines (Viña et al., 1990). Erythrocytes, in particular, are known not to need ATP to transport amino acids, while the γ-glutamyl cycle involves ATP cleavage. If the first step in the utilization of exogenous PCA is its conversion to

glutamate via 5-oxoprolinase, and if that enzyme activity is not universally present in cells, then those cells lacking the γ-glutamyl cycle would be unable to incorporate PCA into proteins.

The indication that PCA is incorporated into proteins by the transfectoma cells used in these experiments is based on several lines of evidence:

i) PCA is consumed by the cells at a high rate.

ii) The enzymes to convert PCA to glutamate are known to be widely distributed.

iii) PCA uptake is necessary to close the glutamine balance.

Each of these pieces of evidence is discussed below.

i) PCA is consumed by the cells at a high rate

Table III-4 showed the uptake rates for the organic acids PCA and pyruvate. At the high density steady states perfused with whole medium, the PCA uptake rate ranged from 10.8 to 33 fmol/cell-h. These uptake rates for PCA are higher than those for all other nutrients except glucose and glutamine. The other organic acid, pyruvate, which is added deliberately to the medium as a nutrient, had uptake rates which ranged only from 3.9 to 14.3 fmol/cell-h. The uptake rates of other amino acids, which was presented on table III-3, show that none except glutamine is consumed at a rate which

even *approaches* the uptake rate or PCA. Lysine, for instance, which constitutes 12% of the amino acid residues in cell protein, is taken up at rates below 1.5 fmol/cell-h. The amino acids whose uptake is next after glutamine only show uptake rates ranging from 2.8 to 8.2 fmol/cell-h. So, the uptake rate of the second-place amino acid is only 20-25% of the uptake rate of PCA. Under all conditions examined, the uptake rate of PCA is much higher than all but two of the nutrients which are in DMEM*. Figure IV-1 presents a graphic comparison of the uptake rates of PCA and the other amino acids which are consumed at a perfusion rate of 5 volumes/day with whole medium. Not only is PCA second only to glutamine, but the next highest uptake rate, serine, isn't even close.

Figure IV-1.

Relative Uptake Rates of PCA and Amino Acids at 5 Volumes/Day

Uptake Rates (fmol/cell-h)
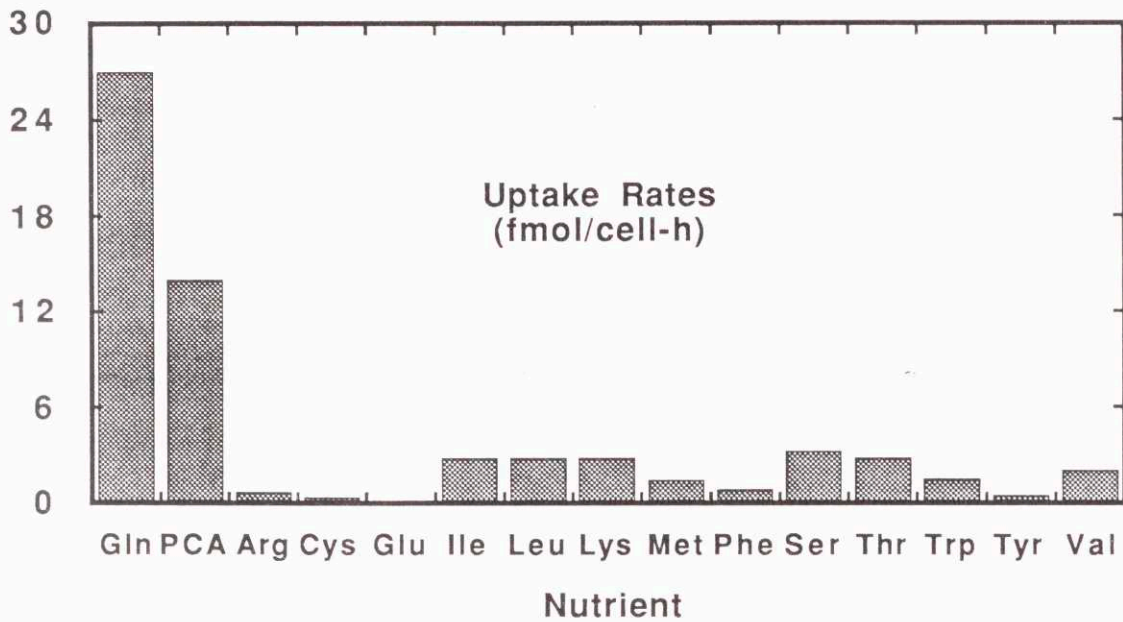
ii) The enzymes to convert PCA to glutamate are known to be widely distributed.

This line of evidence has been discussed earlier, but it will be summarized here. The involvement of the γ-glutamyl cycle in amino acid transport was proposed by Orlowski and Meister (1970). They reported that

PCA was rapidly metabolized in a variety of intact animals and tissue slices, and that the major initial product formed from PCA was glutamate. The existence of the enzyme to convert PCA to glutamate, 5-oxoprolinase, was first isolated by Van der Werf *et al.* (1971). Meister (1974) reported that when a competitive inhibitor of 5-oxoprolinase, L-2-imidazolidone-4-carboxylate, was administered to mice, PCA accumulated in the brain, kidney, liver, and eye, and that unusual amounts of PCA were excreted in the urine. Studies of excessive PCA excretion caused by inborn errors of metabolism in humans reviewed by Van der Werf and Meister (1975) led them to conclude that PCA is a normal metabolite in vivo of quantitative significance. More recently, Viña *et al.* (1986) presented the first evidence that the γ-glutamyl cycle is involved in amino acid uptake by human cells in culture. These studies together indicate that the first enzyme in a pathway to permit PCA to enter the amino acid pool, 5-oxoprolinase, is active in a variety of cells and intact tissues.

iii) PCA uptake is necessary to close the glutamine balance.

Glutamine serves as a precursor for five other amino acids. It is directly converted by glutaminase to glutamate. Glutamate is converted to proline in a two-step process, and can be converted to the tricarboxylic acid (TCA) cycle intermediate 2-oxoglutarate by a variety of paths. One TCA intermediate, malate, serves as precursor to alanine, and another, oxalacetate, can be converted directly to aspartate via transamination with glutamate. Aspartate

itself is converted directly to asparagine. Therefore, the glutamine which the cells consume can supply the needs of a total of six amino acids.

A mass balance on the glutamine family of amino acids requires the uptake or production rates of each of these as well as the biosynthetic demand for each. These amino acids not only supply units for protein synthesis, but one of them, aspartate, also serves as a structural element in the synthesis of pyrimidines. Therefore, we will consider each demand for the amino acids in turn, and then sum them and compare that total to the observed transport rates for the family under some particular defined set of conditions.

The requirements of these amino acids for protein synthesis are based on several assumptions. I am using for these calculations the assumptions that the cells are growing at a doubling time of 22 hours, the protein content is 100 pg/cell, and the nucleic acid content (RNA + DNA) is 40 pg/cell (C. Buser, personal communication). I am further assuming that the sum of purines equals the sum of pyrimidines in the RNA. Therefore, to make new biomass, the cells must synthesize 3.15 pg/hour protein and 0.63 pg/hour pyrimidines. The data from table III-3 presented specific amino acid contents of cell proteins, so we can calculate the requirements for each individual member of the glutamine family to satisfy the needs for protein synthesis. To estimate aspartate requirements to satisfy pyrimidine biosynthesis, I assumed that the average pyrimidine base has a molecular weight of 325. That makes the pyrimidine biosynthetic rate 1.94 fmol/cell-h. Table IV-1 shows the results of these calculations along with the observed uptake rates for members of the glutamine family at a perfusion rate of 5 volumes/day with complete medium. The PCA uptake rate at that condition was 14 fmol/cell-h.

168

Table IV-1
Mass Balance on Glutamine Family

Assumptions: 22 hour doubling time
100 pg protein/cell
40 pg nucleotides/cell

Amino Acid	Needed for Proteins	Needed for Nucleotides	Total Rate	Measured Rate
Alanine	1.5		1.5	-21
Aspartate	0.8	1.9	2.7	-0.4
Asparagine	0.8		0.8	-1.3
Glutamate	1.1		1.1	0.03
Glutamine	1.1		1.1	27
Proline	1.0		1.0	-2.1
Net Totals	6.3	1.9	8.2	2.2
Net Total w/PCA				16.2

The net total uptake rate for the glutamine family was just 2.2 fmol/cell-h. In fact, the only member of the family that was taken up by the cells in quantity was glutamine itself. Alanine, aspartate, asparagine, and proline were all excreted by the cells! Clearly, these amino acids alone cannot account for the requirements to meet biosynthetic demand. The cells maintain sizable pools of free amino acids and nucleotides, the supply for which was not included in the analysis. In addition, these calculations leave no room for excretion of proteins by the cells, so they represent a minimum requirement for these amino acids. However, if we include the PCA uptake

into the balance, we see a net uptake which is more than adequate to satisfy the demand, with plenty of room for protein excretion and turnover. The mass balance on the glutamine family of amino acids can only be closed if we include the PCA uptake in the total. This is the strongest piece of evidence implicating PCA in amino acid metabolism.

If the mass balance is extended to include all the amino acids, the conclusion remains. Table IV-2 presents a balance for the consumption or production of all the amino acids. Data collected during perfusion at 5 volume/day with complete medium was used for the observed rates. In order to calculate the amino acid requirement, the same assumptions were made that were used to create table IV-1. The additional calculations required were to account for the glycine and serine involvement in purine biosynthesis. Since purines are built around a nucleus of glycine, it seems logical that purine biosynthesis would create a demand for glycine. However, two single carbon units in the form of THF-bound methyl groups are required in the synthesis of purines, and thymidine also requires a THF-bound methyl group. The source of these methyl groups is serine. Through the action of serine hydroxy-methyltransferase, a carbon atom is transferred from serine to THF. The remainder of the serine molecule is released by the enzyme as glycine. Thus, nucleotide synthesis generates more glycine than it consumes, creating a net surplus of glycine. These considerations have been made for the serine and glycine balance in the calculations used to prepare table III-1.

170

Table IV-2.

Mass Balance on Amino Acids

Assumptions: 22 hour doubling time
100 pg protein/cell
40 pg nucleotides/cell

Amino Acid	Needed for Proteins	Needed for Nucleotides	Total Rate	Measured Rate
Alanine*	1.5		1.5	-21
Arginine	3.3		3.3	.7
Aspartate*	0.8	1.9	2.7	-0.4
Asparagine*	0.8		0.8	-1.3
Cysteine	0.3		0.3	.3
Glutamate*	1.1		1.1	0.03
Glutamine	1.1		1.1	27
Glycine*	1.4	-2.9	-1.5	-3.2
Isoleucine	0.8		0.8	2.8
Leucine	1.7		1.7	2.8
Lysine	2.9		2.9	2.8
Methionine	0.6		0.6	1.4
Phenylalanine	0.8		0.8	0.8
Proline*	1.0		1.0	-2.1
Serine*	1.2	4.9	6.1	2.6
Threonine	1.0		1.0	2.8
Tryptophan	0.3		0.3	1.5
Tyrosine	0.6		0.6	0.5
Valine	1.2		1.2	2.0
Totals	22	3.9	26	20.0
Total w/PCA				34

* denotes non-essential amino acid

171

Table IV-2 shows that without the addition of the PCA uptake to the balance, insufficient quantities of amino acids are consumed by the cells to account for the observed rates of protein and nucleic acid biosynthesis. Moreover, it shows the source of the glycine which is produced by the cells. Since nucleic acid biosynthesis produces more glycine than is needed to satisfy the demands of protein synthesis, the excess is excreted into the medium. That more glycine is actually excreted under these conditions than calculated is an indication of the requirement for single carbon units in other biosynthetic pathways which were not considered here.

A final consideration that a mechanism exists for the utilization of PCA in the amino acid pool is based on the argument that since glutamine is unstable in aqueous solutions, PCA formation in vivo must occur constantly, and the PCA must be returned to the amino acid pool. Wilk and Orlowski (1973) reported that PCA levels in human blood and cerebrospinal fluid were 20 and 60 μM, respectively. The normal daily urinary excretion of PCA in man is quite low, probably in the range of 4 to 40 μmoles/day (Van der Werf and Meister, 1975). These facts together suggest that a metabolic pathway exists in vivo for the reutilization of PCA formed from spontaneous breakdown of glutamine as well as from metabolic processes.

Considering all these pieces of evidence, I now conclude that PCA is indeed utilized as an amino acid by cells in culture. The route of incorporation presumably follows that of glutamate, once the PCA is converted to glutamate by the action of 5-oxoprolinase. Although the evidence presented here is insufficient to prove that the cells are using PCA

as a source of amino acids, it is highly suggestive. A simple radiolabelling experiment could quickly resolve whether PCA does indeed enter the amino acid pool.

The hypothesis that PCA can be used to help satisfy the requirements for the glutamine family of amino acids generates the intriguing possibility of substituting some or all of the glutamine in cell culture medium with PCA. Griffiths and Pirt (1967) showed that cells could be grown in media containing glutamate rather than glutamine. Hassell and Butler (1990) showed that a substitution of glutamate or oxoglutarate for glutamine in cell culture media will, after a period of adaptation, lead to increased yields and decreased ammonia production. In addition, they reported a 70% decline in cellular glycolytic rates in substituted media. Since an active system for the conversion of PCA to glutamate exists, there is good reason to believe that PCA can replace glutamine in cell culture media. The advantages of PCA over glutamine might the same as the advantages of glutamate or oxoglutarate: decreased ammonia formation, decreased glycolysis, and a far more thermo-stable medium.

C. Metabolic Shifts During Transition from Low to High Cell Density

Section III-B presented a variety of data indicating that a major down-shift in most metabolic rates occurred as the cells grew from 5×10^5 to 10^7 cells/ml. The sole exception to these declines in metabolic rates was the glycolytic rate, which remained about 200 fmol/cell-h (glucose consumption). Not only did the rates of uptake and production of metabolites decrease, but also the rate of IgG production decreased. The data gathered was insufficient to point clearly to a single causative factor for these declines. In fact, there is no evidence whatsoever that there was only a single cause for the change in individual rates seen. A multiplicity of individual causes cannot be ruled out. It is tempting, however, to apply Ockham's razor to the situation, and assume that there was a single, unifying cause which can explain all the diverse phenomena observed during the course of the transition to high cell density.

Several possibilities to explain these changes in metabolism must be considered. A simple explanation is that as the cells increased in number, they exhausted one or more nutrients in the medium. Concentrations of amino acids, glucose, pyruvate, and PCA which were observed during the transient were all presented in section III-B. It can be readily seen from these figures that the uptake rates of these nutrients were never sufficient to deplete them. Even the amino acids with the greatest percent depletion, methionine and cysteine, were never depleted by more than 50 and 75%, respectively. Their levels did not stay low very long, either, since down-regulation of their uptake rates resulted in rising concentrations. Moreover,

174

the metabolic shift was already long underway by the time these low levels were briefly attained. The only amino acid for which the DABS-Cl HPLC technique gave less than satisfactory results, histidine, was probably not depleted much more than 40%. This calculation is based on a cell density of 10^7 cells/ml, a estimated histidine uptake rate of 1 fmol/cell-h, and a dilution rate of 3 volumes/day. The estimated histidine uptake rate is based on an average of the histidine uptake rates of other cell lines from the literature for which cell densities were reported (table IV-2). However, one cannot exclude or confirm histidine limitation from these data, and *if* the histidine uptake rate was over 2.5 fmol/cell-h under these conditions, the histidine would have been exhausted. With the exception of glucose, concentrations of most of the nutrients actually *increased* in concentration as the cells increased in density due to the reduction in specific uptake rates which was more than enough to overcome the increase in cell density. Consequently, one can reject the nutritional insufficiency theory with regard to the nutrients measured.

A hypothesis which was examined in more detail to explain the transient's decrease in metabolic rates involved the state of the intracellular redox potential. Figure III-34 showed the specific IgG productivity as a function of the corresponding redox potentials. Figure III-35 showed the relationship which was observed between the total amino acid transport and the corresponding redox potential. Each of these rate parameters correlated very well with the redox potential. Some important metabolic systems, such as the fatty acid synthesis pathway, are rate controlled by the redox potential (Newsholme and Start, 1973), so it is reasonable to expect that the shifts of the redox potential to nonphysiological levels which were observed to correlate

with alterations in metabolism might play a causative role. However, mere correlation does not prove causality.

Since the changes in redox potential during the transient phase (figure III-33) were driven primarily by changes in the lactate concentration, it might be inferred that lactate concentration is the critical parameter in controlling metabolic rates. However, several investigators have attempted to correlate metabolic behavior with lactate concentrations, with limited success. Reuveny *et al.* (1986) showed that lactate at 22 mM was without detrimental effect, but 28 mM lactate reduced growth of hybridoma cells in low density batch cultures. Hu *et al.* (1987) measured initial growth rates of cells exposed to varying lactate concentrations and found that 33 mM lactate in the medium reduced initial growth rate and final cell density by only about 15%. Glacken *et al.* (1988) reported that the lactate ion itself has only a small effect on the growth rate of hybridoma cells.

As an alternative hypothesis to explain the decline in metabolic rates as the cells reached high density, one might suspect that the density of the cells itself might be the critical causative factor. Cell density effects on metabolism have appeared repeatedly in the scientific literature. The rates of very wide range of metabolic systems have been shown to correlate with cell density even when attempts to control other parameters have been made.

Foster and Pardee (1969) used the nonmetabolizable amino analogue α-aminoisobutyric acid (aib) to measure amino acid transport systems operating in 3T3 murine fibroblasts as they grow to confluence on glass. They found that a 30% drop in aib transport rate accompanied the transition from

subconfluent to confluent states. Griffiths (1972) specifically examined the effects of cell density on nutrient uptake by MRC-5 human fibroblasts. As the cell density increased from 2.4×10^5 to 5.2×10^5 cells/ml, specific uptake rates for amino acids decreased up to three-fold. Examining amino acid transport kinetics, Otsuka and Moskowitz (1974) measured the rates of leucine transport in 3T3 cells as a function of leucine concentration for cells attached to a solid surface. They examined the uptake rates for both subconfluent (low density) and confluent cultures. From this data they made Lineweaver-Burk plots and assigned values to the maximum velocity of transport (V_{max}). They showed that V_{max} was 2.4 times higher in the subconfluent cultures. Robinson (1976), in his study of mouse mammary carcinoma cells, looked at the operation of several of the amino acid transport systems as a function of cell density. Interestingly, he found that there were differences between the L-system (sodium-independent system for transporting neutral amino acids, leucine preferring) and the A-system (sodium dependent system for transporting neutral amino acids, alanine preferring) with regard to their sensitivity to cell density. The A-system is sensitive to cell density, showing a 67% drop in V_{max} as the cell density increased 16-fold, while the L-system was independent of cell density. Bhargava et al. (1975) measured the accumulation of several amino acids into rat liver parenchymal cells in solution at different cell concentrations. They saw a 70% drop in amino acid uptake as the cell density increased from 0.5×10^6 to 5.0×10^6 cells/ml. They presented evidence to indicate that this inhibition is mediated by a material released into the medium by the cells in suspension.

The effects of cell density on protein synthesis rates were also examined in Bhargava's laboratory. A very strong cell concentration dependence on protein synthesis rates was reported by Bhargava and Bhargava (1962). They saw a 71% drop in rate of incorporated ^{14}C-labelled amino acids into proteins by hepatic cord cells in suspension as the cell density was increased from 0.5×10^6 to 2.5×10^6 cells/ml. Bladé and Harel (1967) diluted mouse ascites cells from 10^7 to 2×10^5 cells/ml and observed a 4-fold increase in both the rates of protein synthesis and amino acid uptake. In an effort to model the observed behavior of the cells, they calculated a parameter related to the mean intracellular distance. This parameter correlated very closely with amino acid transport over several orders of magnitude of cell density. They also considered that the cells might be secreting an inhibitory compound to cause this effect, but their efforts to prove this were unsuccessful. Medium containing cells in suspension at 10^7 cells/ml was incubated for 15 minutes, and then centrifuged. Fresh cells were then placed in the medium at a density of 10^6 cells/ml. The rates of amino acid uptake and protein synthesis for these cells was the same as for control cells incubated in fresh medium at the same concentration. This experiment does not rule out the hypothesis that some unstable factor was involved.

Immunoglobulin production has also been shown to be sensitive to cell density. McHeyzer-Williams and Nossal (1989) examined IgG production by murine lymphocytes at very low cell density. They found maximum antibody production occurred at a density of just 10^4 cells/ml. As the cells were allowed to grow to 3.2×10^5, antibody production fell 600-fold! They concluded that

antibody production is grossly suboptimal at cell densities frequently reported in the literature.

Oxygen uptake rates were found to be quite sensitive to cell density by Sand *et al.* (1977). The specific oxygen uptake rate of lymphocyte cells increased 100-fold as the density decreased 1000-fold over a range of 10^7 to 10^3 cells/ml. The authors were able to exclude the effects of dissolved oxygen, CO_2, and lactate. They concluded that the effect was mediated by humoral factors produced by the cells. Wohlpart *et al.* (1990) placed hybridoma cells in suspension at densities ranging from 10^5 to 10^7 cells/ml and found that the specific oxygen uptake rate declined from 400 fmol/cell-h to 120 fmol/cell-h, a 75% decline. Respiration rates were unaffected by the selection of fresh or conditioned medium. In contrast to these reports, Sener *et al.*(1987) measured oxygen uptake rates of tumoral insulin-producing RIN cells at different cell densities. Over a range from 5×10^6 to 2×10^7 cells/ml, the oxygen uptake rate remained constant at 250 fmol/cell-h.

Other metabolites have been show to exhibit density-dependence in their uptake rates. Bladé *et al.*(1966) investigated phosphate uptake by ascites tumor cells. They incubated radiolabelled phosphate with cells at densities ranging from 5×10^5 to 3×10^7 cells/ml and found that the acid insoluble phosphate incorporation declined from 1.9 µg phosphate/mg protein to .019 µg phosphate/mg protein, representing a drop of 99%. Even puromycin resistance in cell cultures was found to be density-dependent. Working with pig kidney cells in monolayer culture, Cass (1979) found that the LD_{50} for puromycin increased as the cell density increased. She showed that this resistance to puromycin was mediated by a cell density-dependent reduction

in puromycin uptake. After 2 hours exposure to labelled puromycin, cells plated at 0.18×10^5 cells/cm^2 took up 5 times as much puromycin as did cells plated at 1.75×10^5 cells/cm^2.

From this review of cell density dependence on metabolic rates, we have seen that rates of amino acid uptake, protein synthesis, IgG production, oxygen uptake, phosphate incorporation, and even puromycin uptake are all sensitive to increased cell density. However, no direct evidence has been offered by the authors of these papers regarding the specific mechanism(s) by which the cells respond to high density conditions.

In an effort to determine the mechanism of density-dependent regulation of growth, Holley *et al.* (1978) found evidence for an unstable protein produced by African green monkey kidney epithelial cells which inhibited the incorporation of ^{3}H-labelled thymidine into cells. If the solution containing the putative inhibitor was shaken, its inhibitory properties were lost. Freeze-thawing, bubbling with gases, heating, or storage at 37°C also destroyed the inhibitory properties. On the other hand, Stallcup *et al.* (1984a) showed evidence for growth inhibitory activity of membranes isolated from normal spleen cells and lymphoid tumor cells. These membrane preparations could produce a 50% reduction in the growth rate of hybridoma cells. They showed that this reduction in growth was not caused by an increase in the death rate, but was a the result of a direct modulation of the cell growth rate. Stallcup *et al.* (1984b) further characterized the inhibitory activity, showing that it co-purified with the major histocompatibility class I antigens H-2 K and D by affinity column chromatography using monoclonal antibody columns. When incorporated into liposomes, the affinity purified antigens inhibited

the growth of tumor cells by 75% at concentrations of 1-3 µg/ml. The inhibition was readily reversible, since removal of the liposome preparation restored the growth rate to control values. Stallcup *et al.* (1986) presented evidence that a lipid-like component of macrophage hybridoma cells could profoundly inhibit the proliferation of B-lymphocytes. Unfortunately, the identity of the inhibitory compound(s) was never established in any of these studies.

As a result of studies such as the ones described above, we can see that there is a wide variety of inhibitory responses to the condition of high cell density. The response that was observed with the cells in the experiments described in this document, a generalized down-regulation of metabolic rates, is in excellent agreement with the body of literature concerning the effects of high density on mammalian cells.

D. Comparative Amino Acid Uptake Rates

Over the last three decades, a number of laboratories have been concerned with quantitative determinations of the metabolic requirements of cells in cultures. A variety of cell types, representing both normal and transformed cells, have been subjected to metabolic rate determinations. A driving force behind these efforts has been the realization that most cell culture media have been developed empirically, without a rational basis for the selection of nutrient concentrations. The components of cell culture media were developed by the process of elimination. One by one, ingredients in a complex mixture were omitted, and the resulting medium was evaluated for the ability to support the growth of cells. Eagle (1959) published one of the first reports of amino acid requirements for cells in culture, as opposed to the requirements of whole animals. He found that, in addition to the eight amino acids necessary for growth of humans (isoleucine, leucine, lysine, methionine, phenylalanine, threonine, tryptophan, and valine), every cell type tested, normal or transformed, required at least 5 additional amino acids (arginine, cyst(e)ine, glutamine, histidine, and tyrosine). Some substitution in the forms of these amino acids was found to be acceptable. For instance, he found that high levels of glutamate could satisfy the requirement for glutamine. Additionally, owing to the widespread activity of transaminases, the keto acid analogues of several of the essential amino acids could serve in their place.

One of the first quantitative analyses of amino acid uptake rates was published by McCarty (1962). He examined both normal and tumor human cells, publishing rates of uptake or formation of amino acids, glucose, and lactate. All the cells produced alanine, and glutamate. Most of the cell lines produced glycine and proline, as well. Metabolic rates were determined in stationary batch cultures after 48 hours of growth, starting with an initial density of 10^5 cells/ml. Griffiths and Pirt (1967) examined the uptake rates of the thirteen essential amino acids by mouse LS cells in both batch and chemostat perfusion culture. Through the use of the chemostat, they were able to investigate the effect of cell growth rate on the specific amino acid uptake rates. They reported that at doubling times shorter than 43 hours, amino acid uptake was stimulated, and that essential amino acids were consumed increasingly at rates higher than required to synthesize new cell material.

Stoner and Merchant (1972) used a chemically defined medium to examine the uptake and production of amino acids by mouse fibroblast cells in batch stationary cultures. The medium contained only the 13 essential amino acids at twice the concentrations suggested by Eagle (1959). They reported the production of glutamate, glycine, proline, alanine, serine, and aspartate. Of these produced amino acids, only serine was consumed by the cells if added to the basal medium. Also working with fibroblasts, Lambert and Pirt (1975) determined the uptakes of all essential amino acids, in addition to vitamins, glucose, and serum factors. They reported that human MRC-5 cells grew at a much faster rate (doubling time of 23 hr vs. 39 hr) if a rich supplement containing some 62 components was added to the medium.

Butler and Thilly examined amino acid utilization by MDCK cells in microcarrier cultures. They found net alanine and glycine production. In addition, they found a strong cell concentration dependence on amino acid uptake rates. As the initial inoculum density was raised from 1.6×10^5 to 4.0×10^5 cells/ml, the total amino acid transport rate (uptake + production) decreased 57%, from 269 to 116 fmol/cell-h.

More recently, Delhotal et al. (1984) compared amino acid utilization patterns obtained when fibroblast cells were grown with glucose and fructose. Compared to uptakes when the cells were grown on glucose, cells grown on fructose consumed more glutamine and many other amino acids, but produced less alanine and proline. Much more glycine was produced by cells grown on fructose.

Using the published results of the previous authors as a guideline, it is possible to compare the amino acid uptake rates measured in the high density perfusion cultures to the rates observed by other investigators in low density systems using a variety of cell types. Table IV-2 presents a comparison of the amino acid uptake or production rates. Values for this study were taken from the low density early transient phase and the high density steady state with 5 volumes/day perfusion. Negative values indicate amino acid production. Notes describing the published rates are on the page following table IV-2.

Table IV-2
Comparative Amino Acid Uptake Rates
fmol/cell-h

Amino Acid	This Study Low Dens.	This Study High Dens.	Published Amino Acid Uptake Rates (see notes for publication code)							
			1	2	3	4	5	6a Low Dens.	6b High Dens.	7
Ala	-36	-21	-1.4	-15.8	-9.0	-6.4	NR	-24	-4	-5.6
Arg	2.6	0.7	20	17	4	3.0	5.2	10.8	5.6	3.1
Asp	-0.5	-.4	-3.1	-1.1	NR	-0.5	NR	NR	NR	2.5
Asn	-4.4	-1.3	NR	NR	NR	NR	NR	NR	NR	0.2
Cys	3.4	0.3	-0.5	5.4	3.8	1.6	9.8	3.5	1.1	1.8
Glu	-.1	0.03	-16	-7.8	-15	-9.6	NR	NR	NR	NR
Gln	41	27	51.2	58.0	71.7	92	44	132	51.6	NR
Gly	-4.3	-2.5	-5.0	-1.5	-0.3	-7.2	NR	-3.3	-1.0	-5.6
His	NR	NR	5.6	5.6	2.9	0.7	0.3	2.7	1.0	0.8
Ile	14	2.8	9.9	9.0	12.1	4.7	9.4	16.9	10.6	5.2
Leu	16	2.8	11.7	10.2	13.6	5.2	9.9	19.8	11.3	3.7
Lys	7.5	2.8	9.9	10.2	9.8	0.5	5.2	8.2	3.6	0.8
Met	1.5	1.4	0.3	0.3	3.1	1.5	2.0	5.5	2.0	0.6
Phe	2.8	0.9	5.1	2.4	1.5	1.2	0.3	3.9	2.2	0.8
Pro	-7.8	-2.1	-1.5	-2.6	-1.4	-4.0	NR	NR	NR	-3.2
Ser	3.6	3.2	-.1	NR	NR	-0.7	NR	12.8	5.9	2.6
Thr	12.8	2.8	1.3	3.1	3.5	3.2	7.8	10.1	4.9	3.5
Trp	2.8	1.5	2.0	3.1	0.5	0.4	0.5	NR	NR	NR
Tyr	13.4	0.5	5.8	2.4	4.6	1.7	1.8	2.9	1.9	0.4
Val	14	2.0	8.8	0.5	9.7	3.7	8.6	13.2	9.4	3.2

NR = Not Reported

Notes for Table IV-2:

1.McCarty (1962): HeLa (human cervical carcinoma) (density unreported)

2. McCarty (1962): KB (human squamous cell carcinoma of lip)
(density unreported)

3. McCarty (1962): Hep2 (human epithelioma of larynx) (density unreported)

4. Stoner and Merchant (1972): L-M (murine fibroblasts) ($\overline{X}_{LM} = 4 \times 10^5$/ml)

5. Lambert and Pirt (1975): MRC-5 (human diploid fibroblasts)
($\overline{X}_{LM} = 10^5$/ml)

6a. Butler and Thilly (1982): MDCK (canine kidney epithelial)
($\overline{X}_{LM} \approx 5 \times 10^5$/ml)

6b. Butler and Thilly (1982): MDCK (canine kidney epithelial)

($\overline{X}_{LM} \approx 1.2 \times 10^6$/ml)

7. Delhotal *et al.*(1984): neonatal human fibroblasts   ($\overline{X}_{LM} \approx 10^6$/ml)

A comparison of the amino acid uptake rates observed in the present study with results published earlier shows that there is good agreement overall. Some particular exceptions do stand out, however.

Each of the previously published results show net production of alanine, glycine, proline, and glutamate (where data was reported). Alanine formation rates observed in this study at both high and low density are much higher than those reported in any other study. Proline formation was higher in the low density portion of this study than any other study, but the high density proline formation rate was comparable to other reports. Glycine

formation rates at high and low density were similar to other published reports. Glutamate formation was reported at high rates by other laboratories, but the cells in this study failed to produce significant amounts of glutamate. Since glutamate is produced from glutamine by the action of glutaminase, and generates no net energy when it is formed, glutamate excretion can be seen as a 'wasteful' loss of potential biomass and energy by the cells. In that regard, the failure of the cells in this study to produce glutamate is accounted for by their increased production of alanine and proline.

Most of the essential amino acids were consumed by the cells in this study at rates comparable to the published rates, with a few exceptions. The branched-chain group, isoleucine, leucine, and valine, were taken up at comparable rates by the cells at low density during the early transient, but at the high density condition, branched-chain amino acid uptake was lower than almost all the reported rates. This may reflect the much higher density that the cells in this study were maintained, 1.4×10^7 viable cells/ml. At the high density state, arginine, cysteine, threonine, and tryptophan were taken up at rates generally lower than most published rates. The arginine uptake rate at high density in particular was much lower than all published rates. This may be an artifact of arginine breakdown in the fresh medium samples during the analytical preparation, because the measured arginine concentrations in medium samples was about 250 μM, rather than the nominal value of 400 μM. Had the higher value for medium concentration been used in the calculations of arginine uptake rates, then the calculated rate would have been much more in line with published results.

The glutamine uptake rates observed during this study were lower than published rates, especially for the high density condition. Although there is no obvious explanation for this finding, it may simply reflect cell line differences. Previously published rates for glutamine uptake rates vary over a three-fold range, and the glutamine uptake rate observed at the low density condition was very close to the rate published for Lambert and Pirt (1975) for human diploid fibroblasts at a similar density. Thilly and Butler (1982) reported a 2.5-fold increase in glutamine uptake rate for cells at lower density (log-mean average density $\approx 5 \times 10^5$) as compared to the same cells at higher density (log-mean average density $\approx 12 \times 10^5$). The cells in this study showed a 1.5-fold increase in glutamine uptake for cells at lower density (density = 10^6) as compared to high density (density = 1.4×10^7).

Overall, the amino acid uptake rates observed in this study are generally comparable to published values, with a few exceptions. The lack of glutamate production was balanced by relatively increased formation of alanine and proline. Essential amino acid uptake was significantly lower than published rates at high cell density. Finally, the reduction in overall amino acid transport observed at high cell density is in concordance with many reports of high cell density-associated reduction in metabolic processes.

A consequence of the high amino acid uptake rates at low cell density is that far greater amounts of amino acids are actually brought into the cells than can be accounted for by the demands for protein and nucleic acid biosynthesis. Table IV-2 showed that for the cells growing at high density, and accounting for the PCA which was consumed, the net amino

consumption was 34 fmol/cell-h. The calculated demand was only 26 fmol/cell-h. This discrepancy widens considerably for the cells during the early transient phase, when the cells were growing rapidly at low density. The net amino acid uptake during this phase was 82 fmol/cell-h, while the calculated requirement was only 27 fmol/cell-h. It is interesting to note that the only condition in which the cells demonstrated high levels of IgG production coincided with a period of gross imbalance in amino acid uptake.

Other investigators have observed that amino acid uptake rates can be much higher than their rates of incorporation into proteins. Mohberg and Johnson (1963) measured amino acid uptake rates in 929-L murine fibroblasts and noted that most amino acids were used in 1.5 to 2.5 times the quantities needed for protein synthesis. In their review of amino acid transport in tumor cells, Johnstone and Scholefield (1965) state that the rate of amino acid uptake by tumor cells frequently is 10 to 100 times the rate of their utilization in protein synthesis. Bhargava *et al.* (1976a) reported that asparagine-dependent BHK cells consumed much more valine, leucine, lysine, and methionine than could be accounted for in the cellular proteins. They hypothesized that a high fraction of newly-synthesized proteins were either rapidly degraded or are excreted by the cells. Since they were studying a mitotically synchronized cell population (using asparagine starvation), they also saw that various amino acids were preferentially taken up at different portions of the cell cycle, and concluded that proteins made at different parts of the cycle contain different amino acid proportions. Bhargava *et al.* (1976b) reported that malignant liver cells consume amino acids at rates much higher than their rates of incorporation into proteins. They measured intracellular

free amino acid pools, and found them to contain the bulk of the excess amino acids ingested. Apparently, tumor cells respond to the demands of increased protein synthesis by storing sizable quantities of free amino acids.

An example of the interactions between protein synthesis by amino acid levels was shown by the work of Christensen *et al.* (1948). They performed a partial hepatectomy on adult rats, and then observed sharply increased intracellular concentrations of amino acids and glutathione in the rapidly regenerating new liver tissue. Donner *et al.* (1978) pointed out that increased intracellular levels of free amino acids resulted in increased protein synthesis in mammalian cells. However, Riggs and Walker (1962), using the non-metabolizable amino acid analogue cycloleucine, showed that the two processes of amino acid uptake and incorporation of amino acids into proteins are regulated independently. Either process could be altered without a direct effect on the other, and the two processes could even be altered in opposite directions at the same time. It remains unclear to what extent amino acid uptake and amino acid transport control each other.

As cells grow, so must the pools of intracellular free amino acids. If these pools are large enough, they could contain a significant fraction of the cell's total amino acids. This could account for the findings of Griffiths and Pirt (1967), who maintained tumor cells at steady state in chemostat perfusion culture and observed that the specific uptake rates of amino acids increased rapidly once the cells growth rate exceeded 0.4 day^{-1} (0.017 hr^{-1}). To analyze the possibility that uptake for intracellular free amino acid pools accounts for a large fraction of total amino acid uptake, the intracellular concentrations of several amino acids were obtained from literature values. Table IV-4 lists the

concentrations of a few essential amino acids reported for both tumor and normal cells. Two of the studies compared the amino acid pool sizes of non-growing normal cells with rapidly growing tumor cells. These studies, in particular, confirm the hypothesis that the pools of free amino acids are much larger in rapidly growing cells. However, exponential growth of the pools along with the cells cannot explain the increase seen in amino acid uptake. For instance, the average tumor cell intracellular leucine concentration reported in table IV-4 is 6 mM. Frame and Hu (1990b) showed that rapidly growing hybridoma cells have an modal volume of about 2000 μ^3, which corresponds to a diameter of approximately 15 μ and agrees approximately with the data presented in figure III-4. Therefore, each cell contains about 12 fmole free leucine. From tables III-3 and IV-2, the total leucine content of the proteins in the cell is about 50 fmole. Therefore, most of the leucine in the cells is in the form of proteins. Another explanation for the imbalance in amino acid uptake associated with rapid cell growth must be found.

Table IV-4.
Reported Intracellular Amino Acid Concentrations

Amino Acid	Conc'n (mM)		Reference
	Cell Type		
	Normal	Tumor	
tryptophan		2.2	Schafer and Jacquez (1967)
leucine	2.7		Reiser and Christiansen (1971)
lysine	2.3		
alanine	4.6		
valine	2.0		
arginine	1.4	4.4	Griffiths (1972)
leucine	2.0	4.6	
valine	2.1	3.0	
valine	4.0		Tucker and Kimmich (1973)
leucine	0.4	7.6	Bhargava *et al.* (1976b)
valine	0.8	11.3	
lysine	1.2	8.5	
arginine	0.6	4.7	

Another hypothesis to account for the imbalance in amino acid uptake is the possibility that cells are rapidly secreting proteins. If protein secretion were rapid enough, amino acid uptake would have to increase to accommodate the demand. Table III-3 showed that the leucine uptake during the early transient phase was 16 fmol/cell-h. The calculated leucine requirement for cell protein synthesis was given on table IV-2 as 1.7

fmol/cell-h. To account for the imbalance in leucine uptake relative to cell protein synthesis, a total of 14.3 fmol/cell-h would have to be secreted in the form of proteins. If leucine constituted 7.2% of extracellular as well as intracellular protein, the protein secretion rate would be 26 pg/cell-h. A cell containing 100 pg of intracellular proteins would have to secrete over 6 times its weight in proteins daily! At a density of 1.6×10^6 cells/ml and a dilution rate of 2 vol/day, the steady-state extracellular secreted protein concentration would be about 500 µg/ml. The total protein concentration in the medium from serum proteins was about 4 mg/ml, so even if the cells were secreting proteins at this prodigious rate, it would have been hard to detect them against the background of serum proteins. Still, the possibility that the cells are secreting (non-IgG) proteins into the medium at a high rate remains to be examined.

An alternative hypothesis concerning the imbalance in amino acid consumption during periods of high growth is that they are being used for the synthesis of non-proteinaceous materials. Lipids, in particular, can be synthesized from the ketogenic amino acids leucine, isoleucine, lysine, phenylalanine, and tyrosine. If ketogenic amino acids were being diverted to support lipid synthesis, their uptake rates would be much higher than other amino acids. Table III-3 listed the uptake rates of amino acids during the low density transient phase, and it can been seen that all the ketogenic amino acids are indeed utilized especially rapidly during the low density transient phase. However, the non-ketogenic amino acids serine and threonine are also consumed rapidly at this time, so the significance of high ketogenic amino acid uptake is unclear. Moreover, since the lipid content of a cell is much

lower than the protein content, lipid synthesis cannot account for more amino acid uptake than protein synthesis.

E. Effects of Waste and Nutrient Limitation

An original aim of this research effort was to evaluate the different effects of waste metabolite limitation and nutrient limitation on the metabolic rates of cells at high density. To accomplish this goal, a series of perfusion cultures was grown and maintained at several steady states. At each steady state, samples were collected and analyzed to determine metabolite concentrations. From this concentration data, kinetic rate parameters were calculated for cell growth and death rates, energy-yielding metabolic rates, and amino acid uptake rates.

Three different steady state conditions were maintained in order to independently vary waste and nutrient levels. The control condition, representing the best environment obtainable with this experimental system, was maintained by perfusing the bioreactor with whole medium at the fastest flow rate possible. A perfusion rate of 9 volumes/day achieved the highest steady-state cell density and viability. Growth rates were high and death rates were low in this condition, indicating that this was a relatively good environment for the cells. Perfusion at just 3 volumes/day with whole medium created an environment with high levels of waste products. Because the medium chosen for these experiments, DMEM* (see Appendix 3 for composition), is a rich medium with regard to nutrient concentrations, and

because the cells did not consume the nutrients rapidly in this state, nutrient levels remained high. The rate of removal of waste metabolites was low at this perfusion rate, and this permitted wastes to accumulate to high concentrations. Therefore, cells growing at the 3 volume/day perfusion condition were waste-limited. Nutrient limitation was induced by increasing the perfusion rate to 5 volumes/day (to aid the removal of wastes and thus prevent waste limitation) and diluting the medium with buffered saline. Since the nutrients entered the bioreactor at half strength, the cells were able to nearly exhaust several of them. Therefore, cells growing at the 5 volume/day perfusion with dilute medium were nutrient limited.

Table III-1 presented the different environmental conditions to which the cells were exposed as a result of the manipulations described above. At the 3 volume/day perfusion rate, waste metabolites, as exemplified by lactate, were at the highest concentrations observed during the course of these experiments. Glucose and glutamine concentrations were adequate, though not as high as they were during perfusion at 9 volumes/day. 5 volumes/day perfusion with diluted medium created a condition with very low residual glucose and glutamine concentrations. The redox potentials were nearly identical at all high density conditions.

The response of the cells to these different conditions was shown in table III-2. At 9 volumes/day, the cells grew to 1.56×10^7 viable cells/ml with a viability of 81%. The waste limited culture grew to only 9.8×10^6 cells/ml with a viability of 63%, and the nutrient limited culture grew to only 8×10^6 cells/ml with a viability of just 58%. The differences in growth and death rates observed at these different conditions helps explain the differences in

195

cell density and viability. At the 9 volumes/day condition, the growth rate was 0.024 hr^{-1}, and the death rate was 0.013 hr^{-1}. Waste limited cultures showed a much lower growth rate, 0.016 hr^{-1}, but the same death rate as the control culture. The nutrient-limited culture, on the other hand, had a good growth rate (0.027 hr^{-1}) but the death rate was increased to 0.021 hr^{-1}. Consequently, we can see that waste limitation reduced the growth rate and nutrient limitation increased the death rate.

Glycolytic and glutaminolytic rates were presented in table III-5, and the conversion efficiencies were presented in table III-6. The glutaminolytic rates included PCA uptake for reasons discussed earlier. The effect of waste limitation was to decrease glycolytic rates, whereas nutrient limitation slightly increased the glycolytic rate. Glutaminolytic rates were substantially depressed in both the waste and the nutrient limited cultures, with the waste limited condition showing a greater degree of depression. The conversion efficiency of glycolysis remained fairly constant, about 90-100%. Glutaminolytic conversion efficiencies were affected by waste limitation, increasing the yield of alanine from (glutamine + PCA) by 36%. Nutrient limitation left glutaminolytic conversion yields unaffected. The net effects of these alterations of energy-yielding metabolic pathways on the rate of ATP formation were shown in table III-6. As compared to the control culture perfused at 9 volumes/day, both the waste limited and the nutrient limited cultures had reduced rates of ATP production. Waste limitation reduced ATP production to a greater extent than did nutrient limitation, due both to the stimulation of glycolysis by nutrient limitation and the severe depression of glutaminolysis by waste limitation.

Amino acid metabolic rates were presented in table III-3. There are two different ways to summarize amino acid rates: **total** transport rates, which are the sum of the absolute values for uptake; and **net** transport rates, which are the arithmetic sum of individual uptake rates. The total transport rate for the control culture was 123 fmol/cell-h, while the net transport rate was 38 fmol/cell-h. Waste limitation produced a 59% reduction in total amino acid transport, while nutrient limitation reduced total amino acid transport by only 23%. The net amino acid transport rates were reduced by waste and nutrient limitations by 73% and 12%, respectively. Whether total or net rates are considered, waste limitation produced a much more profound inhibition in amino acid transport than did nutrient limitation.

Organic acid uptake rates were reduced by both nutrient and waste limitation. Nutrient and waste limitations reduced pyruvate uptake rates by 91% and 73%, respectively, and PCA uptake rates by 57% and 66%, respectively. Pyruvate uptake was one of the few metabolic rates more affected by nutritional limitation than waste limitation.

The overall effects of nutrient and waste limitation on cellular metabolism were quite different. In general, metabolic rates were more affected by waste limitation than by nutrient limitation. The particular control mechanisms which operate within the cells to regulate these many different metabolic pathways in concert so as to produce a coherent response to suboptimal conditions remains a matter for conjecture. It is the express desire of the author that future efforts with high density perfusion systems shed more light on this interesting aspect of regulation in metabolism.

197

V. Conclusions

The influences of nutritional limitation and waste product limitation were examined in high density cell cultures at steady state in a perfusion bioreactor system. In addition, the behavior of the system during the transition from low to high cell density was studied. Table V-1 summarizes the results of these conditions.

Table V-1.

Summary of Results with High-Density Perfusion Culture

Experimental Condition	Viable Cell/ml $\times 10^6$	μ hr^{-1}	α hr^{-1}	Glyco. rate fm/c-h	Glutam. rate fm/c-h	Net aa uptake fm/c-h	IgG rate fg/c-h	Redox Value m V
Transient Growth Phase	1.6	.033	.004	247	93	82	200	-241
Steady States								
Control	15.6	.024	.013	265	71	38	N/A	-266
Nutr. limited	8.0	.027	.021	278	46	34	7.7	-265
Waste limited	9.8	.016	.013	187	28	10.4	9.5	-266

N/A = Not Applicable (Cells had irreversibly drifted to non-production prior to culture)

198

The conclusions reached from this study are as follows:

The amino acid-to-protein mass balance fails to close under conditions favoring high IgG secretion. At the high cell densities examined at steady-state, when the IgG productivity is very low, the observed amino acid uptake rates approximate the calculated rates necessary to meet the demands of protein and nucleotide synthesis. During the initial transient growth phase, coincident with the period of high immunoglobulin secretion, the rates of some amino acid uptake are tenfold higher than those required, and the overall net amino acid uptake rate was threefold higher than required to satisfy protein and nucleic acid rates. Several hypotheses were advanced to explain the imbalance in amino acid uptake during periods of high growth rate:

1) The cells are creating a large pool of intracellular free amino acids which must grow exponentially along with the cells.

2) The cells are excreting much of the newly formed protein into the medium, and consequently must consume amino acids at high rates to satisfy the demand for exported proteins.

3) The cells are utilizing some of the amino acids as raw material for the synthesis of other biochemicals, such as lipids or sterols.

However, analysis of these hypotheses has found serious arguments against each. The fate of the excess amino acids remains undetermined.

A precipitous decline in specific amino acid rates accompanied the initial rise in cell density of the cells. Some of the observed amino acid uptake or production rates declined five- to ten-fold as the cell density increased from 10^6 to 10^7. At the same time, secretion rates for immunoglobulin declined tenfold or more. The declines in amino acid uptake rates and IgG secretion rates were comparable to declines in the rates of a wide variety of metabolic processes which have been reported in the literature. Glycolytic rates, on the other hand, were relatively constant during the transient growth phase to high cell density.

PCA is consumed by cells. An unintended medium component resulting from the spontaneous breakdown of glutamine, pyrollidone carboxylic acid (PCA, also known as 5-oxoproline), appears to play an important role in amino acid metabolism. A hypothesis for the role of PCA has been advanced which involves its uptake by the cells, followed by ATP-dependent cleavage to L-glutamic acid by 5-oxoprolinase followed by the subsequent normal metabolic utilization of glutamate. Calculated amino acid requirements for cell protein synthesis plus nucleotide synthesis can **only** be met by the observed amino acid uptake rates by including PCA uptake and its subsequent conversion to glutamate. A mass balance on the glutamine-derived family of amino acids, in particular, requires the inclusion of PCA uptake rates to close.

ATP production rates increased with increasing perfusion rates. As the perfusion rate was increased from 3 to 9 volumes/day, waste metabolite-induced limitations were relieved. Energy-producing metabolic rates increased substantially with increasing perfusion rates. As the perfusion rate was increased, glycolytic rates increased by about 50% and glutaminolytic rates increased by about 125%.

The nested conical separator provides effective cell recycle capability. Designed to separate mammalian cells through sedimentation, it maintains a high viability in the bioreactor. This is accomplished through two aspects of the separator. Being internal, it obviates the need for an external pumps and filter devices, which can account for a significant fraction of cell death in those systems which use them. In addition, because it acts as a differential sedimentation device, it selectively removes dead cells from the culture. Perfusion rates up to 9 volumes/day were possible with this system. These extremely rapid dilution rates, which have not been previously reported, permit the rapid removal of metabolic wastes and thus permit the long-term cultivation of mammalian cells at very high density and viability.

VI. Suggestions for Future Research

The findings of this research project lead to some interesting possibilities for follow-up research in the areas of amino acid metabolism, regulation of protein synthesis, PCA utilization, and bioreactor design. Some particular suggestions which I would be gratified to see explored are:

1) **Determine the mechanism of cell density-dependent down-regulation of metabolic rates**. This field has been only slightly explored by others, yet discovery of the molecular details involved in down-regulation offers the possibility of rational intervention to overcome this phenomenon. The full potential for economic realization of the benefits inherent in high density cell cultures must await a better understanding of the events leading to the unfortunate reduction in metabolic rates which accompanies high density cell culture.

2) **Determine the fate of the excessive amino acids which are taken up by cells growing rapidly**. Since the state of rapid cell division with attendant high amino acid consumption is coincident with high IgG productivity in the cells used for these experiments, it is imperative that we obtain a better understanding of the quantitative relationships between amino acid uptake and protein secretion. Just where *are* all these amino acids going, anyway?

3) **Prove that PCA is entering the intracellular pool of the glutamine family of amino acids**. This has already been done for fresh tissue slices, so the same kind of radiolabelling experiments shouldn't be too hard to repeat for cell cultures. In a perfect world, cell culture media wouldn't

have an opportunity to degrade prior to use by the cells, so PCA wouldn't be a component of media. However, due to the widespread (and useful!) practice of incubating freshly prepared medium for a few days at 37°C to establish its sterility, glutamine breakdown forms PCA. In any event, even without preincubation, the glutamine within a culture will break down at the same time that the cells are consuming it, so PCA will always be present in glutamine-containing media. This leads naturally to the next suggestion...

4) **Try to replace all the glutamine in media with PCA.** Since a substantial portion of glutamine is going to form PCA anyway, along with ammonia, why not avoid ammonia production altogether and start off with PCA? Others have used glutamate and 2-oxoglutarate as media glutamine replacements, but many cells require a lengthy period of adaptation before they can grow with a normal doubling time on these media. It is not unreasonable to speculate that because of the role of PCA in the γ-glutamyl cycle for amino acid transport, many cells will already express the necessary enzymes for its rapid uptake. In any event, PCA is much, much cheaper than the glutaminyl dipeptides currently being investigated as glutamine replacements.

5) **Improve the design of the nested conical sedimentation separator.** In a sense, I feel fortunate that the separator functioned so well, considering that it underwent only a few cycles of design revision before the present design was developed. Had that not been the case, more effort would have been made to understand the mechanics of lamella-type separation systems with conical geometry. It is entirely possible that a little tweaking here and there in the design of the separator could result in major improvements in separation or cell size selectivity. On the other hand, maybe it's already optimal. No one can know whether functional improvements can be made until they have tried.

6) **Try operating the bioreactor system so as to avoid any air bubbles passing through the separator.** The passage of air bubbles through the separator has the undesired effect of disturbing the laminar flow pattern within the separator plates upon which sedimentation depends. The rapidly rising bubbles entrain cells and carry them out the top of the separator. Not only does this render difficult the analytical task of determining growth and death rates, but it also puts an artificial ceiling on the perfusion rate (and hence the maximum cell density) of the system. Some mechanically simple system of maintaining exactly equal flow rates in and out of the system will permit the inlet to the separator to remain submerged, preventing air from disturbing the separation.

Appendix 1.

BASIC program used to estimate particle capture efficiencies

```
1 OPEN "epsfile.txt" FOR OUTPUT AS #4
5 gap = .5
  pi=3.14159265#
6 theta = 30/180*pi:alpha=pi/2-theta
7 sn=SIN(theta)
12 FOR l=5 TO 9 STEP 2
14 FOR dp=7 TO 15 STEP 2
15 FOR q0=875 TO 2500 STEP (2500-875)/4
20 q=q0/3600/24
30 velt=(dp*.0001)^2*.05*981/18/.01
32 co=velt*COS(theta)
37 da=-1:hi=-1:lo=1
40 tau=gap/2*(1-da)/velt/SIN(theta)
50 dt=tau/100
53 z=gap/2*TAN(alpha)
62 FOR t=0 TO tau STEP dt
70 fz=q/pi/z/sn/gap
80 ft=1-(((1-da)*t/tau+da)^2)
85 vz=fz*ft-co
90 z=z+vz*dt
100 NEXT t
105 IF da=-1 AND z<l THEN 900
120 IF ABS(z-l) <.01 THEN 900
130 IF z>l THEN hi=da:da=(lo+da)/2:GOTO 40
140 lo=da:da=(hi+da)/2:GOTO 40
900 delta=.02:sum=0
1000 FOR d=-1 TO da STEP delta
1010 sum=sum+3/4*(1-d*d)*delta
1020 NEXT d
1030 a$=STR$(q0)+" "+CHR$(9)+STR$(dp)+" "+CHR$(9)+STR$(l)+
         " "+CHR$(9)+LEFT$(STR$(sum),4)+" ":PRINT#4,a$
     PRINT a$
1040 NEXT q0
     NEXT dp
     NEXT l
1070 CLOSE#4
```

Appendix 2.

Formulation of Growth Medium used in Experiments.

Component	Concentration	
	mg/l	μM
Inorganic Ions		
$CaCl_2 \cdot H_2O$	265	2000
$FeNO_3 \cdot 9H_2O$	0.1	0.25
$MgSO_4$	97.67	0.8
KCl	400	5.4
NaCl	6400	109000
KH_2PO_4	109	800
$NaHCO_3$	3700	44000
Amino Acids		
L-Arginine·HCl	84	400
L-Cystine·HCl	62.6	200
L-Glutamine	876	6000
Glycine	30	400
L-Histidine·HCl·H_2O	42	200
L-Isoleucine	105	800
L-Leucine	105	800
L-Lysine·HCl	146	800
L-Methionine	30	200
L-Phenylalanine	66	400
L-Serine	42	400
L-Threonine	95	800
L-Tryptophan	16	78
L-Tyrosine·2Na·$2H_2O$	104	400
L-Valine	94	800

Component	Concentration	
	mg/l	μM
Vitamins		
Choline Chloride	4	25
Folic Acid	4	0.9
myo-inositol	7.2	40
Niacinamide	4	32.8
D-Pantothenic Acid·Ca	4	8.4
Pyridoxal·HCl	4	20
Riboflavin	0.4	1
Thiamine·HCl	4	12
Other		
D-Glucose	4500	25000
Phenol Red (Na)	15.9	42
Pyruvic Acid (Na)	220	2000
β-Mercaptoethanol		50

(Dulbecco and Freeman, 1959.)

Appendix 3.

Dimensions of Bioreactor used for Experimental Cultures.

(Not drawn to scale)

Waste Outlet .... .5 in

Outer Cone (glass) .... 30°

Inner Solid Cone (glass) .... 2.5 in

Inner Cone (glass) .... 2 in / 1.5 in / .25 in

Outer Cone (glass) .... 30° / 1/8 in / 1/8 in

Teflon Adaptor .... 1 in / .5 in / 1.75 in / 5.5 in

Glass Rod .... .25 in

Teflon Magnet

Fermentor (glass)

Teflon Paddle .... 2 in

3 in
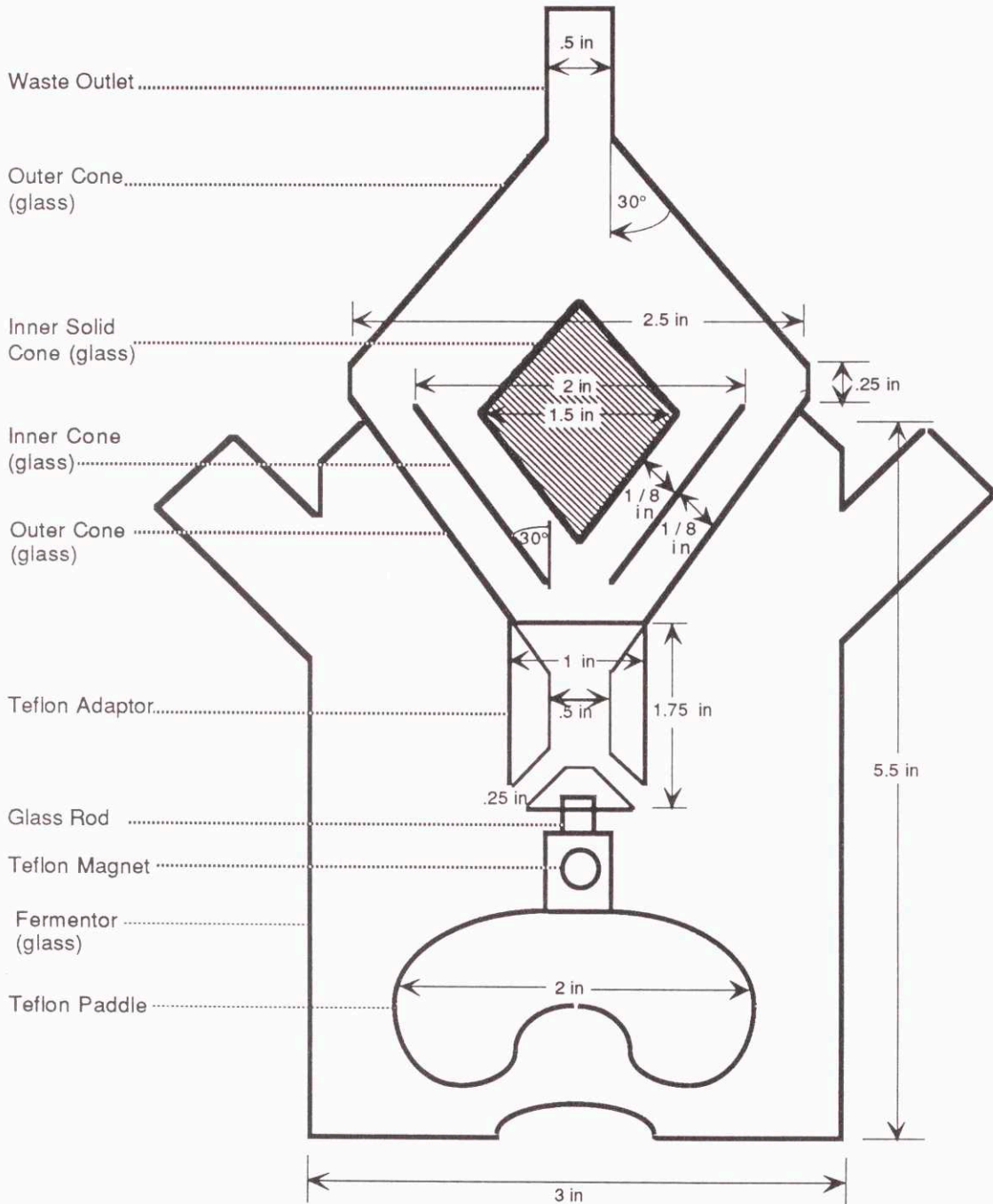
VII. References

Abraham, G. N. and D. N. Podell (1981). Pyroglutamic acid. Mol. Cell. Biochem. **38**: 181-190.

Avgerinos, G. C., D. Drapeau, J. S. Socolow, J. Mao, K. Hsiao, and R. J. Broeze (1990). Spin filter perfusion system for high density cell culture: Production of recombinant urinary type plasminogen activator in CHO cells. Bio/technology **8**: 54-58.

Baglioni, C. (1970). The role of pyrrolidone carboxylic acid in the initiation of immunoglobulin peptide chains. Biochem. Biophys. Res. Commun. **38**: 212-219.

Barbehenn, E. K., E. Masterson, S-W. Koh, J. V. Passonneau, and G. J. Chader (1984). An examination of the efficiency of glucose and glutamine as energy sources for cultured chick pigment epithelial cells. J. Cell. Physiol. **118**: 262-266.

Baechtel, F. S., D. E. Gregg, and M. D. Prager (1976). The influence of glutamine, its decomposition products, and glutaminase on the transformation of human and mouse lymphocytes. Biochim. Biophys. Acta **421**: 33-43.

Bertoncello, I. (1987). A comparison of cell separations obtained with centrifugal elutriation and separation at unit gravity. In: Pretlow, T. G. and T. P. Pretlow (editors), Cell separation: Methods and selected applications. Vol 4, pp. 89-108. New York: Academic Press.

Bhargava, K. and Bhargava, P.M. (1962). The incorporation of labelled amino acids into the proteins of liver cells in suspension. Life Sci. **9**: 477-482.

Bhargava, P. M., M. A. Siddiqui, G. Kranti Kumar, and K. S. N. Prasad (1975). Effect of cell concentration on the uptake of amino acids by rat liver parenchymal cells in suspension. J. Membr. Biol. **22**: 357-368.

Bhargava, P. M., E. P. Allin, and L. Montagnier (1976a). Uptake of amino acids and thymidine during the first cell cycle of synchronized hamster cells. J. Membr. Biol. **26**: 1-17.

Bhargava, P. M., D. Szafarz, C. A. Bornecque, and F. Zajdela (1976b). A comparison of the ability of normal liver, a premalignant liver, a solid hepatoma and the Zajdela ascitic hepatoma, to take up amino acids *in vitro*. J. Membr. Biol. **26**: 31-41.

Birch, J. R., and S. J. Pirt (1969). The choline and serum protein requirements of mouse fibroblast cells (strain LS) in culture. J. Cell Sci. **5**: 135-142.

Birch, J. R., and S. J. Pirt (1970) .Improvements in a chemically defined medium for the growth of mouse cells (strain LS) in suspension. J. Cell Sci. **7**: 661-670.

Bladé, E., L. Harel, and N. Hanania (1966). Variation du taux d'incorporation du phosphore dans des cellules en fonction de leurs concentrations et inhibition de contact. Exp. Cell Res. **41**: 473-482.

Bladé, E. and L. Harel (1968). Interaction between cells. I. Influence of cell concentration on amino acid transport and protein synthesis. Biochim. Biophys. Acta **156**: 148-156.

Boycott, A.E. (1920). Sedimentation of blood corpuscles. Nature **104**: 532.

Brand, K., W. Fekl, J. von Hintzenstern, K. Langer, P. Luppa, and C. Schoerner (1989). Metabolism of glutamine in lymphocytes. Metabolism **38**: 29-33

Brunengraber, H., M. Boutry, and J. M. Lowenstein (1973). Fatty acid and 3-β-hydroxysterol synthesis in the perfused rat liver. Including measurements on the production of lactate, pyruvate, β-hydroxy-butyrate, and acetoacetate by the fed liver. J. Biol. Chem **248**: 2656-2669.

Butler, M., and W. G. Thilly (1982). MDCK Microcarrier Cultures: Seeding Density Effects and Amino Acid Utilization. In Vitro **18**: 213-219.

Butler, M., T. Imamura, J. Thomas, and W. G. Thilly (1983). High yields from microcarriers by medium perfusion. J. Cell Sci. **61**: 351-363.

Carrel, A. (1912). On the permanent life of tissues outside of the organism. J. Exp. Med. **15**: 516-528.

Chang, J. Y., R. Knecht, and D. G. Braun (1983). Amino acid analysis in the picomole range by precolumn derivatization and high-performance liquid chromatography. Meth. Enzymol. **91**: 41-48.

Chmielewska, I., B. Bulhak, and K. Toczko (1967). Diketo piperazines and pyroglutamic acid utilization in humans. Bull. Acad. Pol. Sci. Biol. **15**: 719-721.

Christensen, H. N,. J. T. Rothwell, R. A. Sears, and J. Streicher (1948). Association between rapid growth and elevated cell concentrations of amino acids. II. In regenerating liver after partial hepatectomy in the rat. J. Biol. Chem. **175**: 101-105.

Dalili, M., G. D. Sayles, and D. F. Ollis (1990). Glutamine-limited batch hybridoma growth and antibody production: Experiment and model. Biotech Bioeng **36**: 74-82.

Darnell, J. E., and H. Eagle (1958). Glucose and Glutamine in Poliovirus Production by HeLa Cells. Vir. **6**: 556-566.

Delhotal, B., F. Lemonnier, M. Couturier, C. Wolfrom, M. Gautier, and A. Lemonnier (1984). Comparative use of fructose and glucose in human liver and fibroblastic cultures.

Donner, D. B., K. Nakayama, U. Lutz, and M. Sonnenberg (1978). The effects of bioregulators upon amino acid transport and protein synthesis in isolated rate hepatocytes. Biochim. Biophys. Acta **507**: 322-336.

Downie, N. M. and R. W. Heath (1983). In: Basic Statistical Methods, Fifth edition, pp 75-91. New York: Harper & Row.

Dulbecco, R. and G. Freeman (1959). Plaque production by polyoma virus. Virology **8**: 396-397.

Eagle, H. (1955). Nutrition needs of mammalian cells in tissue culture. Science **122**: 501-504.

Eagle, H. (1959). Amino acid metabolism in mammalian cell cultures. Science **130**: 432-437.

Eagle, H., and K. Piez (1962). The population-dependent requirement by cultured mammalian cells for metabolites which they can synthesize. J. Exp. Med. **116**: 29-43.

Evans,V. J., J. C Bryant, W. T. McQuilken, M. C. Fioramonti, K. K. Sanford, B. B. Westfall, and W. R. Earle (1956). Studies on nutrient media for tissue cells *in vitro*. II. An improved protein-free chemically defined medium for long-term cultivation of strain L-929 cells. Cancer Res. **16**: 87-94.

Foster, D. O. and A. B. Pardee (1969). Transport of amino acids by confluent and nonconfluent 3T3 and polyoma virus-transformed 3T3 cells growing on glass cover slips. J. Biol. Chem. **244**: 2675-2681.

Frame, K. K. and W-S. Hu (1990a). The loss of antibody productivity in continuous culture of hybridoma cells. Biotech. Bioeng. **35**: 469-476.

Frame, K. K. and W-S. Hu (1990b). Cell volume measurement as an estimation of mammalian cell biomass. Bioeng. **36**: 191-197.

Glacken, M. W., R. J. Fleischaker, and A. J. Sinskey (1986). Reduction of Waste Product Excretion via Nutrient Control: Possible Strategies for Maximizing Product and Cell Yields on Serum in Cultures of Mammalian Cells. Biotech. Bioeng. **28**: 1376-1389.

Glacken, M. W., E. Adema, and A. J. Sinskey (1988). Mathematical descriptions of hybridoma culture kinetics. I. Initial metabolic rates. Biotech. Bioeng **32**: 491-506.

Griffiths, J. B. and G. J. Pirt (1967). The uptake of amino acids by mouse cells (strain LS) during growth in batch culture and chemostat culture: The influence of cell growth rate. Proc. R. Soc. B. **168**: 421-438.

Griffiths, J. B. (1972). The effect of cell population density on nutrient uptake and cell metabolism: A comparative study of human diploid and heterodiploid cell lines. J. Cell Sci. **10**: 515-524.

Hamamoto, K., K. Ishimaru, and M. Tokashiki (1989). Perfusion culture of hybridoma cells using a centrifuge to separate cells from culture mixture. J. Ferm. Bioeng. **67**: 190-194.

Hamel. (1916). Spiralformige Bewegungen zaher Flussigkeiten. Jahresber. d. Deutschen Mathematiker-Vereinigung **25**: 34.

Hassell, T. and M. Butler (1990). Adaptation to non-ammoniagenic medium and selective substrate feeding lead to enhanced yields in animal cell cultures. J. Cell Sci. **96**: 501-508.

Hill, W. D., R. R. Rothfus, & Li, K. (1977). Boundary-enhanced sedimentation due to settling convection. Int. J. Multiphase Flow **3**: 561-583.

Himmelfarb,P., P. S. Thayer, and H. E. Martin (1969). Spin filter culture: The propagation of mammalian cells in suspension. Science **164**: 555-557.

Holley, R. W., R. Armour, and J. H. Baldwin (1978). Density-dependent regulation of growth of BSC-1 cells in cell culture: Growth inhibitors formed by the cells. Proc. Nat. Acad. Sci. USA **75**: 1864-1866.

Hu W-S., T. C. Dodge, K. K. Frame, and V. B. Himes (1987). Effect of glucose on the cultivation of mammalian cells. Dev. Biol. Stand. **66**: 279-290.

Imamura, I., C. L. Crespi, W. G. Thilly, and H. Brunengraber (1982). Fructose as a carbohydrate source yields stable pH and redox potential in microcarrier cell culture. Anal. Biochem. **124**: 353-358.

Johnstone, R. M. and P. G. Scholefield (1965). Amino acid transport in tumor cells. In: Haddow, A. and S. Weinhouse (editors), Advances in Cancer Research, volume 9, pp 143-227. New York: Academic Press.

Kitano, K., Y. Shintani, Y. Ichimore, K. Tsukamoto, S. Sasai, and M. Kida (1986). Production of human monoclonal antibodies by heterohybridomas. Appl. Micr. Biotechnol. **24**: 282-286.

Kitos, P. A., and C. Waymouth (1967). The metabolism of L-glutamate and L-5-carboxy-pyrrolidone by mouse cells (NCTC clone 929) under conditions of defined nutrition. J. Cell. Physiol **67**: 383-398.

Köhler G, Howe SC, and Milstein C. (1976). Fusion between immunoglobulin-secreting and nonsecreting myeloma cell lines. Eur J Immunol **4**: 292-295

Kovacevic, Z. and and H. P. Morris (1972). The role of glutamine in the oxidative metabolism of malignant cells. Cancer Res. **32**: 326-333.

Lange, W. E. and E. F. Carey (1966). Metabolism of ^{14}C-labeled glutamic acid and pyroglutamic acid. J. Pharm. Sci. **55**: 1147-1149.

Langlois, W. E. (1964). *in* "Slow viscous flow." p 109-111. Macmillan Co., NY.

Lanks, K. W., I. F. Hitti, and N. W. Chin (1986). Substrate utilization for lactate and energy production in heat-shocked L929 cells. J. Cell. Physiol. **127**: 451-456.

Lanks, K.W. and P-W. Li (1988). End products of glucose and glutamine metabolism by cultured cell lines. J. Cell Physiol **135**: 151-155.

Leibovitz, A. (1963). The growth and maintenance of tissue-cell cultures in free gas exchange with the atmosphere. Amer. J. Hyg. **78**: 173-180.

LoBuglio, A. F., R. H. Wheeler, J. Trang, A. Haynes, K. Rogers, E. B. Harvey, L. Sun, J. Ghrayeb, & M. B. Khazaeli (1989). Mouse/human chimeric monoclonal antibody in man: kinetics and immune response. Proc Natl Acad Sci U S A **86**: 4220-4224.

Maiorella, B., G. Dorin, A. Carion, and D. Harano (1991). Crossflow microfiltration of animal cells. Biotech. Bioeng. **37**: 121-126.

Martin, N. J., A. J. Brennan, and J. Shevitz (1987). A perfusion system for high productivity in cell culture. Biomed. Prod. October 1987: 33-43.

McCarty, K. (1962). Selective utilization of amino acids by mammalian cell cultures. Exp. Cell Res. **27**: 230-240.

McHeyzer-Williams, M. G. and G. J. V. Nossal (1989). Inhibition of antibody production at high cell density following mitogen stimulation and isotype switching in vitro. J. Immunol. Meth. **119**: 9-17.

McKeehan, W. L. (1982). Glycolysis, glutaminolysis and cell proliferation. Cell Biol. Int. Rep. **6**: 635-660.

Meister, A. (1973). On the enzymology of amino acid transport. Science **180**: 33-39.

Meister, A. (1974). Glutathione: metabolism and function via the γ-glutamyl cycle. Life Sci. **15**: 177-190.

Merten, O. W. (1987). "Concentrating mammalian cells I. Large-scale animal cell culture." Trends in Biotech. **5**: 230-237.

Moav B. and T. N. Harris (1967). Pyrrolid-2-one-5 carboxylic acid involvement in the biosynthesis of rabbit immunoglobulin. Biochem. Biophys. Res. Commun. **26**: 773-776.

Mohberg, J., and M. J. Johnson (1963). Amino acid utilization by 929-L fibroblasts in chemically defined media. J. Nat. Cancer Inst. **31**: 611-625.

Monod, J. (1942). Recherches sur la croissance bactériennes. Paris: Masson.

Moreadith, R. W, and A. L. Lehninger (1983). The pathways of glutamate and glutamine oxidation by tumor cell mitochondria. J. Biol. Chem **259**: 6215-6221.

Murakami, H., H. Masui, G. H. Sato, N. Sueoka, T. P. Chow, and T. Sueoka (1982). Growth of hybridoma cells in serum-free medium: Ethanolamine is an essential component. Proc. Nat. Acad. Sci. USA **77**: 5429-5431.

Nagle, S.C., H. R. Tribble, R. G. Anderson, and N. D. Gary (1963). A chemically defined medium for the growth of animal cells in suspension. Proc. Soc. exp. Biol. Med. **113**: 340-344.

Nahapetian, A. T., J. N. Thomas, and W. G. Thilly (1986). Optimization of environment for high density vero cell culture: Effect of dissolved oxygen and nutrient supply on cell growth and changes in metabolites. J. Cell Sci. **81**: 65-103.

Newsholme, E. A. and C. Start (1973). Regulation of fat metabolism in liver. In: Regulation in metabolism. pp. 293-328. London: John Wiley & Sons.

Oller, A. R., C. W. Buser, M. A. Tyo, and W. G. Thilly (1989). Growth of mammalian cells at high oxygen concentrations. J. Cell Sci. **94**: 43-49.

Orlowski M , and A. Meister (1970). The gamma-glutamyl cycle: a possible transport system for amino acids. Proc. Natl. Acad. Sci. USA **67**: 1248-1255.

Otsuka, H. and M. Moskowitz (1974). Difference in transport of leucine in attached and suspended 3T3 cells. J. Cell Physiol. **85**: 665-674.

Ozturk, S. S., and B. O. Palsson (1990). Chemical decomposition of glutamine in cell culture media: Effect of media type, pH, and serum concentration. Biotechnol. Prog. **6**: 121-128.

Pascher, G. (1956). Arch. klin. exp. Dermatol. **203**: 234-238.

Pirt, S. J. (1965). The maintenance energy of bacteria in growing cultures. Proc. Roy. Soc. Lond. (Biol.) **163(B)**: 224-231.

Pirt, S. J., and Callow, D. S. (1964). Continuous-flow culture of the ERK and L types of mammalian cells. Exp. Cell Res. **33**: 413-421.

Pretlow, T. G. and T. P. Pretlow (1982). Sedimentation of cells: An overview and discussion of artifacts. In: Pretlow, T. G. and T. P. Pretlow (editors), Cell separation: Methods and selected applications. Vol 1, pp. 41-60. New York: Academic Press.

Reed, W. D., H. R. Zielke, P. J. Baab, and P.T. Ozand (1981). Ketone bodies, glucose, and glutamine as lipogenic precursors in human diploid fibroblasts. Lipids **16**: 677-684.

Reitzer, L. J., B. M. Wise, and D. Kennell (1979). Evidence that Glutamine,not Sugar, is the Major Energy Source for Cultured HeLa Cells.J. Biol. Chem. **254**: 2669-2676.

Reuveny, S., D. Velez, J. D. Macmillan, and L. Miller (1986). Factors affecting cell growth and monoclonal antibody production in stirred reactors. J. Immunol. Meth. **86**: 53-59.

Riggs, T. R. and L. M. Walker (1962). Some relations between activetransport of free amino acids into cells and thair incorporation into protein. J. Biol. Chem. **238**: 2663-2668.

Robinson, J. H. (1976). Density regulation of amino acid transport in cultured, androgen-responsive tumour cells. J. Cell Physiol. **89**: 101-110.

Rose, W.C., R. L. Wixom, H. B. Lockhart, and G. F. Lambert (1955). The amino acid requirements of man. XV. The valine requirement: summary and final observations. J Biol. Chem. **217**: 987-1004.

Rush, E. A. and J. L. Starr (1970). The indirect incorporation of pyrrolidone carboxylic acid into transfer ribonucleic acid. Biochim. Biophys. Acta **199**: 41-55.

Sand,T., R. Condie and A. Rosenberg (1977). Metabolic crowding effect in suspension of cultured lymphocytes. Blood **50**: 337-346.

Sanford, K. K., W. R. Earle, and G. D. Likely (1948). The growth in vitro of single isolated tissue cells. J. Nat. Cancer Inst. **9**: 229-246.

Sasai, S., S. Umemoto, and T. Fujimoto (1985). Establishment of a medium for the mass culture of mammalian cells. Abst. 3rd Intl. Cell Culture Congr. (Sendai). p 46.

Sato, S., K. Kawamura, and N. Fujiyoshi (1983). Animal cell cultivation for production of biological substances with a novel perfusion culture apparatus. J. Tiss. Cult. Meth. **8**: 167-171.

Schafer, J. A. and J. A. Jacquez (1967). Transport of amino acids in Ehrlich ascites cells: Competitive stimulation. Biochim. Biophys. Acta **135**:741-750.

Schmid, G., H. W. Blanch, and C. R. Wilke (1990). Hybridoma growth, metabolism, and product formation in HEPES-buffered medium: I. Effect of passage number. Biotechnol. Lett. **12**: 627-632.

Sener, A., V. Leclercq-Meyer, M. Giroix, W. Malaisse, and C. Hellerström (1987). Opposite effects of D-glucose and a nonmetabolized analogue of l-leucine on respiration and secretion in insulin-producing tumoral cells (RINm5F). Diabetes **36**: 187-192.

Siano, S. A. and R. Mutharasan (1991). NADH fluorescence and oxygen uptake responses of hybridoma cultures to substrate pulse and step changes. Biotech. Bioeng. **37**: 141-159.

Sinclair, R. (1966). Steady-state suspension culture and metabolism is strain L mouse cells in simple defined medium. Exp. Cell Res. **41**: 20-33.

Stallcup, K. C., A. Dawson, and M. F. Mescher (1984a). Growth-inhibitory activity of lymphoid cell plasma membranes. I. Inhibition of lymphocyte and lymphoid tumor cell growth. J. Cell Biol. **99**: 1221-1226.

Stallcup, K. C., S. J. Burakoff, and M. F. Mescher (1984b). Growth-inhibitory activity of lymphoid cell plasma membranes. II. Partial Characterization of the inhibitor. J. Cell Biol. **99**: 1227-1234.

Stallcup, K. C., Y-N. Liu, M. E. Dorf, and M. F. Mescher (1986). Inhibition of lymphoid cell growth by a lipid-like component of macrophage hybridoma cells. J. Immunol. **136**: 2723-2728.

Stoner, G. D. and D. J. Merchant (1972). Amino acid utilization by L-M strain mouse cells in a chemically defined medium. In Vitro **7**: 330-343.

Stott, D. I. and A. J. Munro (1972). The formation of pyrrolid-2-one-5-carboxylic acid at the N-terminus of immunoglobulin G heavy chain. Biochem J. **128**: 1221-1227.

Sumbilla, C. M., C. L. Zielke, W. D. Reed, P.T. Ozand, and H. R. Zielke (1981). Comparison of the oxidation of glutamine, glucose, ketone bodies, and fatty acids by human diploid fibroblasts. Biochim. Biophys. Acta **675**: 301-304.

Sun, L. K., P. Curtis, E. Rakowicz-Szulczynska, J. Ghrayeb, N. Chang, S. L. Morrison, and H. Koprowski (1987) Chimeric Antibody with Human Constant Regions and Mouse Variable Regions Directed Against Carcinoma-associated Antigen 17-1A. Proc. Nat. Acad. Sci. USA **84**: 214-218.

Suzuki, E., and D. F. Ollis (1989). Cell cycle model for antibody production kinetics. Biotech. Bioeng. **34**: 1398-1402.

Takazawa, Y. and M. Tokashiki (1989). High cell density perfusion culture of mouse-human hybridomas. Appl. Microbiol. Biotechnol. **32**: 280-284.

Thilly, W. G., D. Barngrover, and J. N. Thomas (1982). Microcarriers and the problem of high density cell culture. *in* From Gene to Protein: Translation into Biotechnology. pp 75-103. New York: Academic Press.

Tritsch, G. L., and G. E. Moore (1962). Spontaneous decomposition of glutamine in cell culture media. Exp. Cell Res. **28**: 360-364.

Tokashiki, M., K. Hamamoto, Y. Takazawa, and Y. Ichikawa (1988). High density culture of mouse-human hybridoma cells using a new perfusion culture vessel. J. Ferm. Tech. **14**: 337-341.

Tolbert, W. R., J. Feder, and R. C. Kimes (1981). Large-scale rotating filter perfusion system for high-density growth of mammalian suspension cultures. In Vitro **17**: 885-890.

Tolbert, W. R., W. R. Srigley, and C. P. Prior (1988). Perfusion culture systems for large-scale pharmaceutical production. *in* Animal Cell Biotechnology, Vol 3. pp 373-393. Spier, R. E. and J. B. Griffiths, eds. Academic Press: New York.

Tucker, A. M. and G. A. Kimmich (1973). Characteristics of amino acid accumulation by isolated intestinal epithelial cells. J. Membr. Biol.**12**: 1-22.

Tyo, M. A. and W.G. Thilly (1989). Novel High Density Perfusion System For Suspension Culture Metabolic Studies. Presented at the 1989 Annual Meeting of the American Institute of Chemical Engineers, San Francisco, CA, November , 1989.

Van Der Werf, P. and A. Meister (1975). The metabolic formation and utilization of 5-oxo-L-Proline (L-pyroglutamate, L-pyrrolidone carboxylate). Adv. Enzymol. **43**: 519-566.

Van der Werf, P., M. Orlowski and A. Meister (1971). Enzymatic conversion of 5-oxo-L-proline (L-pyrrolidone carboxylate) to L-glutamate coupled with cleavage of adenosine triphosphate to adenosine diphosphate, a reaction in the γ-glutamyl cycle. Proc. Natl. Acad. Sci. USA **68**: 2982-2985.

Velez, D., L. Miller, and J. D. MacMillan (1989). Use of tangential flow filtration in perfusion propagation of hybridoma cells for production of monoclonal antibodies. Biotech. Bioeng **33**: 938-940.

Viña J. R., M. Palacin, I. R. Puertes, R. Hernandez, and J. Viña. (1989). Role of the gamma-glutamyl cycle in the regulation of amino acid translocation. Am. J. Physiol. **257**: E916-E922.

Viña J. R, P. Blay, A. Ramirez, A. Castells, and J. Viña. (1990). Inhibition of γ-glutamyl transpeptidase deceases amino acid uptake in human keratinocytes in culture. FEBS Lett. **269**: 86-88.

Waymouth, C. (1959). Rapid proliferation of sub-lines of NCTC clone 929 (strain L) mouse cells in a simple chemically defined medium (MB 752/1). J. Nat. Cancer Inst. **22**: 1003-1017.

Wilk, S. and M.Orlowski (1973). The occurrence of free L-pyrrolidone carboxylic acid in body fluids and tissues. FEBS Lett. **33**:157-160.

Williamson, D. H., Pl Lund, and H. A. Krebs (1966). The redox state of free nicotinamide-adenine dinucleotide in the cytoplasm and mitochondria of rat liver. Biochem. J. **103**: 514-527.

Wohlpart, D., D. Kirwan, and J. Gainer (1990). Effects of cell density and glucose and glutamine levels on the respiration rates of hybridoma cells. Biotech. Bioeng. **36**: 630-635.

Zielke, H. R., P. T. Ozand, J. T. Tildon, D. A. Sevdalian, and M. Cornblath (1976). Growth of human diploid fibroblasts in the absence of glucose utilization. Proc. Nat. Acad. Sci. USA **73**: 4110-4114.

Zielke, H. R., P. T. Ozand, J. T. Tildon, D. A. Sevdalian, and M. Cornblath (1978). Reciprocal regulation of glucose and glutamine utilization by cultured human fibroblasts. J. Cell. Physiol. **95**: 41-48.

Zielke, H.R., C. M. Sumbilla, D. A. Sevdalian, R. L. Hawkins, and P. T. Ozand (1980). Lactate: A major product of glutamine metabolism by human diploid fibroblasts. J. Cell. Physiol. **104**: 433-441.